Dissertations

Theses and Dissertations

Spring 2000

Active feedback control of a wake flow via forced oscillations based on a reduced model

Fu Li
New Jersey Institute of Technology

ABSTRACT

ACTIVE FEEDBACK CONTROL OF A WAKE FLOW VIA FORCED OSCILLATIONS BASED ON A REDUCED MODEL

by
Fu Li

As it is well known, the flow past a cylinder consists of a symmetric recirculation bubble of vortices at small Reynolds numbers. As Reynolds number increases, the bubble becomes unstable and develops into a Karman vortex street of alternating vortices. This instability is responsible for the occurrence of large amplitude oscillations in the lift and an increase in the mean drag. It was previously shown by numerical simulation that the mechanism driving the bubble instability is well mimicked by Foppl's four dimensional potential flow model where the bubble is represented by a saddle point. In this work, we design two active feedback control algorithms for the model based on small perturbations applied to the cylinder in order to control the flow slightly perturbed away from the fixed point. We use the domain perturbation method and asymptotic expansions to derive control algorithms analytically. In the first algorithm, we displace the cylinder by a small vertical distance such that the lift remains zero at all times. We also show by direct numerical simulation of the flow (based on the full N-S equations) that our feedback control system is capable of preventing vortex shedding from occurring in the impulsively started viscous flow at Reynolds number Re = 100. In the second algorithm, we deform the cylinder uniformly so that the drag remains the drag of the steady recirculation bubble.

ACTIVE FEEDBACK CONTROL OF A WAKE FLOW VIA FORCED OSCILLATIONS BASED ON A REDUCED MODEL

by
Fu Li

A Dissertation
Submitted to the Faculty of
New Jersey Institute of Technology
in Partial Fulfillment of the Requirements for the Degree of
Doctor of Philosophy in Mathematical Sciences

Department of Mathematical Sciences

May 2000

APPROVAL PAGE

ACTIVE FEEDBACK CONTROL OF A WAKE FLOW VIA FORCED OSCILLATIONS BASED ON A REDUCED MODEL

Fu Li

Dr. Nadine Aubry, Dissertation Advisor	Date
Professor/Jacobus Chair of Mechanical Engineering, NJIT	
Professor of Mathematical Sciences, NJIT	

Dr. Demetrius T. Papageorgiou, Committee Member	Date
Associate Professor of Mathematical Sciences, NJIT	

Dr. Michael Siegel, Committee Member	Date
Associate Professor of Mathematical Sciences, NJIT	

Dr. Burt Tilley, Committee Member	Date
Assistant Professor of Mathematical Sciences, NJIT	

Dr. Pushpendra Singh, Committee Member	Date
Assistant Professor of Mechanical Engineering, NJIT	

BIOGRAPHICAL SKETCH

Author: Fu Li

Degree: Doctor of Philosophy in Mathematical Sciences

Date: May 2000

Undergraduate and Graduate Education:

- Doctor of Philosophy in Mathematical Sciences, 2000
  New Jersey Institute of Technology, Newark, NJ

- Master of Science in Applied Mathematics, 1997
  New Jersey Institute of Technology, Newark, NJ

- Master of Science in Engineering Mechanics, 1992
  Shanghai Jiao Tong University, Shanghai, P. R. China

- Bachelor of Science in Engineering Mechanics, 1988
  Shanghai Jiao Tong University, Shanghai, P. R. China

Major: Mathematical Sciences

Publications:

Fu Li and Nadine Aubry,   Reactive flow control for a wake flow based on a reduced model, AIAA paper 2531, 2000.

Fu Li and Nadine Aubry,   Active feedback control of the instability leading to vortex shedding, 52nd APS/DFD Meeting, Nov. 1999, New Orleans, Louisiana.

Fu Li and Nadine Aubry, Active feedback control of vortex shedding past a cylinder based on a low dimensional model, 51st APS/DFD Meeting, Nov. 1998, Philadelphia, PA.

To my Parents and PangPang

ACKNOWLEDGMENT

TABLE OF CONTENTS

LIST OF FIGURES

CHAPTER 1

INTRODUCTION

1.1 Background

The control of fluid flow has attracted much attention in both the fluid mechanics and control communities in the past decade. Controlling fluid flows aims at drag reduction, lift enhancement as well as noise and vibration reduction in practical applications.

The goal of this study is to design a feedback loop control algorithm to manipulate the flow past a cylinder. As it is well-known, the flow consists of a symmetric recirculation bubble of vortices at low Reynolds numbers. As Reynolds number increases, the bubble becomes unstable and develops into a Karman vortex street of alternating vortices. There are two major consequences of this instability: (i) the lift becomes non-zero and oscillates in time, (ii) the drag increases significantly. These two features are often undesired in practical applications.

Two different types of control can be identified. The first, and most common, method — referred to as **passive control** — consists of a suitable modification of boundary conditions. Typical examples of this type of control are the insertion of a splitter plate behind a cylinder (Unal & Rockwell 1988, Kwon & Choi 1996), the introduction of a small secondary cylinder in the near wake (Strykowski & Sreenivasan 1990), base bleed and suction (Oertel H. Jr. 1990), and near wake heating (Schumm et al. 1994). The second type — or **active control** — requires the introduction of energy to the flow. Active control can be achieved either via closed (feedback) loop or open loop. Open loop control requires one or more actuators, but no information on the flow (Gad-el-Hak 1996), while closed loop (feedback) control

1

requires both actuators and sensors, using a control law to sense the flow in real time (Monkewitz 1992).

In this thesis, we concentrate on the active feedback (closed loop) control of the flow past a circular cylinder. The goal of our study is to cancel the unsteady oscillating lift on the cylinder which occurs as vortex shedding develops.

An interesting observation on wake dynamics is that a very small alteration in the near wake may have a global effect on the flow. So far the mechanism behind this phenomenon is still unclear. Some researchers have studied the relation between the formation of vortex shedding and absolute/convective instabilities of the mean flow (Provansal et al. 1987, Jackson 1987, Hannemann et al. 1989, Dusek et al. 1994, Schumm et al. 1994). In certain cases, the Ginzburg-Landau equation has been used to describe the temporal and spatial development of the instability, as well as to control vortex shedding by measuring the temporal growth of the instability near the critical Reynolds number. The realized control is, however, restricted to a small range of Reynolds numbers above the critical Reynolds number.

Although much attention has been given to active flow control over the past decade (Moin et al. 1994, Gad-el-Hak 1996, Lumley 1999), the active control of vortex shedding behind a circular cylinder still remains an interesting challenge and has not been implemented in practice.

The earliest experiments of feedback control of vortex shedding were probably carried out by Berger (1967) who showed that vortex shedding can be suppressed within a small range of Reynolds numbers. Williams & Zhao (1989) applied active control to suppress vortex shedding behind a circular cylinder. In their experiment, they used a hot-wire located in the near wake as sensor, and a loudspeaker in the wind tunnel wall as actuator. They showed that in the range of Reynolds numbers from $Re = 400$ to $Re = 10^4$, vortex shedding can significantly be reduced throughout

the wake. Roussopoulos (1993) also performed similar experiments using a single–channel feedback mechanism. He pointed out that at high Reynolds number, the flow can be stabilized only near the location of the sensor.

Computationally, most researchers use suction/blowing techniques on the cylinder surface in order to prevent vortex shedding from occurring. Park et al. (1994) used suction/blowing actuation and reported a successful feedback control of vortex shedding at $Re = 60$. More recently, Gunzburger et al. (1996) designed the same feedback control scheme. They sensed the pressure distribution on the cylinder surface and used injection and suction of fluid through orifices on the surface as actuators. They reported a remarkable lift reduction without suppressing vortex shedding completely. Min & Choi (1999) designed a suboptimal feedback control scheme by evaluating three cost functions which are all related to the pressure distribution on the cylinder surface. They showed that the drag and lift can be reduced significantly at the low Reynolds number values $Re = 60$ and $Re = 80$.

Except for a few contributions such as that of Min & Choi, most techniques have been empirical. Another approach consists in looking for a model, particularly a low dimensional dynamical system, capable of capturing the main physics of the real flow. Cortelezzi (1996) developed a nonlinear feedback control loop to manipulate the flow past a plate, based on a point vortex model simulating vortex shedding. He used the circulation produced by the plate as sensor and a suction point behind the plate as actuator. However, to our knowledge, his technique was not applied to any viscous flow.

Since vortex shedding is born from the break-up of the recirculating bubble of two symmetric, counter-rotating vortices, it seems appropriate to design a control technique based on the instability the bubble undergoes. The bubble of twin vortices, together with its instability, is itself a complex phenomenon which needs to be

modeled in order to be useful in a feedback control loop. The model we use here is that of Foppl (1913). It consists of the two-dimensional, incompressible potential flow resulting from the superposition of a uniform incoming flow, a pair of point vortices symmetrically located with respect to the centerline behind the cylinder, and inner vortices placed within the cylinder in order to satisfy the boundary conditions on the body. Foppl found the fixed point (steady solutions) of the system and partially carried out the linear stability analysis of the model. He showed that the flow is unstable to asymmetric perturbations and neutrally stable to symmetric perturbations. His stability analysis was reviewed later by Smith (1973) and, more recently, generalized by Tang and Aubry (1997) who showed that the fixed point is indeed unstable to a certain type of asymmetric perturbations, but stable to another type of asymmetric disturbances. They also demonstrated computationally the relevance of Foppl's model to the viscous flow. Some researchers (Widnall 1985, Rusak et al. 1991) studied the three-dimensional stability of Foppl's model.

In the following sections, we first recall Foppl's model and then qualitatively describe an active feedback control strategy to control the oscillating lift on the cylinder.

1.2 Foppl's Model

We consider the two-dimensional, incompressible, potential flow resulting from the superposition of an incoming flow, two point vortices of opposite circulation Γ located symmetricly behind the cylinder at $z_1(x_1, y_1)$, $z_2(x_2, y_2)$ ($x_1 = x_2$, $y_1 = -y_2$) and two inner vortices placed within the body to guarantee zero normal velocity at the boundary, see figure 1.1.
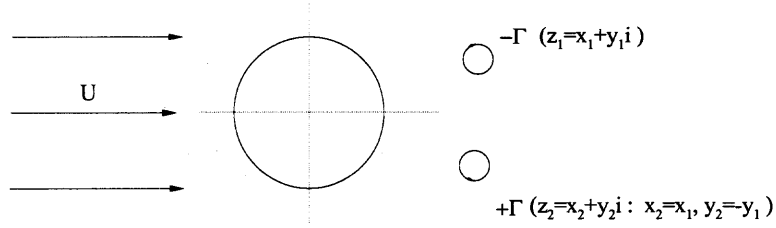
Figure 1.1 Foppl's vortex model

Assuming that the incoming free stream is $U_\infty = 1$ and the radius of the cylinder is equal to $r_0 = 1$, the complex potential of the system is:

$$w(z) = z + \frac{1}{z} - \frac{\Gamma}{2\pi i} ln(z - z_1) + \frac{\Gamma}{2\pi i} ln(z - \frac{1}{\overline{z_1}}) + \frac{\Gamma}{2\pi i} ln(z - z_2) - \frac{\Gamma}{2\pi i} ln(z - \frac{1}{\overline{z_2}})$$

The dynamics of the two point vortices located at $z_1 = x_1 + y_1 i$ and $z_2 = x_2 + y_2 i$, where $z_1 = \overline{z_2}$ ($x_1 = x_2$, $y_1 = -y_2$) is given by the ordinary differential equations (ODE's):

$$\frac{d\overline{z}_1}{dt} = 1 - \frac{1}{z_1^2} + \frac{\Gamma}{2\pi i}\frac{1}{z_1 - z_2} + \frac{\Gamma}{2\pi i}\frac{1}{z_1 - \frac{1}{\overline{z_1}}} - \frac{\Gamma}{2\pi i}\frac{1}{z_1 - \frac{1}{\overline{z_2}}}$$

$$\frac{d\overline{z}_2}{dt} = 1 - \frac{1}{z_2^2} - \frac{\Gamma}{2\pi i}\frac{1}{z_2 - z_1} + \frac{\Gamma}{2\pi i}\frac{1}{z_2 - \frac{1}{\overline{z_1}}} - \frac{\Gamma}{2\pi i}\frac{1}{z_2 - \frac{1}{\overline{z_2}}}$$

The fixed point solution is obtained by setting $\frac{d\overline{z}_1}{dt} = 0$, $\frac{d\overline{z}_2}{dt} = 0$, which leads to the equations:

$$(r^2 - 1)^2 = 4r^2 y^2 \tag{1.1}$$

$$\frac{\Gamma}{2\pi} = \frac{(r^2 + 1)(r^2 - 1)^2}{r^5} \tag{1.2}$$

where $r^2 = x^2 + y^2$, ($x = x_1 = x_2$, $y = y_1 = -y_2$) is the distance between the point vortex and the center of the cylinder. While the first equation defines two lines of
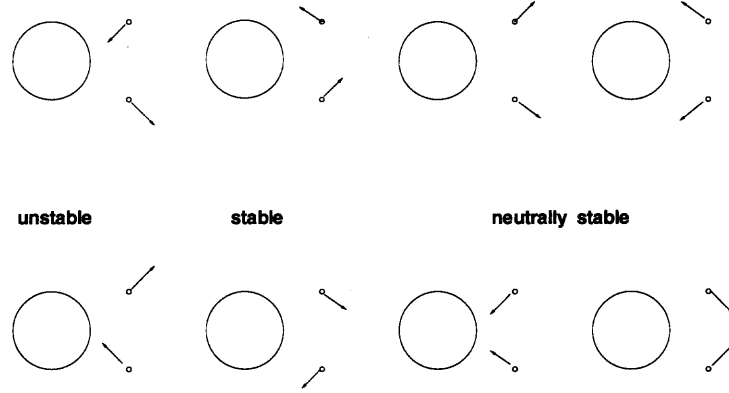
Figure 1.2 Stability of Foppl's model

fixed points, the second equation determines the circulation Γ of each pair of twin vortices in terms of their location in the plane.

Performing the linear stability analysis for the fixed points, we find the eigenvalues:

$$\lambda_{1,2}^2 = \frac{1}{r^{10}} - \frac{3}{r^8} + \frac{3}{r^6} + \frac{3}{r^4}$$

$$\lambda_{3,4}^2 = \frac{5}{r^{10}} - \frac{13}{r^8} - \frac{5}{r^6} - \frac{3}{r^4}$$

as a function of the location of each pair of fixed points. Since one of the eigenvalues $\lambda_{1,2}$ is always negative, and the other one positive, the fixed point is always unstable. Furthermore, by studying the expressions of the eigenvectors associated with the eigenvalues, we can show that the fixed point is neutrally stable to all symmetric perturbations, unstable to certain asymmetric perturbations and stable to other asymmetric perturbations (Tang & Aubry 1997). Figure 1.2 schematically reproduces the shape of the neutrally stable modes, that of the unstable mode and that of the stable one.

In a numerical simulation of the viscous flow from the Navier-Stokes equations, a small perturbation along the stable manifold was found to decay as time evolved

center   saddle point

$Re \ (\lambda^2){=}0$

neutrally stable

$Re \ (\lambda^2){>}0$
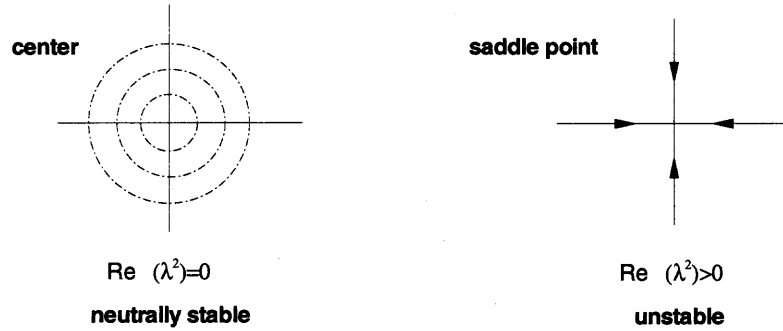
unstable

Figure 1.3 Eigenspaces of Foppl's model

while a small perturbation along the unstable manifold was observed to grow with time (Tang & Aubry 1997). The stability property of Foppl's model thus shows some connection to that of the real, viscous flow. In this thesis, we explore this connection further. Our technique consists in controlling the stability property of the potential model. Such technique will be tested in our numerical simulation of the viscous flow by integrating the full Navier-Stokes equations.

1.3 Objective and Control Strategy

The linear stability analysis of Foppl's model has shown that the steady twin vortices are dynamically unstable. It is therefore natural to wonder whether one can control the flow in the vicinity of the fixed point by keeping the orbit (in phase space) close to the stable eigenspace, and therefore, close to the fixed point.

The fixed point is actually a saddle point with a two-dimensional center eigenspace, a one-dimensional stable eigenspace, and a one-dimensional unstable eigenspace, see figure 1.3 for the eigenspaces of Foppl's model. Our idea is to keep the orbit close to the stable eigenspace by oscillating the cylinder vertically.

Before applying any control, the cylinder's surface can be expressed by the curve $r_0^2 - 1 = 0$. Our control technique will specifically aim at counteracting the motion of the vortices along the unstable eigenspace. Our goal is to find a displacement control function $\delta(t)$ which varies with time t in order to kill the instability along the unstable eigenspace, see figure 1.4. As the cylinder is displaced from the initial t_0, the zero normal velocity boundary condition needs to be satisfied at every time step. This is achieved by imposing a small vortex distribution $\Gamma_\epsilon(\gamma, t)$ on the cylinder surface.

It is well known that vortex shedding behind a free cylinder will cause oscillations of the cylinder which, in turn, will interact with the flow. Oscillations induced by vortex shedding is another area of active research and numerous contributions can be found in the literature (Bearman 1984, Brika & Laneville 1993, Blackburn& Henderson 1999). In this study, we concentrate on the active control of the unsteady lift by forced oscillations of the cylinder.

This thesis is organized as follows. In Chapter 2, we present our mathematical model and active feedback control system of Foppl's vortex model by means of a control function $\delta(t)$ representing the small displacement of the cylinder. In Chapter 3, we apply our control scheme to the real flow by numerically integrating the Navier-Stokes equations for the impulsively started flow past a cylinder. Finally, Chapter 4 will be dedicated to the analysis of a control system based on a symmetric deformation of the cylinder surface.

Solid line: Steady state circular cylinder at $t_0=0$

Dashed line: Cylinder surface after oscillation at time $t>0$

Oscillated cylinder

$-\Gamma$

U

$\delta(t)$

Original cylinder $r_0^2-1=0$

$+\Gamma$
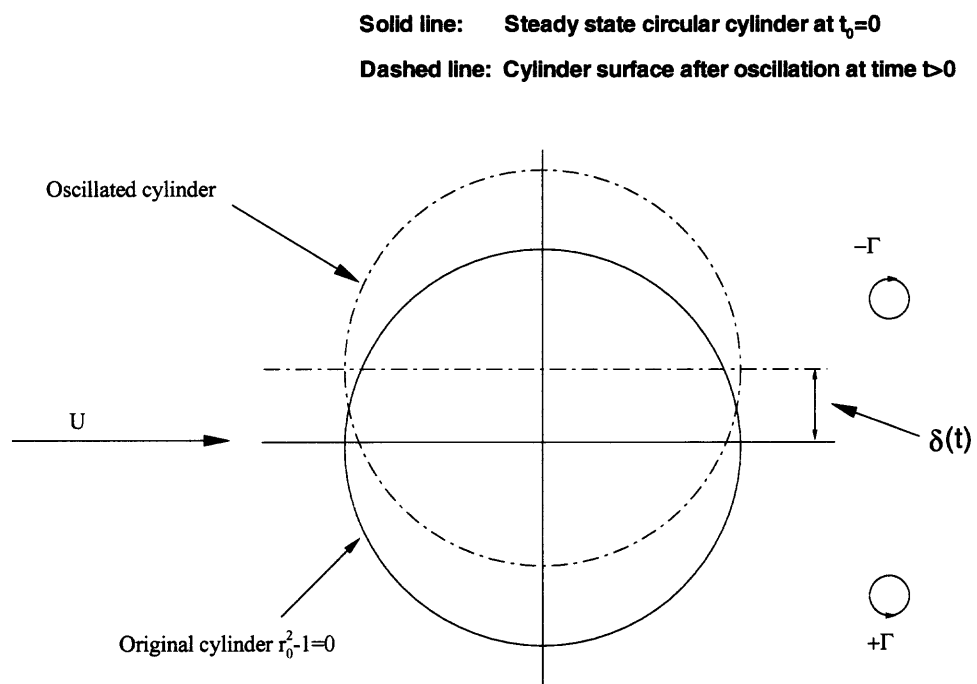
Figure 1.4 Control of the lift by oscillating the cylinder

CHAPTER 2

CONTROL OF FOPPL'S VORTICES BY FORCED OSCILLATIONS OF THE CYLINDER

2.1 Mathematical Model

In this chapter, we study to control the lift on the cylinder to be zero in the unsteady state. For this purpose, We displace the cylinder vertically by a distance $\delta(t)$ in order to cancel the life coefficient $C_L(t)$ at all time $t > 0$. The problem here is to determine $\delta(t)$ at each time *analytically* in order to reach this goal.

We now approach the previous problem by using the perturbation method and asymptotic expansion in order to enforce the boundary condition on the surface of the cylinder. We consider the incoming flow onto a body whose surface is given by the function $F(r, \gamma, t) = 0$ where (r, γ) define the position of the point in polar coordinates; for a displaced solid surface, the flow-tangency boundary condition is given by the equation:

$$\frac{DF}{Dt} = \frac{\partial F}{\partial t} + \vec{u} \cdot \nabla F = 0 \qquad (2.1)$$

at all points on the body surface $F(r, \gamma, t) = 0$. Here, $\vec{u}$ is the velocity at any point on the surface and the vector ∇F is normal to the body surface $F(r, \gamma, t) = 0$. In order for the boundary condition to be satisfied at any time t, a small vortex distribution $\Gamma_\epsilon(\gamma, t)$, where $\Gamma_\epsilon(\gamma, t) \ll 1$, is imposed on the boundary surface.

At the initial time $t = 0$, $r = r_0$, the solid surface is a circle with unit radius:

$$F(r_0, \gamma, 0) = r_0^2 - 1 = 0 \qquad (2.2)$$

Let $\delta(t)$ be a small displacement of the cylinder surface with respect to the initial circular cylinder $r_0 = 1$, see figure 2.1. The goal of our study is to find a

Solid line: Steady state circular cylinder at $t_0=0$

Dashed line: Cylinder surface after displacement at time $t>0$

$F(r, \gamma, t) = 0$

$-\Gamma \ (z_1{}'=x_1{}'+y_1{}'i)$

U

γ

$\delta(t)$

$r_0=1$

$+\Gamma \ (z_2{}'=x_2{}'+y_2{}'i)$
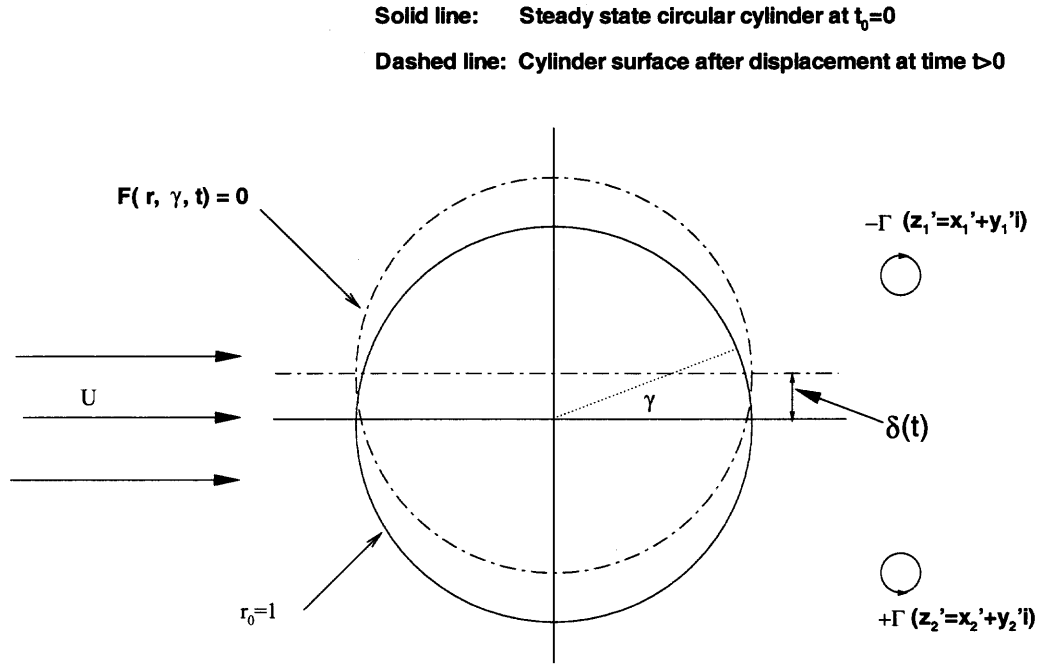
Figure 2.1 The displacement control function $\delta(t)$

function $\delta(t)$ which stabilizes the system. The small displacement of the cylinder $\delta(t)$ is thus our control function and we assume $\delta(t) \ll 1$, $\quad \frac{d\delta(t)}{dt} \ll 1$.

The velocity $\vec{u}$ at any point on the solid surface is the sum of the velocities induced by the free stream, the Foppl's vortices and the vortex distribution on the surface. It can then be written as:

$$\vec{u} = \vec{u}^U + \vec{u}^v + \vec{u}^c$$

where:

$\vec{u}^U$ is the velocity induced by the free-stream velocity $U = 1$.

$\vec{u}^v$ is the velocity induced by Foppl's vortices: Vortex 1 and Vortex 2.

$\vec{u}^c$ is the velocity induced by the vortex distribution $\Gamma_\epsilon(\gamma, t)$ on the surface, where the superscript 'c' represents the velocity induced by the control.

We can then rewrite equation (2.1) as:

$$\frac{\partial F}{\partial t} + (u_r^U + u_r^v + u_r^c)\frac{\partial F}{\partial r} + (u_\gamma^U + u_\gamma^v + u_\gamma^c)\frac{1}{r}\frac{\partial F}{\partial \gamma} = 0 \tag{2.3}$$

where the subscripts r and γ denote the radial and azimuthal components, respectively.

In the basic state, the point on the cylinder surface can be expressed as $(\cos\gamma, \sin\gamma)$ and the distance to the origin of the coordinates is $r_0 = 1$. When the cylinder displacement function $\delta(t)$ is applied, the cylinder moves in the vertical direction and a point on the cylinder surface is defined as $(\cos\gamma, \sin\gamma + \delta(t))$. For any point, this results in a change of the distance to the origin O of the coordinates (see figure 2.1). Denoting this change by $r_\epsilon(\gamma, t)$, we can write:

$$(r_0\cos\gamma)^2 + (r_0\sin\gamma + \delta(t))^2 = (r_0 + r_\epsilon(\gamma, t))^2 \tag{2.4}$$

Using the fact that in our control scheme the displacement function is very small, that is $\delta(t) \ll 1$, we can neglect the higher order term $(\delta(t))^2$ and write:

$$r_\epsilon(\gamma, t) = \sin\gamma\delta(t) \tag{2.5}$$

Recall that the basic state is one of the fixed points described by equations (1.1), (1.2) corresponding to the steady circular cylinder. In the more general model where the cylinder undergoes a displacement, the velocity at any point is composed of the zeroth order term corresponding to the basic state and the first order term induced by the small displacement. Generally, we have:

$$u_r = u_{r0} + u_{r1} \tag{2.6}$$

$$u_\gamma = u_{\gamma0} + u_{\gamma1} \tag{2.7}$$

We now introduce the function $F(r, \gamma, t)$ defining the displaced cylinder:

$$F(r, \gamma, t) = r - r_0 - r_\epsilon(\gamma, t) \tag{2.8}$$

This gives us the derivatives of F as follows:

$$\begin{aligned}
\frac{\partial F}{\partial t} &= -\frac{\partial r_\epsilon(\gamma, t)}{\partial t} = -\sin\gamma\frac{d\delta(t)}{dt}\\
\frac{\partial F}{\partial r} &= 1\\
\frac{\partial F}{\partial \gamma} &= -\frac{\partial r_\epsilon(\gamma, t)}{\partial \gamma} = -\cos\gamma\delta(t)
\end{aligned}$$

Substituting these derivatives and expression (2.6) (2.7) in equation (2.3) leads to:

$$-\sin\gamma\frac{d\delta(t)}{dt} + [(u_{r0}^U + u_{r1}^U) + (u_{r0}^v + u_{r1}^v) + (u_{r0}^c + u_{r1}^c)]$$
$$+[(u_{\gamma0}^U + u_{\gamma1}^U) + (u_{\gamma0}^v + u_{\gamma1}^v) + (u_{\gamma0}^c + u_{\gamma1}^c)]\frac{1}{r_0}(-\cos\gamma\delta(t)) = 0$$

where the indices 0 and 1 refer to zeroth order and first order terms respectively.

We notice that in the basic state, we do not apply our control scheme and the vortex distribution on the surface is zero. The vortex distribution function is therefore a first order term and $u_{r0}^c = u_{\gamma0}^c = 0$. Noticing that $\delta(t) \ll 1$, $\frac{d\delta(t)}{dt} \ll 1$, the first order term of the boundary condition becomes:

$$u_{r1}^U + u_{r1}^v + u_{r1}^c = \sin\gamma\frac{d\delta(t)}{dt} + (u_{\gamma0}^U + u_{\gamma0}^v)\cos\gamma\delta(t) \tag{2.9}$$

This is the theoretical boundary condition we obtain on the displaced cylinder surface $(\cos\gamma, \sin\gamma + \delta(t))$ at any time $t > 0$. In the next sections, we concentrate on finding appropriate expressions for the various velocity components $u_{\gamma0}^U$, $u_{\gamma0}^v$, u_{r1}^U, u_{r1}^v and u_{r1}^c.

2.2   Induced Velocity for a Point Located on the Displaced Surface

In this section, we consider any point on the displaced surface and calculate the velocity at that point. For this, we calculate the various induced velocities, that is the velocity induced by the incoming free stream U, that induced by the Foppl's vortices $\pm\Gamma$, and that induced by the vortex distribution $\Gamma_\epsilon(\gamma, t)$ on the cylinder surface (imposed by our control strategy). We carry out our analysis in polar coordinates.

2.2.1   Polar Coordinates

The location (x, y) of any point can be expressed in polar coordinates, that is:

$$x = r\cos\theta$$

$$y = r\sin\theta$$

$$z = re^{i\theta}$$

where $z(r, \theta)$ denotes the position (x, y) by complex variable $z = x + iy$. The relation between the velocity in polar coordinates and that in Cartesian coordinates is given by the rotation:

$$u_r = u_x\cos\theta + u_y\sin\theta \tag{2.10}$$

$$u_\theta = -u_x\sin\theta + u_y\cos\theta \tag{2.11}$$

Using the fact that $u_x = \frac{dx}{dt}$, $u_y = \frac{dy}{dt}$ and $\cos\theta + i\sin\theta = \frac{z}{r}$, we can write:

$$u_r - iu_\theta = \frac{d\bar{z}}{dt}\frac{z}{r} \tag{2.12}$$

or, equivalently,

$$u_r = \frac{1}{r}Re[\frac{d\bar{z}}{dt}z] \tag{2.13}$$

$$u_\theta = -\frac{1}{r}Im[\frac{d\bar{z}}{dt}z] \tag{2.14}$$

We now consider a small perturbation (ρ, α) to an arbitrary point $z(r, \theta)$, and denote the new position after perturbation by $z^{'}(r^{'}, \theta^{'})$, such that:

$$r^{'} = r + \rho$$

$$\theta^{'} = \theta + \alpha$$

Since we consider small perturbations only, i.e. $\rho \ll 1, \alpha \ll 1$, we can neglect high order terms and write:

$$
\begin{aligned}
z^{'} &= (r + \rho)e^{i(\theta + \alpha)} \\
&= (re^{i\theta} + \rho e^{i\theta})e^{i\alpha} \\
&= (z + \frac{\rho}{r}z)(1 + i\alpha) \\
&= z + z(\frac{\rho}{r} + i\alpha)
\end{aligned}
$$

This leads to the final expressions for the perturbed point $z^{'}$ and its complex conjugate $\overline{z'}$:

$$z^{'} = z + z(\frac{\rho}{r} + i\alpha) \tag{2.15}$$

$$\overline{z'} = \overline{z'} + \overline{z'}(\frac{\rho}{r} - i\alpha) \tag{2.16}$$

In the next sections, we use equations (2.12), (2.13), (2.14), (2.15), (2.16) in the calculation of the induced velocity at any arbitrary point on the displaced surface of the cylinder.

2.2.2 Velocity Induced by the Free Stream

Our control strategy will constantly compensate for any motion the flow undertakes away from zero lift. This compensation will be achieved by displacing the cylinder at any time accordingly. In this sense, the controlled flow is time dependent, i.e. unsteady. In the controlled regime, we consider an arbitrary point $z^{'}_0(r^{'}_0, \gamma)$ on the

surface $F(r, \gamma, t) = 0$. The unsteady flow can be treated as the superimposition of the steady flow and a small perturbation. The velocity induced by the free stream at any point $z'_0(r'_0, \gamma)$ can be obtained from the complex potential:

$$w(z'_0) = U(z'_0 - i\delta(t) + \frac{1}{z'_0 - i\delta(t)}) \tag{2.17}$$

and

$$\frac{d\overline{z'_0}}{dt} = \frac{dw}{dz'_0} = U(1 - \frac{1}{(z'_0 - i\delta(t))^2}) \tag{2.18}$$

where $\delta(t)$ is the displacement of the cylinder at any time t.

Using equations (2.12), (2.13), (2.14) from the previous section, we have:

$$u'_r - iu'_\gamma = \frac{d\overline{z'_0}}{dt}\frac{z'_0}{r'_0} = \frac{U}{r'_0}(z'_0 - \frac{z'_0}{(z'_0 - i\delta(t))^2})$$

or, equivalently:

$$u'_r(z'_0) = \frac{U}{r'_0}Re(z'_0 - \frac{1}{(z'_0 - i\delta(t))^2})$$

$$u'_\gamma(z'_0) = -\frac{U}{r'_0}Im(z'_0 - \frac{1}{(z'_0 - i\delta(t))^2})$$

The position of any material point on the surface of the cylinder can be written as:

$$z'_0 = z_0 + i\delta(t) \tag{2.19}$$

Using Taylor's series expansion and neglecting second and higher order terms, we now expand the unsteady velocity in terms of the leading order term (steady state) and the first order term, that is:

$$u'_r(z'_0) = u^U_{r0}(z_0) + u^U_{r1}(z_0)$$

$$u'_\gamma(z'_0) = u^U_{\gamma0}(z_0) + u^U_{\gamma1}(z_0)$$

where:

$$u_{r0}^{U}(z_0) = \frac{U}{r_0} Re(z_0 - \frac{1}{z_0})$$

$$u_{\gamma 0}^{U}(z_0) = -\frac{U}{r_0} Im(z_0 - \frac{1}{z_0})$$

$$u_{r1}^{U}(z_0) = -\frac{Ur_\epsilon}{r_0^2} Re(z_0 - \frac{1}{z_0}) + \frac{U}{r_0} Re(i\delta(t) - \frac{i\delta(t)}{z_0^2})$$

$$u_{\gamma 1}^{U}(z_0) = \frac{Ur_\epsilon}{r_0^2} Im(z_0 - \frac{1}{z_0}) - \frac{U}{r_0} Im(i\delta(t) - \frac{i\delta(t)}{z_0^2})$$

Since $U = 1$ and $r_0 = 1$, we write the velocity at any point on the displaced surface induced by the free stream as follows.

$$u_{r0}^{U} = 0 \qquad (2.20)$$

$$u_{\gamma 0}^{U}(\gamma) = -2\sin\gamma \qquad (2.21)$$

$$u_{r1}^{U}(\gamma, t) = -\sin 2\gamma \delta(t) \qquad (2.22)$$

$$u_{\gamma 1}^{U}(\gamma, t) = 0 \qquad (2.23)$$

We notice that here the zeroth order radial velocity $u_{r0}^{U} = 0$ actually reflects the normal boundary condition on the solid surface satisfied by the basic state.

2.2.3 Position of the Image Vortex Pair for the Displaced Cylinder

We know that for the cylinder whose center is located at the origin $(0,0)$ of the coordinates, the position of the image vortex corresponding to the point vortex located at $z = x + iy$ is $\frac{1}{\bar{z}}$.

We now consider the cylinder whose center is displaced and located at $(0, \delta(t))$. For the point vortex located at $z = x + iy$, we denote the position of the image vortex by $z^I = x^I + iy^I$. We then calculate this position and find, see figure 2.2:
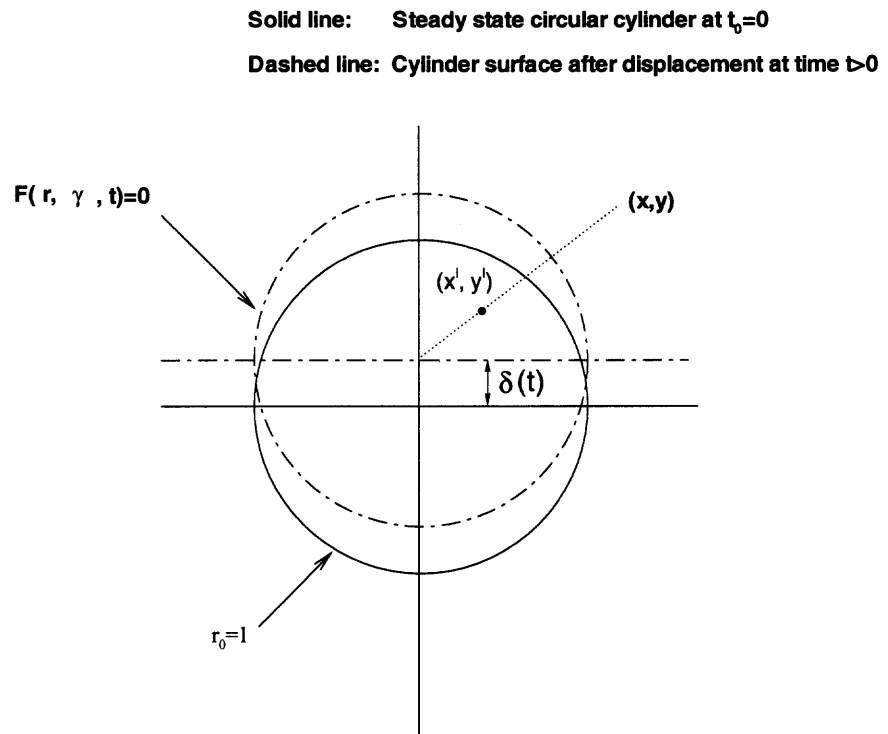
Figure 2.2 Position of image point (x^I, y^I) for point (x, y) after displacement of the cylinder

$$x^I = \frac{x}{x^2 + (y - \delta(t))^2}$$

$$y^I = \frac{y - \delta(t)}{x^2 + (y - \delta(t))^2} + \delta(t)$$

Our next goal is to linearize the position of the image vortex (x^I, y^I) in terms of the displacement function of the cylinder $\delta(t)$. For this purpose, we expand x^I, y^I, keep the first term in $\delta(t)$ and neglect the higher order term. This leads to:

$$x^I = \frac{x}{x^2 + y^2} + \frac{2xy}{(x^2 + y^2)^2}\delta(t)$$

$$y^I = \frac{y}{x^2 + y^2} + \frac{y^2 - x^2}{(x^2 + y^2)^2}\delta(t) + \delta(t)$$

We can write the linearized complex position in the form:

$$z^I = x^I + iy^I = \frac{1}{\bar{z}} + i\delta(t)(1 - \frac{1}{\bar{z}^2}) \tag{2.24}$$

This is the linearized position of the image vortex for the displaced cylinder whose center is at $(0, \delta(t))$. We will use this result in the next section.

2.2.4 Velocity Induced by Foppl's Vortices

We can calculate the velocity at the point z'_0 on the displaced surface induced by the two point vortices located at points z'_1, z'_2 and their images located at points z^I_1, z^I_2 in the controlled flow.

We now suppose that the positions of the two vortices in the basic state are $z_1(r_1, \theta_1)$, $z_2(r_2, \theta_2)$, respectively, and that we apply small perturbations (ρ_1, α_1), (ρ_2, α_2) to such positions such that ρ_1, $\rho_2 \ll 1$, θ_1, $\theta_2 \ll 1$. The new position of the vortices are defined by $z'_1(r'_1, \theta'_1)$, $z'_2(r'_2, \theta'_2)$, respectively, such that:

$$r'_1 = r_1 + \rho_1$$

$$\theta_1' = \theta_1 + \alpha_1$$

$$r_2' = r_2 + \rho_2$$

$$\theta_2' = \theta_2 + \alpha_2$$

Using complex variables, the flow dynamics induced by the point vortices at the point z_0' on the displaced surface is given by:

$$\frac{d\overline{z'}_0}{dt} = -\frac{\Gamma}{2\pi i}\frac{1}{z_0' - z_1'} + \frac{\Gamma}{2\pi i}\frac{1}{z_0' - z_1^I} + \frac{\Gamma}{2\pi i}\frac{1}{z_0' - z_2'} - \frac{\Gamma}{2\pi i}\frac{1}{z_0' - z_2^I}$$

where z_1^I, z_2^I are the linearized positions of the image vortices in the unsteady state corresponding to z_1', z_2', respectively. Recalling equation (2.12), we can deduce:

$$u_r^{'v}(z_0') - iu_\gamma^{'v}(z_0') = [-\frac{\Gamma}{2\pi i}\frac{1}{z_0' - z_1'} + \frac{\Gamma}{2\pi i}\frac{1}{z_0' - z_1^I} + \frac{\Gamma}{2\pi i}\frac{1}{z_0' - z_2'} - \frac{\Gamma}{2\pi i}\frac{1}{z_0' - z_2^I}]\frac{z_0'}{r_0'} \quad (2.25)$$

Using (2.15) and (2.24), we obtain the zeroth order and first order terms of all position variables in the unsteady state:

$$z_1' = z_1 + z_1(\frac{\rho_1}{r_1} + i\alpha_1) \quad (2.26)$$

$$z_2' = z_2 + z_2(\frac{\rho_1}{r_2} + i\alpha_2) \quad (2.27)$$

$$z_0' = z_0 + i\delta(t) \quad (2.28)$$

$$z_1^I = \frac{1}{\overline{z}_1} - \frac{1}{\overline{z}_1}(\frac{\rho_1}{r_1} - i\alpha_1) + i\delta(t)(1 - \frac{1}{\overline{z}_1^2}) \quad (2.29)$$

$$z_2^I = \frac{1}{\overline{z}_2} - \frac{1}{\overline{z}_2}(\frac{\rho_2}{r_2} - i\alpha_2) + i\delta(t)(1 - \frac{1}{\overline{z}_2^2}) \quad (2.30)$$

We express the unsteady velocity in terms of the zeroth order term (basic state) and the first order term, neglecting the higher order terms:

$$u_r^{'v}(z_0') = u_{r0}^v + u_{r1}^v$$

$$u_\gamma^{'v}(z_0') = u_{\gamma0}^v + u_{\gamma1}^v$$

We now expand (2.25) to obtain the expression of the velocity induced by Foppl's vortices, the details of our expansion are:

$$u_r^{'v}(z_0') - iu_\gamma^{'v}(z_0')$$

$$= [-\frac{\Gamma}{2\pi i}\frac{1}{(z_0' - z_1')} + \frac{\Gamma}{2\pi i}\frac{1}{(z_0' - z_1^I)} + \frac{\Gamma}{2\pi i}\frac{1}{(z_0' - z_2')} - \frac{\Gamma}{2\pi i}\frac{1}{(z_0' - z_2^I)}]\frac{z_0'}{r_0'}$$

$$= [-\frac{\Gamma}{2\pi i}\frac{(z_1\bar{z}_1 - 1)}{(z_0 - z_1)(z_0\bar{z}_1 - 1)} + \frac{\Gamma}{2\pi i}\frac{(z_2\bar{z}_2 - 1)}{(z_0 - z_2)(z_0\bar{z}_2 - 1)}]\frac{z_0}{r_0}$$

$$+\frac{i\delta(t)}{r_0}[-\frac{\Gamma}{2\pi i}\frac{(z_1\bar{z}_1 - 1)}{(z_0 - z_1)(z_0\bar{z}_1 - 1)} + \frac{\Gamma}{2\pi i}\frac{(z_2\bar{z}_2 - 1)}{(z_0 - z_2)(z_0\bar{z}_2 - 1)}]$$

$$-\frac{z_0\sin\gamma\delta(t)}{r_0^2}[-\frac{\Gamma}{2\pi i}\frac{(z_1\bar{z}_1 - 1)}{(z_0 - z_1)(z_0\bar{z}_1 - 1)} + \frac{\Gamma}{2\pi i}\frac{(z_2\bar{z}_2 - 1)}{(z_0 - z_2)(z_0\bar{z}_2 - 1)}]$$

$$+[\frac{\Gamma}{2\pi i}\frac{i\delta(t) - z_1(\frac{\rho_1}{r_1} + i\alpha_1)}{(z_0 - z_1)^2} - \frac{\Gamma}{2\pi i}\frac{\frac{1}{\bar{z}_1}(\frac{\rho_1}{r_1} - i\alpha_1) + i\delta(t)\frac{1}{\bar{z}_1^2}}{(z_0 - \frac{1}{\bar{z}_1})^2}$$

$$-\frac{\Gamma}{2\pi i}\frac{i\delta(t) - z_2(\frac{\rho_2}{r_2} + i\alpha_2)}{(z_0 - z_2)^2} + \frac{\Gamma}{2\pi i}\frac{\frac{1}{\bar{z}_2}(\frac{\rho_2}{r_2} - i\alpha_2) + i\delta(t)\frac{1}{\bar{z}_2^2}}{(z_0 - \frac{1}{\bar{z}_2})^2}]\frac{z_0}{r_0}$$

$$= \frac{1}{r_0}[\frac{\Gamma}{2\pi i}\frac{(r_1^2 - 1)}{r_{01}^2} - \frac{\Gamma}{2\pi i}\frac{(r_2^2 - 1)}{r_{02}^2}]$$

$$+\frac{1}{r_0}(i\cos\gamma\delta(t))[\frac{\Gamma}{2\pi i}\frac{(r_1^2 - 1)}{r_{01}^2} - \frac{\Gamma}{2\pi i}\frac{(r_2^2 - 1)}{r_{02}^2}]$$

$$+\frac{\Gamma}{2\pi i}[\frac{(i\delta(t) - z_1(\frac{\rho_1}{r_1} + i\alpha_1))(z_0\bar{z}_1 - 1)^2 - (\bar{z}_1(\frac{\rho_1}{r_1} - i\alpha_1) + i\delta(t))(z_0 - z_1)^2}{(z_0 - z_1)^2(z_0\bar{z}_1 - 1)^2}]\frac{z_0}{r_0}$$

$$-\frac{\Gamma}{2\pi i}[\frac{(i\delta(t) - z_2(\frac{\rho_2}{r_2} + i\alpha_2))(z_0\bar{z}_2 - 1)^2 - (\bar{z}_2(\frac{\rho_2}{r_2} - i\alpha_2) + i\delta(t))(z_0 - z_2)^2}{(z_0 - z_2)^2(z_0\bar{z}_2 - 1)^2}]\frac{z_0}{r_0}$$

$$= \frac{1}{r_0}\left[\frac{\Gamma}{2\pi i}\frac{(r_1^2-1)}{r_{01}^2} - \frac{\Gamma}{2\pi i}\frac{(r_2^2-1)}{r_{02}^2}\right]$$

$$+\left[\frac{\Gamma}{2\pi}\frac{(r_1^2-1)}{r_{01}^2} - \frac{\Gamma}{2\pi}\frac{(r_2^2-1)}{r_{02}^2}\right](\cos\gamma\delta(t))$$

$$-i\delta(t)\frac{\Gamma}{2\pi}\left[\frac{2\sin\gamma - 4r_1\sin\theta_1 - 2r_1^2\sin(\gamma-2\theta_1)}{r_{01}^4} - \frac{2\sin\gamma - 4r_2\sin\theta_2 - 2r_2^2\sin(\gamma-2\theta_2)}{r_{02}^4}\right]$$

$$-i\frac{\Gamma}{2\pi}\left[\frac{4r-2(r^2+1)\cos(\gamma-\theta_1)}{r_{01}^4}\rho_1 + \frac{2r(r^2-1)\sin(\gamma-\theta_1)}{r_{01}^4}\alpha_1\right]$$

$$+i\frac{\Gamma}{2\pi}\left[\frac{4r-2(r^2+1)\cos(\gamma-\theta_2)}{r_{02}^4}\rho_2 + \frac{2r(r^2-1)\sin(\gamma-\theta_2)}{r_{02}^4}\alpha_2\right]$$

where $r_{01} = |z_1 - z_0|$, r_{01} is the distance between Foppl's Vortex 1 and the cylinder surface in the basic state; $r_{02} = |z_2 - z_0|$, r_{02} is the distance between Foppl's Vortex 2 and the cylinder surface in the basic state; $r_1^2 = x_1^2 + y_1^2$, r_1 is the distance between Foppl's Vortex 1 and the center of the cylinder in the basic state; $r_2^2 = x_2^2 + y_2^2$, r_2 is the distance between Foppl's Vortex 2 and the center of the cylinder in the basic state. Since the two Foppl vortices are symmetric with respect to the center line of the cylinder: $r_1 = r_2$, we simplify the notation by setting $r = r_1 = r_2$.

Noticing that we are dealing with a unit circle $r_0 = 1$, we can write the zeroth and first order induced velocity components as follows.

$$u_{r0}^v = 0 \tag{2.31}$$

$$u_{\gamma 0}^v(\gamma) = \frac{\Gamma}{2\pi}(r^2-1)\left(\frac{1}{r_{01}^2} - \frac{1}{r_{02}^2}\right) \tag{2.32}$$

$$u_{r1}^v(\gamma,t) = \frac{\Gamma}{2\pi}(r^2-1)\left(\frac{1}{r_{01}^2} - \frac{1}{r_{02}^2}\right)\cos\gamma\delta(t) \tag{2.33}$$

$$u_{\gamma 1}^v(\gamma, t) = \delta(t)\frac{\Gamma}{2\pi}\left[\frac{2\sin\gamma - 4r\sin\theta_1 - 2r^2\sin(\gamma - 2\theta_1)}{r_{01}^4} - \frac{2\sin\gamma - 4r\sin\theta_2 - 2r^2\sin(\gamma - 2\theta_2)}{r_{02}^4}\right]$$

$$+\frac{\Gamma}{2\pi}(2)\left(\frac{2r - (r^2 + 1)\cos(\gamma - \theta_1)}{r_{01}^4}\rho_1 - \frac{2r - (r^2 + 1)\cos(\gamma - \theta_2)}{r_{02}^4}\rho_2\right) \tag{2.34}$$

$$+\frac{\Gamma}{2\pi}(r^2 - 1)(2)\left(\frac{r\sin(\gamma - \theta_1)}{r_{01}^4}\alpha_1 - \frac{r\sin(\gamma - \theta_2)}{r_{02}^4}\alpha_2\right)$$

These expressions give us the induced velocity at the point z_0' on the solid surface induced by the two point vortices and their images at time t. Here, the leading order radial velocity $u_{r0}^v = 0$ reflects the normal boundary condition on the solid surface satisfied by the basic state.

2.2.5 Velocity Induced by the Vortex Distribution along the Cylinder Surface

Since the basic state is unstable (saddle point), any perturbed orbit will drift away from the saddle point. While the lift of the basic state is zero, the motion of the solution along the perturbed orbit is accompanied by a deviation of the lift from zero. Such a deviation occurs also in the viscous flow as the flow drifts away from bubble of vortices in the regime where the latter is unstable. Our objective is to prevent any deviation of the lift from zero. In order to satisfy the no-slip normal boundary condition on the solid surface (2.1) at any time t, we place a small vortex distribution $\Gamma_\epsilon(\gamma, t)$ along the surface. The velocity at any point z_0' on the solid surface induced by the vortex distribution is given by the expression:

$$v_x(\gamma, t) = -\int_0^{2\pi}\frac{\Gamma_\epsilon(\tau, t)}{2\pi}\frac{y - y_{\Gamma_\epsilon}}{(x - x_{\Gamma_\epsilon})^2 + (y - y_{\Gamma_\epsilon})^2}d\tau$$

$$= -\int_0^{2\pi}\frac{\Gamma_\epsilon(\tau, t)}{2\pi}\frac{\sin\gamma - \sin\tau}{(\cos\gamma - \cos\tau)^2 + (\sin\gamma - \sin\tau)^2}d\tau$$

$$v_y(\gamma, t) = \int_0^{2\pi}\frac{\Gamma_\epsilon(\tau, t)}{2\pi}\frac{x - x_{\Gamma_\epsilon}}{(x - x_{\Gamma_\epsilon})^2 + (y - y_{\Gamma_\epsilon})^2}d\tau$$

$$= \int_0^{2\pi} \frac{\Gamma_\epsilon(\tau, t)}{2\pi} \frac{\cos\gamma - \cos\tau}{(\cos\gamma - \cos\tau)^2 + (\sin\gamma - \sin\tau)^2} d\tau.$$

Using the relation between polar coordinates and Cartesian coordinates (2.10) (2.11), we can write:

$$v_r^c(\gamma, t) = \int_0^{2\pi} \frac{\Gamma_\epsilon(\tau, t)}{2\pi} \frac{-(\sin\gamma - \sin\tau)\cos\gamma + (\cos\gamma - \cos\tau)\sin\gamma}{(\cos\gamma - \cos\tau)^2 + (\sin\gamma - \sin\tau)^2} d\tau$$

$$= \int_0^{2\pi} \frac{\Gamma_\epsilon(\tau, t)}{2\pi} \frac{\sin(\tau - \gamma)}{2(1 - \cos(\tau - \gamma))} d\tau$$

$$v_\gamma^c(\gamma, t) = \int_0^{2\pi} \frac{\Gamma_\epsilon(\tau, t)}{2\pi} \frac{(\sin\gamma - \sin\tau)\sin\gamma + (\cos\gamma - \cos\tau)\cos\gamma}{(\cos\gamma - \cos\tau)^2 + (\sin\gamma - \sin\tau)^2} d\tau$$

$$= \frac{1}{2} \int_0^{2\pi} \frac{\Gamma(\tau, t)}{2\pi} d\tau$$

Therefore, the velocity at a point on the solid surface induced by the vortex distribution can be expressed as:

$$v_r^c(\gamma, t) = \int_0^{2\pi} \frac{\Gamma_\epsilon(\tau, t)}{2\pi} \frac{\sin(\tau - \gamma)}{2(1 - \cos(\tau - \gamma))} d\tau \qquad (2.35)$$

$$v_\gamma^c(\gamma, t) = \frac{1}{2} \int_0^{2\pi} \frac{\Gamma_\epsilon(\tau, t)}{2\pi} d\tau \qquad (2.36)$$

We notice that the azimuthal velocity $v_\gamma^c(\gamma, t)$ at any point z_0' is dependent on time t only and independent of the angle γ. This shows that, at every point z_0' on the solid surface, the azimuthal velocity $v_\gamma^c(\gamma, t)$ is only a function of time t.

2.2.6 Vortex Distribution Function on the Cylinder Surface

Summarizing the previous results (2.31), (2.32), (2.33), (2.34), (2.35), (2.36), the various induced velocities at any point on the solid surface take the expressions:

$$u_{r0}^U(\gamma) = 0 \qquad (2.37)$$

$$u_{\gamma 0}^{U}(\gamma) = -2\sin\gamma \tag{2.38}$$

$$u_{r0}^{v}(\gamma) = 0 \tag{2.39}$$

$$u_{\gamma 0}^{v}(\gamma) = (r^2 - 1)\frac{\Gamma}{2\pi}(\frac{1}{r_{01}^2} - \frac{1}{r_{02}^2}) \tag{2.40}$$

$$u_{r1}^{U}(\gamma, t) = \sin 2\gamma\delta(t) \tag{2.41}$$

$$u_{\gamma 1}^{U}(\gamma, t) = -2\cos 2\gamma\delta(t) \tag{2.42}$$

$$u_{r1}^{v}(\gamma, t) = \frac{\Gamma}{2\pi}(r^2 - 1)(\frac{1}{r_{01}^2} - \frac{1}{r_{02}^2})\cos\gamma\delta(t) \tag{2.43}$$

$$u_{\gamma 1}^{v}(\gamma, t) = \delta(t)\frac{\Gamma}{2\pi}[\frac{2\sin\gamma - 4r\sin\theta_1 - 2r^2\sin(\gamma - 2\theta_1)}{r_{01}^4} - \frac{2\sin\gamma - 4r\sin\theta_2 - 2r^2\sin(\gamma - 2\theta_2)}{r_{02}^4}]$$

$$+\frac{\Gamma}{2\pi}(2)(\frac{2r - (r^2 + 1)\cos(\gamma - \theta_1)}{r_{01}^4}\rho_1 - \frac{2r - (r^2 + 1)\cos(\gamma - \theta_2)}{r_{02}^4}\rho_2) \tag{2.44}$$

$$+\frac{\Gamma}{2\pi}(r^2 - 1)(2)(\frac{r\sin(\gamma - \theta_1)}{r_{01}^4}\alpha_1 - \frac{r\sin(\gamma - \theta_2)}{r_{02}^4}\alpha_2)$$

$$u_{r1}^{c}(\gamma, t) = \int_0^{2\pi} \frac{\Gamma_\epsilon(\tau, t)}{2\pi}\frac{\sin(\tau - \gamma)}{2(1 - \cos(\tau - \gamma))}d\tau \tag{2.45}$$

$$u_{\gamma 1}^{c}(\gamma, t) = \frac{1}{2}\int_0^{2\pi} \frac{\Gamma_\epsilon(\tau, t)}{2\pi}d\tau \tag{2.46}$$

The zeroth order of the radial velocities $u_{r0}^{U} = 0$ and $u_{r0}^{v} = 0$ guarantees the no-slip normal boundary condition on the solid surface for the basic state.

We now return to the boundary condition on the cylinder surface (2.9). Substituting expressions (2.37)–(2.46) into this boundary condition for the controlled flow, we obtain the vortex distribution along the surface:

$$[-\sin 2\gamma\delta(t) + \frac{\Gamma}{2\pi}(r^2 - 1)(\frac{1}{r_{01}^2} - \frac{1}{r_{02}^2})\cos\gamma\delta(t)] + \int_0^{2\pi}\frac{\Gamma_\epsilon(\tau, t)}{2\pi}\frac{\sin(\tau - \gamma)}{2(1 - \cos(\tau - \gamma))}d\tau$$

$$= \sin\gamma\frac{d\delta(t)}{dt} + [-2\sin\gamma + \frac{\Gamma}{2\pi}(r^2 - 1)(\frac{1}{r_{01}^2} - \frac{1}{r_{02}^2})]\cos\gamma\delta(t)$$

which leads to the final expression:

$$\int_0^{2\pi}\frac{\Gamma_\epsilon(\tau, t)}{2\pi}\frac{\sin(\tau - \gamma)}{2(1 - \cos(\tau - \gamma))}d\tau = \sin\gamma\frac{d\delta(t)}{dt} \tag{2.47}$$

This is the vortex distribution function $\Gamma_\epsilon(\gamma, t)$ along the surface of the cylinder. The result of (2.47) is quite intuitive, as we now explain. Since we use the quasi-steady position of the image vortex, we know that the normal velocity at any point z_0' on the surface of the cylinder caused by the incoming flow U and the Foppl vortices $\pm\Gamma$ is identically zero. Therefore, the normal velocity at the location z_0' due to the motion of the cylinder $\sin\gamma\frac{d\delta(t)}{dt}$ is exactly equal to the normal velocity caused by the vortex distribution $\Gamma_\epsilon(\gamma, t)$.

We can see that the kernel of the integral (2.47) has a singularity at $\tau = \gamma$. The integral is therefore a Principal Value (P. V.) integral. However, by using a change of variable and Fourier series, we can see that the singularity at $\tau = \gamma$ is a removable singularity. We now seek a solution of $\Gamma_\epsilon(\gamma, t)$ in the form:

$$\Gamma_\epsilon(\gamma, t) = p(\gamma)\frac{d\delta(t)}{dt}$$

This gives us:

$$\int_0^{2\pi} \frac{p(\tau)}{2\pi} \frac{\sin(\tau - \gamma)}{2(1 - \cos(\tau - \gamma))} d\tau = \sin\gamma \tag{2.48}$$

We use Fourier series to solve this equation for $p(\gamma)$ and set:

$$p(\gamma) = \sum_{k=1}^{\infty} (a_k \cos k\gamma + b_k \sin k\gamma)$$

We now make a change of variable and set $\tau - \gamma = \theta$. In the new variable, the Fourier series becomes:

$$p(\tau) = \sum_{k=1}^{\infty} [(a_k \cos k\theta + b_k \sin k\theta) \cos k\gamma + (b_k \cos k\theta - a_k \sin k\theta) \sin k\gamma]$$

Now the left hand side of (2.48) can be expanded as:

$$\int_0^{2\pi} \frac{p(\tau)}{2\pi} \frac{\sin(\tau - \gamma)}{2(1 - \cos(\tau - \gamma))} d\tau$$

$$= \sum_{k=1}^{\infty} \left(\int_{-\gamma}^{2\pi-\gamma} \frac{a_k \cos k\theta + b_k \sin k\theta}{2\pi} \frac{\sin \theta}{2(1 - \cos \theta)} d\theta \right) \cos k\gamma$$

$$+ \sum_{k=1}^{\infty} \left(\int_{-\gamma}^{2\pi-\gamma} \frac{b_k \cos k\theta - a_k \sin k\theta}{2\pi} \frac{\sin \theta}{2(1 - \cos \theta)} d\theta \right) \sin k\gamma$$

$$= \sum_{k=1}^{\infty} \left(\int_{0}^{2\pi} \frac{a_k \cos k\theta + b_k \sin k\theta}{2\pi} \frac{\sin \theta}{2(1 - \cos \theta)} d\theta \right) \cos k\gamma$$

$$+ \sum_{k=1}^{\infty} \left(\int_{0}^{2\pi} \frac{b_k \cos k\theta - a_k \sin k\theta}{2\pi} \frac{\sin \theta}{2(1 - \cos \theta)} d\theta \right) \sin k\gamma$$

We notice here that:

$$\int_{0}^{2\pi} \frac{\cos k\theta}{2\pi} \frac{\sin \theta}{2(1 - \cos \theta)} d\theta = 0$$

Defining:

$$I_k = \int_{0}^{2\pi} \frac{\sin k\theta}{2\pi} \frac{\sin \theta}{2(1 - \cos \theta)} d\theta$$

We can write:

$$\int_{0}^{2\pi} \frac{p(\tau)}{2\pi} \frac{\sin(\tau - \gamma)}{2(1 - \cos(\tau - \gamma))} d\tau = \sum_{k=1}^{\infty} (b_k I_k) \cos k\gamma + \sum_{k=1}^{\infty} (-a_k I_k) \sin k\gamma$$

Comparing the two sides of equation (2.48), we have:

$$\int_{0}^{2\pi} \frac{p(\tau)}{2\pi} \frac{\sin(\tau - \gamma)}{2(1 - \cos(\tau - \gamma))} d\tau = \sum_{k=1}^{\infty} (b_k I_k) \cos k\gamma + \sum_{k=1}^{\infty} (-a_k I_k) \sin k\gamma$$

$$= \sin \gamma$$

This implies that:

$$b_k = 0, \qquad for \; k \geq 1$$

$$a_k = 0, \qquad for \; k \geq 2$$

$$a_1 = -\frac{1}{I_1}$$

where:

$$I_1 = \int_0^{2\pi} \frac{\sin\theta}{2\pi} \frac{\sin\theta}{2(1-\cos\theta)} d\theta = \frac{1}{2}.$$

This completes our findings. The solution for the vortex distribution function $\Gamma_\epsilon(\gamma, t)$ can be expressed as:

$$\Gamma_\epsilon(\gamma, t) = -2\cos\gamma \frac{d\delta(t)}{dt} \qquad (2.49)$$

We notice here that $\cos\gamma$ is an even function about γ, which implies that the vortex distribution function $\Gamma_\epsilon(\gamma, t)$ is also an even function. Hereafter, we say that $\Gamma_\epsilon(\gamma, t)$ is symmetricly distributed about γ.

The fact that the vortex distribution function $\Gamma_\epsilon(\gamma, t)$ is proportional to $\cos\gamma$ implies that the corresponding induced tangential velocity v_θ^ς given by equation (2.46) is zero. As it is well known, an ideal flow allows the flow to slip along the wall. For example, Foppl's model allows tangential slip along the cylinder surface as described in equation (2.40).

We should mention here that the previous solution is *one* solution and that there may be other solutions to the mathematical problem (2.47). The solution (2.49) does satisfy the normal no slip boundary condition on the surface of the cylinder, that is:

$$v_r = \sin\gamma \frac{d\delta(t)}{dt}$$

as well as the boundary condition at infinity, that is:

$$\lim_{r\to\infty} \vec{v}^c = 0$$

2.3 Control by Displacement of the Cylinder

2.3.1 Linearization of the Control System

We now derive our feedback control law. For this purpose, we consider the flow dynamics in its unsteady state at any time t. The point vortices $\pm\Gamma$ are perturbed from the fixed point locations at z_1, z_2 to the new positions z_1', z_2', and the material point on the surface of the cylinder is perturbed from z_0 to z_0'. The variables z_1^I, z_2^I denote the location of the image vortices with respect to the displaced cylinder $F(r, \gamma, t) = 0, t > 0$ in the unsteady state, corresponding to z_1', z_2'. In Cartesian coordinates, the complex potential of the system is:

$$
\begin{aligned}
w(z) &= z - i\delta(t) + \frac{1}{z - i\delta(t)} - \frac{\Gamma}{2\pi i}\frac{1}{z - z_1'} + \frac{\Gamma}{2\pi i}\frac{1}{z - z_1^I} + \frac{\Gamma}{2\pi i}\frac{1}{z - z_2'} - \frac{\Gamma}{2\pi i}\frac{1}{z - z_2^I} \\
&\quad + \frac{1}{2\pi i}\int_0^{2\pi} \Gamma_\epsilon(\gamma, t)\ln(z - z_0')d\gamma
\end{aligned}
$$

Here, $\Gamma_\epsilon(\gamma, t)$ is the vortex distribution on the cylinder surface $F(r, \gamma, t)$ imposed to satisfy the boundary condition of the cylinder surface in the unsteady state. The expression of $\Gamma_\epsilon(\gamma, t)$ has been obtained in (2.49). The dynamics of the point vortex model is then given by:

$$
\frac{d\overline{z'}_1}{dt} = 1 - \frac{1}{(z_1' - i\delta(t))^2} + \frac{\Gamma}{2\pi i}\frac{1}{z_1' - z_2'} + \frac{\Gamma}{2\pi i}\frac{1}{z_1' - z_1^I} - \frac{\Gamma}{2\pi i}\frac{1}{z_1' - z_2^I}
$$

$$
+ \frac{1}{2\pi i}\int_0^{2\pi}\frac{\Gamma_\epsilon(\gamma, t)}{z_1' - z_0'}d\gamma
$$

$$
\frac{d\overline{z'}_2}{dt} = 1 - \frac{1}{(z_2' - i\delta(t))^2} - \frac{\Gamma}{2\pi i}\frac{1}{z_2' - z_1'} + \frac{\Gamma}{2\pi i}\frac{1}{z_2' - z_1^I} - \frac{\Gamma}{2\pi i}\frac{1}{z_2' - z_2^I}
$$

$$
+ \frac{1}{2\pi i}\int_0^{2\pi}\frac{\Gamma_\epsilon(\gamma, t)}{z_2' - z_0'}d\gamma
$$

where the incoming free stream velocity is denoted by $U = 1$. Using equation (2.12), we can rewrite the above expressions in polar coordinates:

$$\frac{dr'_1}{dt} - ir'_1\frac{d\theta'_1}{dt} = \frac{1}{r'_1}[z'_1 - \frac{z'_1}{(z'_1 - i\delta(t))^2} + \frac{\Gamma}{2\pi i}\frac{z'_1}{z'_1 - z'_2} + \frac{\Gamma}{2\pi i}\frac{z'_1}{z'_1 - z^I_1} - \frac{\Gamma}{2\pi i}\frac{z'_1}{z'_1 - z^I_2}$$

$$+\frac{1}{2\pi i}\int_0^{2\pi}\frac{\Gamma_\epsilon(\gamma,t)z'_1}{z'_1 - z'_0}d\gamma]$$

$$\frac{dr'_2}{dt} - ir'_2\frac{d\theta'_2}{dt} = \frac{1}{r'_2}[z'_2 - \frac{z'_2}{(z'_2 - i\delta(t))^2} - \frac{\Gamma}{2\pi i}\frac{z'_2}{z'_2 - z'_1} + \frac{\Gamma}{2\pi i}\frac{z'_2}{z'_2 - z^I_1} - \frac{\Gamma}{2\pi i}\frac{z'_2}{z'_2 - z^I_2}$$

$$+\frac{1}{2\pi i}\int_0^{2\pi}\frac{\Gamma_\epsilon(\gamma,t)z'_2}{z'_2 - z'_0}d\gamma]$$

Here, we use the same notation (as in the previous section) to linearize the system with respect to the fixed point positions $z_1(r_1,\theta_1)$, $z_2(r_2,\theta_2)$ and the circular cylinder surface $z_0(r_0,\gamma)$. The positions of the vortices are perturbed by means of small disturbances (ρ_1,α_1), (ρ_2,α_2), where ρ_1, $\rho_2 \ll 1$, θ_1, $\theta_2 \ll 1$. The new positions of the point vortices after perturbation are defined by $z'_1(r'_1,\theta'_1)$. Using the results of the linearized new position after perturbation (2.26) (2.27) (2.28) (2.29) (2.30) in the previous section and substituting these expansions into the our control system equations, we have:

$$\frac{d\rho_1}{dt} = -\frac{\rho_1}{r_1^2}Re[z_1 - \frac{1}{z_1} + \frac{\Gamma}{2\pi i}\frac{z_1}{z_1 - z_2} + \frac{\Gamma}{2\pi i}\frac{1}{z_1\bar{z}_1 - 1} - \frac{\Gamma}{2\pi i}\frac{1}{z_1\bar{z}_2 - 1}]$$

$$+ \frac{1}{r_1}Re[z_1(\frac{\rho_1}{r_1} + i\alpha_1) + \frac{1}{z_1^2}z_1(\frac{\rho_1}{r_1} + i\alpha_1)$$

$$+ \frac{\Gamma}{2\pi i}(\frac{1}{z_1 - z_2}z_1(\frac{\rho_1}{r_1} + i\alpha_1) - \frac{z_1}{(z_1 - z_2)^2}(z_1(\frac{\rho_1}{r_1} + i\alpha_1) - z_2(\frac{\rho_2}{r_2} + i\alpha_2))$$

$$- \frac{\Gamma}{2\pi i}\frac{2r_1\rho_1}{(r_1^2 - 1)^2} + \frac{\Gamma}{2\pi i}\frac{1}{(z_1\bar{z}_2 - 1)^2}(z_1\bar{z}_2(\frac{\rho_1}{r_1} + i\alpha_1) + z_1\bar{z}_2(\frac{\rho_2}{r_2} - i\alpha_2))]$$

$$+ \ \frac{1}{r_1} Re[-\frac{2i}{z_1^2} + \frac{\Gamma}{2\pi} z_1 (\frac{\overline{z}_1^2 - 1}{(r_1^2 - 1)^2} - \frac{\overline{z}_2^2 - 1}{(z_1\overline{z}_2 - 1)^2})]\delta(t)$$

$$+ \ \frac{1}{r_1} Re[\int_0^{2\pi} \frac{\Gamma_\epsilon(\gamma, t)}{2\pi i} \frac{z_1}{z_1 - z_0} d\gamma]$$

$$\frac{d\alpha_1}{dt} \ = \ \frac{2\rho_1}{r_1^3} Im[z_1 - \frac{1}{z_1} + \frac{\Gamma}{2\pi i} \frac{z_1}{z_1 - z_2} + \frac{\Gamma}{2\pi i} \frac{1}{z_1\overline{z}_1 - 1} - \frac{\Gamma}{2\pi i} \frac{1}{z_1\overline{z}_2 - 1}]$$

$$- \ \frac{1}{r_1^2} Im[z_1(\frac{\rho_1}{r_1} + i\alpha_1) + \frac{1}{z_1^2} z_1(\frac{\rho_1}{r_1} + i\alpha_1)$$

$$+ \ \frac{\Gamma}{2\pi i} (\frac{1}{z_1 - z_2} z_1(\frac{\rho_1}{r_1} + i\alpha_1) - \frac{z_1}{(z_1 - z_2)^2}(z_1(\frac{\rho_1}{r_1} + i\alpha_1) - z_2(\frac{\rho_2}{r_2} + i\alpha_2))$$

$$- \ \frac{\Gamma}{2\pi i} \frac{2r_1\rho_1}{(r_1^2 - 1)^2} + \frac{\Gamma}{2\pi i} \frac{1}{(z_1\overline{z}_2 - 1)^2}(z_1\overline{z}_2(\frac{\rho_1}{r_1} + i\alpha_1) + z_1\overline{z}_2(\frac{\rho_2}{r_2} - i\alpha_2))]$$

$$- \ \frac{1}{r_1^2} Im[-\frac{2i}{z_1^2} + \frac{\Gamma}{2\pi} z_1 (\frac{\overline{z}_1^2 - 1}{(r_1^2 - 1)^2} - \frac{\overline{z}_2^2 - 1}{(z_1\overline{z}_2 - 1)^2})]\delta(t)$$

$$- \ \frac{1}{r_1^2} Im[\int_0^{2\pi} \frac{\Gamma_\epsilon(\gamma, t)}{2\pi i} \frac{z_1}{z_1 - z_0} d\gamma]$$

$$\frac{d\rho_2}{dt} \ = \ -\frac{\rho_2}{r_2^2} Re[z_2 - \frac{1}{z_2} - \frac{\Gamma}{2\pi i} \frac{z_2}{z_2 - z_1} + \frac{\Gamma}{2\pi i} \frac{1}{z_2\overline{z}_1 - 1} - \frac{\Gamma}{2\pi i} \frac{1}{z_2\overline{z}_2 - 1}]$$

$$+ \ \frac{1}{r_2} Re[z_2(\frac{\rho_2}{r_2} + i\alpha_2) + \frac{1}{z_2^2} z_2(\frac{\rho_2}{r_2} + i\alpha_2)$$

$$- \ \frac{\Gamma}{2\pi i} (\frac{1}{z_2 - z_1} z_2(\frac{\rho_2}{r_2} + i\alpha_2) - \frac{z_2}{(z_2 - z_1)^2}(z_2(\frac{\rho_2}{r_2} + i\alpha_2) - z_1(\frac{\rho_1}{r_1} + i\alpha_1))$$

$$- \ \frac{\Gamma}{2\pi i} \frac{1}{(z_2\overline{z}_1 - 1)^2}(z_2\overline{z}_1(\frac{\rho_2}{r_2} + i\alpha_2) + z_2\overline{z}_1(\frac{\rho_1}{r_1} - i\alpha_1)) + \frac{\Gamma}{2\pi i} \frac{2r_2\rho_2}{(r_2^2 - 1)^2}]$$

$$+ \quad \frac{1}{r_2} Re[-\frac{2i}{z_1^2} + \frac{\Gamma}{2\pi} z_2 (\frac{\bar{z}_1^2 - 1}{(z_2 \bar{z}_1 - 1)^2} - \frac{\bar{z}_2^2 - 1}{(r_2^2 - 1)^2})] \delta(t)$$

$$+ \quad \frac{1}{r_2} Re[\int_0^{2\pi} \frac{\Gamma_\epsilon(\gamma, t)}{2\pi i} \frac{z_2}{z_2 - z_0} d\gamma]$$

$$\frac{d\alpha_2}{dt} = \frac{2\rho_2}{r_2^3} Im[z_2 - \frac{1}{z_2} - \frac{\Gamma}{2\pi i} \frac{z_2}{z_2 - z_1} + \frac{\Gamma}{2\pi i} \frac{1}{z_2 \bar{z}_1 - 1} - \frac{\Gamma}{2\pi i} \frac{1}{z_2 \bar{z}_2 - 1}]$$

$$- \quad \frac{1}{r_2^2} Im[z_2 (\frac{\rho_2}{r_2} + i\alpha_2) + \frac{1}{z_2^2} z_2 (\frac{\rho_2}{r_2} + i\alpha_2)$$

$$- \quad \frac{\Gamma}{2\pi i} (\frac{1}{z_2 - z_1} z_2 (\frac{\rho_2}{r_2} + i\alpha_2) - \frac{z_2}{(z_2 - z_1)^2} (z_2 (\frac{\rho_2}{r_2} + i\alpha_2) - z_1 (\frac{\rho_1}{r_1} + i\alpha_1))$$

$$- \quad \frac{\Gamma}{2\pi i} \frac{1}{(z_2 \bar{z}_1 - 1)^2} (z_2 \bar{z}_1 (\frac{\rho_2}{r_2} + i\alpha_2) + z_2 \bar{z}_1 (\frac{\rho_1}{r_1} - i\alpha_1)) + \frac{\Gamma}{2\pi i} \frac{2r_2 \rho_2}{(r_2^2 - 1)^2}]$$

$$- \quad \frac{1}{r_2^2} Im[-\frac{2i}{z_1^2} + \frac{\Gamma}{2\pi} z_2 (\frac{\bar{z}_1^2 - 1}{(z_2 \bar{z}_1 - 1)^2} - \frac{\bar{z}_2^2 - 1}{(r_2^2 - 1)^2})] \delta(t)$$

$$- \quad \frac{1}{r_2^2} Im[\int_0^{2\pi} \frac{\Gamma_\epsilon(\gamma, t)}{2\pi i} \frac{z_2}{z_2 - z_0} d\gamma]$$

We now proceed by adding and subtracting the equations of motion for the two vortices. In doing so, we use the fact that the vortices are symmetrically located with respect to the x-axis in the basic state, that is $z_1 = \bar{z}_2$, and that:

$$Re[f(z)] = Re[\overline{f(z)}]$$

$$Im[f(z)] = -Im[\overline{f(z)}]$$

Our manipulation leads to:

$$\frac{d(\rho_1 + \rho_2)}{dt} = \frac{1}{r} Re[(z_1 + \frac{1}{z_1} + \frac{\Gamma}{2\pi i} \frac{2z_1^2}{(z_1^2 - 1)^2})(\frac{\rho_1 + \rho_2}{r} + i(\alpha_1 - \alpha_2))]$$

$$- \frac{1}{r} \frac{\Gamma}{2\pi} \frac{2r^2}{(z_1 - z_2)^2} (\alpha_1 - \alpha_2)$$

$$+ \frac{1}{2\pi} \int_0^{2\pi} \Gamma_\epsilon(\gamma, t) \left(\frac{\sin(\gamma - \theta_1)}{r_{01}^2} + \frac{\sin(\gamma - \theta_2)}{r_{02}^2} \right) d\gamma$$

$$\frac{d(\alpha_1 - \alpha_2)}{dt} = -\frac{1}{r^2} Im[(z_1 + \frac{1}{z_1} + \frac{\Gamma}{2\pi i} \frac{2z_1^2}{(z_1^2 - 1)^2})(\frac{\rho_1 + \rho_2}{r} + i(\alpha_1 - \alpha_2))]$$

$$- \frac{1}{r^2} \frac{\Gamma}{2\pi} \frac{2r}{(r^2 - 1)^2} (\rho_1 + \rho_2)$$

$$+ \frac{1}{2\pi r} \int_0^{2\pi} \Gamma_\epsilon(\gamma, t) \left(\frac{r - \cos(\gamma - \theta_1)}{r_{01}^2} - \frac{r - \cos(\gamma - \theta_2)}{r_{02}^2} \right) d\gamma$$

$$\frac{d(\rho_1 - \rho_2)}{dt} = \frac{1}{r} Re[(z_1 + \frac{1}{z_1})(\frac{\rho_1 - \rho_2}{r} + i(\alpha_1 + \alpha_2))]$$

$$+ \frac{1}{r} Re[-\frac{4i}{z_1^2} + \frac{\Gamma}{2\pi} 2z_1 (\frac{\overline{z}_1^2 - 1}{(r^2 - 1)^2} - \frac{1}{z_1^2 - 1})]\delta(t)$$

$$+ \frac{1}{2\pi} \int_0^{2\pi} \Gamma_\epsilon(\gamma, t) \left(\frac{\sin(\gamma - \theta_1)}{r_{01}^2} - \frac{\sin(\gamma - \theta_2)}{r_{02}^2} \right) d\gamma$$

$$\frac{d(\alpha_1 + \alpha_2)}{dt} = -\frac{1}{r^2} Im[(z_1 + \frac{1}{z_1})(\frac{\rho_1 - \rho_2}{r} + i(\alpha_1 + \alpha_2))]$$

$$- \frac{1}{r^2} \frac{\Gamma}{2\pi} (\frac{2r}{(r^2 - 1)^2} - \frac{2r}{(z_1 - z_2)^2})(\rho_1 - \rho_2)$$

$$- \frac{1}{r^2} Im[-\frac{4i}{z_1^2} + \frac{\Gamma}{2\pi} 2z_1 (\frac{\overline{z}_1^2 - 1}{(r^2 - 1)^2} - \frac{1}{z_1^2 - 1})]\delta(t)$$

$$+ \frac{1}{2\pi r} \int_0^{2\pi} \Gamma_\epsilon(\gamma, t) \left(\frac{r - \cos(\gamma - \theta_1)}{r_{01}^2} + \frac{r - \cos(\gamma - \theta_2)}{r_{02}^2} \right) d\gamma.$$

We now introduce the following symmetric and asymmetric modes:

$$
\begin{aligned}
\rho_S &= \rho_1 + \rho_2 \\
\alpha_S &= \alpha_1 - \alpha_2 \\
\rho_A &= \rho_1 - \rho_2 \\
\alpha_A &= \alpha_1 + \alpha_2
\end{aligned}
$$

where the subscript 'S' refers to the symmetric mode, and the subscript 'A' denotes the antisymmetric mode.

For convenience of calculation, we define the real parts, $A(r)$, $B(r)$ and imaginary parts, $C(r)$, $D(r)$ which are all functions of the position of the fixed point r for the two complex-variable functions in the previous expressions, such that:

$$
\begin{aligned}
A(r) + B(r)i &= z_1 + \frac{1}{z_1} + \frac{\Gamma}{2\pi i} \frac{2z_1^2}{(z_1^2 - 1)^2} \\
C(r) + D(r)i &= z_1 + \frac{1}{z_1}
\end{aligned}
$$

Using the fixed point equations (1.1), (1.2), we obtain:

$$
r^4 + 1 - 2r^2 \cos 2\theta = \frac{(r^2 - 1)^2 (r^2 + 1)}{r^2}
$$

We can deduce the functions $A(r)$, $B(r)$, $C(r)$, $D(r)$ taking the form:

$$
A(r) = \left(r + \frac{1}{r}\right) \cos \theta - \frac{2}{r} \cos \theta \tag{2.50}
$$

$$
B(r) = \left(r - \frac{1}{r}\right) \sin \theta + \frac{1 - r^2}{r^3} \tag{2.51}
$$

$$
C(r) = \left(r + \frac{1}{r}\right) \cos \theta \tag{2.52}
$$

$$
D(r) = \left(r - \frac{1}{r}\right) \sin \theta \tag{2.53}
$$

Here, the angles are identical, i.e. $\theta = \theta_1 = -\theta_2$, due to the symmetry of two fixed points $z_1 = \overline{z_2}$.

Using the above results, we deduce the linearized control system:

$$
\frac{d\rho_S}{dt} = \frac{1}{r}(\frac{A}{r}\rho_S - B\alpha_S) - \frac{1}{r}\frac{\Gamma}{2\pi}\frac{2r^2}{(z_1 - z_2)^2}\alpha_S
$$

$$
+ \frac{1}{2\pi}\int_0^{2\pi}\Gamma_\epsilon(\gamma, t)(\frac{\sin(\gamma - \theta_1)}{r_{01}^2} + \frac{\sin(\gamma - \theta_2)}{r_{02}^2})d\gamma
$$

$$
\frac{d\alpha_S}{dt} = -\frac{1}{r^2}(\frac{B}{r}\rho_S + A\alpha_S) - \frac{1}{r^2}\frac{\Gamma}{2\pi}\frac{2r}{(r^2 - 1)^2}\rho_S
$$

$$
- \frac{1}{2\pi r}\int_0^{2\pi}\Gamma_\epsilon(\gamma, t)(\frac{r - \cos(\gamma - \theta_1)}{r_{01}^2} - \frac{r - \cos(\gamma - \theta_2)}{r_{02}^2})d\gamma
$$

$$
\frac{d\rho_A}{dt} = \frac{1}{r}(\frac{C}{r}\rho_A - D\alpha_A)
$$

$$
+ \frac{1}{r}Re[-\frac{4i}{z_1^2} + \frac{\Gamma}{2\pi}2z_1(\frac{\bar{z}_1^2 - 1}{(r^2 - 1)^2} - \frac{1}{z_1^2 - 1})]\delta(t)
$$

$$
+ \frac{1}{2\pi}\int_0^{2\pi}\Gamma_\epsilon(\gamma, t)(\frac{\sin(\gamma - \theta_1)}{r_{01}^2} - \frac{\sin(\gamma - \theta_2)}{r_{02}^2})d\gamma
$$

$$
\frac{d\alpha_A}{dt} = -\frac{1}{r^2}(\frac{D}{r}\rho_A + C\alpha_A) - \frac{1}{r^2}\frac{\Gamma}{2\pi}(\frac{2r}{(r^2 - 1)^2} - \frac{2r}{(z_1 - z_2)^2})\rho_A
$$

$$
- \frac{1}{r^2}Im[-\frac{4i}{z_1^2} + \frac{\Gamma}{2\pi}2z_1(\frac{\bar{z}_1^2 - 1}{(r^2 - 1)^2} - \frac{1}{z_1^2 - 1})]\delta(t)
$$

$$
- \frac{1}{2\pi r}\int_0^{2\pi}\Gamma_\epsilon(\gamma, t)(\frac{r - \cos(\gamma - \theta_1)}{r_{01}^2} + \frac{r - \cos(\gamma - \theta_2)}{r_{02}^2})d\gamma
$$

We recall the expression (2.49) for the vortex distribution function $\Gamma_\epsilon(\gamma, t)$ on the cylinder surface and notice that:

$$\frac{1}{2\pi}\int_0^{2\pi}\cos\gamma\left(\frac{\sin(\gamma-\theta_1)}{r_{01}^2}+\frac{\sin(\gamma-\theta_2)}{r_{02}^2}\right)d\gamma=0$$

$$\frac{1}{2\pi r}\int_0^{2\pi}\cos\gamma\left(\frac{r-\cos(\gamma-\theta_1)}{r_{01}^2}-\frac{r-\cos(\gamma-\theta_2)}{r_{02}^2}\right)d\gamma=0.$$

We now define:

$$P_3 \;=\; \frac{1}{2\pi}\int_0^{2\pi}(-2\cos\gamma)\left(\frac{\sin(\gamma-\theta_1)}{r_{01}^2}-\frac{\sin(\gamma-\theta_2)}{r_{02}^2}\right)d\gamma$$

$$P_4 \;=\; \frac{1}{2\pi r}\int_0^{2\pi}(-2\cos\gamma)\left(\frac{r-\cos(\gamma-\theta_1)}{r_{01}^2}+\frac{r-\cos(\gamma-\theta_2)}{r_{02}^2}\right)d\gamma$$

$$Q_3 \;=\; \frac{1}{r}Re\left[-\frac{4i}{z_1^2}+\frac{\Gamma}{2\pi}2z_1\left(\frac{\bar{z}_1^2-1}{(r^2-1)^2}-\frac{1}{z_1^2-1}\right)\right]$$

$$\;=\; \frac{1}{r}\left[-\frac{4\sin 2\theta}{r^2}+\frac{\Gamma}{2\pi}(2)r(r^2-1)\cos\theta\left(\frac{1}{(r^2-1)^2}-\frac{1}{r^4+1-2r^2\cos 2\theta}\right)\right]$$

$$Q_4 \;=\; -\frac{1}{r^2}Im\left[-\frac{4i}{z_1^2}+\frac{\Gamma}{2\pi}2z_1\left(\frac{\bar{z}_1^2-1}{(r^2-1)^2}-\frac{1}{z_1^2-1}\right)\right]$$

$$\;=\; \frac{1}{r^2}\left[\frac{4\cos 2\theta}{r^2}+\frac{\Gamma}{2\pi}(2)r(r^2+1)\sin\theta\left(\frac{1}{(r^2-1)^2}-\frac{1}{r^4+1-2r^2\cos 2\theta}\right)\right]$$

The control system for the symmetric mode and asymmetric mode takes the following matrix form.

Symmetric mode:

$$\frac{\partial}{\partial t}\begin{bmatrix}\rho_S\\[2mm]\alpha_S\end{bmatrix}=\begin{bmatrix}\dfrac{A}{r^2} & -\dfrac{B}{r}-\dfrac{\Gamma}{2\pi}\dfrac{2r}{(z_1-z_2)^2}\\[4mm] -\dfrac{B}{r^3}-\dfrac{\Gamma}{2\pi}\dfrac{2}{r(r^2-1)^2} & -\dfrac{A}{r^2}\end{bmatrix}\begin{bmatrix}\rho_S\\[2mm]\alpha_S\end{bmatrix}$$

Asymmetric mode:

$$
\frac{\partial}{\partial t}
\begin{bmatrix} \rho_A \\ \alpha_A \end{bmatrix}
=
\begin{bmatrix}
\frac{C}{r^2} & -\frac{D}{r} \\
-\frac{D}{r^3} + \frac{\Gamma}{2\pi}\frac{2}{r(r^2-1)} & -\frac{C}{r^2}
\end{bmatrix}
\begin{bmatrix} \rho_A \\ \alpha_A \end{bmatrix}
+
\begin{bmatrix} P_3 & Q_3 \\ P_4 & Q_4 \end{bmatrix}
\begin{bmatrix} \frac{d\delta(t)}{dt} \\ \delta(t) \end{bmatrix}
$$

We can see here that our control technique has no effect on the center eigenspace, and that the displacement function $\delta(t)$ only modifies the stable/unstable subspace. We will solve this dynamical system numerically and give the expression of the eigenvalues corresponding to the asymmetric mode in the next subsection.

In the basic state, this system simplifies since there is no displacement of the cylinder, i.e. $\delta(t) = 0$, $\frac{d\delta(t)}{dt} = 0$. In this case, the system can be written in the more compact form:

$$
\frac{\partial}{\partial t}
\begin{bmatrix} \rho_S \\ \alpha_S \end{bmatrix}
=
\begin{bmatrix}
\frac{A}{r^2} & -\frac{B}{r} - \frac{\Gamma}{2\pi}\frac{2r}{(z_1-z_2)^2} \\
-\frac{B}{r^3} - \frac{\Gamma}{2\pi}\frac{2}{r(r^2-1)^2} & -\frac{A}{r^2}
\end{bmatrix}
\begin{bmatrix} \rho_S \\ \alpha_S \end{bmatrix}
$$

$$
\frac{\partial}{\partial t}
\begin{bmatrix} \rho_A \\ \alpha_A \end{bmatrix}
=
\begin{bmatrix}
\frac{C}{r^2} & -\frac{D}{r} \\
-\frac{D}{r^3} + \frac{\Gamma}{2\pi}\frac{2}{r(r^2-1)} & -\frac{C}{r^2}
\end{bmatrix}
\begin{bmatrix} \rho_A \\ \alpha_A \end{bmatrix}
$$

We now calculate the eigenvalues of the previous Jacobian matrices and obtain:

$$
\lambda_{1,2}^2 = \frac{A^2 + B^2}{r^4} + \frac{2B}{r^2}\frac{\Gamma}{2\pi}\left[\frac{1}{(z_1 - z_2)^2} + \frac{1}{(r^2 - 1)^2}\right] + \left(\frac{\Gamma}{2\pi}\right)^2\frac{4}{(r^2 - 1)^2(z_1 - z_2)^2}
$$

$$
= \frac{1}{r^{10}}(-3r^6 - 5r^4 - 13r^2 + 5) < 0
$$

$$
\lambda_{3,4}^2 = \frac{C^2 + D^2}{r^4} - \frac{2D}{r^2(r^2 - 1)}\frac{\Gamma}{2\pi}
$$

$$
= \frac{1}{r^{10}}(3r^6 + 3r^4 - 3r^2 + 1) > 0.
$$

Here, we recover the stability results for the basic state obtained in Chapter 1, which shows that the fixed point is a saddle point, with a two-dimensional center eigenspace and a two-dimensional stable/unstable eigenspace.

2.3.2 Pressure Distribution on the Solid Surface

In the following, we design our feedback control algorithm to control the lift of the cylinder at anytime $t > 0$ based on the pressure distribution on the solid surface.

We now perform an analysis for the pressure distribution on the solid surface similar to that previously performed for induced velocities. In other words, we decompose the pressure in terms of a basic state (zeroth order term) and a small first order perturbation. In the following, we work with the pressure coefficient, that is

$$
\begin{aligned}
C_p &= \frac{p - p_\infty}{\frac{1}{2}\rho U_\infty^2} \\
&= \frac{\frac{1}{2}\rho U_\infty^2 - \frac{1}{2}\rho v^2}{\frac{1}{2}\rho U_\infty^2} \\
&= 1 - \frac{(v_{r0} + v_{r1})^2 + (v_{\gamma 0} + v_{\gamma 1})^2}{U_\infty^2} \\
&= 1 - \frac{v_{\gamma 0}^2 + 2 v_{\gamma 0} v_{\gamma 1}}{U_\infty^2}
\end{aligned}
$$

In the above derivation, we have used the fact that the normal velocity on the cylinder surface vanishes at all times $t > 0$ in the basic state. Neglecting the second order terms v_{r1}^2, $v_{\gamma 1}^2$, we obtain the leading order (steady state) and first order pressure coefficient terms:

$$
C_{p0}(\gamma) = 1 - \frac{v_{\gamma 0}^2}{U_\infty^2} \tag{2.54}
$$

$$
C_{p1}(\gamma) = -\frac{2 v_{\gamma 0} v_{\gamma 1}}{U_\infty^2} \tag{2.55}
$$

We recall expression (2.49) that the small vortex distribution on the cylinder surface $\Gamma_\epsilon(\gamma, t)$ is a periodic function about γ which gives us:

$$u_{\gamma 1}^c(\gamma, t) = \frac{1}{2} \int_0^{2\pi} \frac{\Gamma_\epsilon(\tau, t)}{2\pi} d\tau = 0$$

We use the azimuthal induced velocities results in (2.38), (2.40), (2.42), (2.44), (2.46) and calculate the first two terms of the pressure coefficient for a point (r_0', γ) on the surface of the cylinder:

$$C_{p0}(\gamma) = 1 - [2\sin\gamma - \frac{\Gamma}{2\pi}(r^2 - 1)(\frac{1}{r_{01}^2} - \frac{1}{r_{02}^2})]^2 \tag{2.56}$$

$$C_{p1}(\gamma) = 2[2\sin\gamma - \frac{\Gamma}{2\pi}(r^2 - 1)(\frac{1}{r_{01}^2} - \frac{1}{r_{02}^2})]$$

$$[\frac{\Gamma}{2\pi}(\frac{2\sin\gamma - 4r\sin\theta_1 - 2r^2\sin(\gamma - 2\theta_1)}{r_{01}^4} - \frac{2\sin\gamma - 4r\sin\theta_2 - 2r^2\sin(\gamma - 2\theta_2)}{r_{02}^4})\delta(t)$$

$$\tag{2.57}$$

$$+\frac{\Gamma}{2\pi}(2)(\frac{2r - (r^2 + 1)\cos(\gamma - \theta_1)}{r_{01}^4}\rho_1 - \frac{2r - (r^2 + 1)\cos(\gamma - \theta_2)}{r_{02}^4}\rho_2)$$

$$+\frac{\Gamma}{2\pi}(r^2 - 1)(2)(\frac{r\sin(\gamma - \theta_1)}{r_{01}^4}\alpha_1 - \frac{r\sin(\gamma - \theta_2)}{r_{02}^4}\alpha_2)]$$

The first order term of the pressure coefficient for the symmetric point $(r_0', -\gamma)$ on the cylinder surface can be calculated in a similar manner:

$$C_{p1}(-\gamma) = -2[2\sin\gamma - \frac{\Gamma}{2\pi}(r^2 - 1)(\frac{1}{r_{01}^2} - \frac{1}{r_{02}^2})]$$

$$[\frac{\Gamma}{2\pi}(\frac{-2\sin\gamma - 4r\sin\theta_1 + 2r^2\sin(\gamma - 2\theta_2)}{r_{02}^4} - \frac{-2\sin\gamma - 4r\sin\theta_2 + 2r^2\sin(\gamma - 2\theta_1)}{r_{01}^4})\delta(t)$$

$$+\frac{\Gamma}{2\pi}(2)(\frac{2r - (r^2 + 1)\cos(\gamma - \theta_2)}{r_{02}^4}\rho_1 - \frac{2r - (r^2 + 1)\cos(\gamma - \theta_1)}{r_{01}^4}\rho_2)$$

$$+\frac{\Gamma}{2\pi}(r^2 - 1)(2)(-\frac{r\sin(\gamma - \theta_2)}{r_{02}^4}\alpha_1 + \frac{r\sin(\gamma - \theta_1)}{r_{01}^4}\alpha_2)]$$

This leads to a differential pressure coefficient between two points (r'_0, γ) and $(r'_0, -\gamma)$ located symmetrically on both sides of the centerline:

$$\Delta C_{p1} = C_{p1}(\gamma) - C_{p1}(-\gamma)$$

$$= 2[2\sin\gamma - \frac{\Gamma}{2\pi}(r^2 - 1)(\frac{1}{r_{01}^2} - \frac{1}{r_{02}^2})]$$

$$[\frac{\Gamma}{2\pi}(4)(\frac{\sin\gamma - 2r\sin\theta_1 - r^2\sin(\gamma - 2\theta_1)}{r_{01}^4} - \frac{\sin\gamma - 2r\sin\theta_2 - r^2\sin(\gamma - 2\theta_2)}{r_{02}^4})\delta(t) \qquad (2.58)$$

$$+ \frac{\Gamma}{2\pi}(2)(\frac{2r - (r^2 + 1)\cos(\gamma - \theta_1)}{r_{01}^4} + \frac{2r - (r^2 + 1)\cos(\gamma - \theta_1)}{r_{02}^4})\rho_A$$

$$+ \frac{\Gamma}{2\pi}(r^2 - 1)(2)(\frac{r\sin(\gamma - \theta_1)}{r_{01}^4} - \frac{r\sin(\gamma - \theta_2)}{r_{02}^4})\alpha_A]$$

As we expected, the differential pressure coefficient is a function of both $\delta(t)$ and the asymmetric variables ρ_A, α_A.

In the basic state, there is no displacement of the cylinder, i.e. $\delta(t) = 0$. This implies:

$$\Delta C_{p1}(\gamma) = 2[2\sin\gamma - \frac{\Gamma}{2\pi}(r^2 - 1)(\frac{1}{r_{01}^2} - \frac{1}{r_{02}^2})]$$

$$[\frac{\Gamma}{2\pi}(2)(\frac{2r - (r^2 + 1)\cos(\gamma - \theta_1)}{r_{01}^4} + \frac{2r - (r^2 + 1)\cos(\gamma - \theta_1)}{r_{02}^4})\rho_A \qquad (2.59)$$

$$+ \frac{\Gamma}{2\pi}(r^2 - 1)(2)(\frac{r\sin(\gamma - \theta_1)}{r_{01}^4} - \frac{r\sin(\gamma - \theta_2)}{r_{02}^4})\alpha_A]$$

For a symmetric perturbation which implies $\rho_A = 0$, $\alpha_A = 0$, expression (2.59) shows that $\Delta C_p = 0$; however, for an asymmetric perturbation $\rho_A \neq 0$, $\alpha_A \neq 0$, (2.59) shows $\Delta C_p \neq 0$. The amplitude of ΔC_p can thus be considered as a measure of the distance between the flow and the stable/unstable eigenspace.

We know that in the basic state there is no lift on the cylinder. This can be shown from the leading order term of the pressure coefficient. We have indeed:

$$C_{L0} = -\int_0^{2\pi} C_{P0}(\gamma) \sin \gamma \, d\gamma$$

$$= -\int_0^{\pi} [C_{P0}(\gamma) - C_{P0}(-\gamma)] \sin \gamma \, d\gamma$$

$$= 0$$

When a small perturbation is applied to the basic state, the lift of the cylinder becomes non-zero due to the unstable motion of the vortices. In our control scheme, we impose a small displacement on the cylinder, defined by the displacement function $\delta(t)$, in order to counteract the deviation of the lift from zero at any given time. We can find the displacement function $\delta(t)$ by imposing the first order lift coefficient to be zero at any time t. We can thus write:

$$C_{L1} = -\int_0^{2\pi} C_{P1}(\gamma) \sin \gamma \, d\gamma$$

$$= -\int_0^{\pi} [C_{P1}(\gamma) - C_{P1}(-\gamma)] \sin \gamma \, d\gamma$$

$$= 0$$

which leads to the expression of the displacement function of the cylinder:

$$\delta(t) = a(r)\rho_A(t) + b(r)\alpha_A(t) \tag{2.60}$$

where the coefficients $a(r), b(r)$ are independent of γ and t and dependent on r only.

$$a(r) = \frac{N_1(r)}{DEN(r)} \tag{2.61}$$

$$b(r) = \frac{N_2(r)}{DEN(r)} \tag{2.62}$$

$$N_1(r) = 4 \int_0^\pi k(\gamma) \frac{\Gamma}{2\pi} \left[\frac{2r - (r^2 + 1)\cos(\gamma - \theta_1)}{r_{01}^4} + \frac{2r - (r^2 + 1)\cos(\gamma - \theta_2)}{r_{02}^4} \right] \sin \gamma d\gamma \tag{2.63}$$

$$N_2(r) = 4 \int_0^\pi k(\gamma) \frac{\Gamma}{2\pi} (r^2 - 1) \left[\frac{r\sin(\gamma - \theta_1)}{r_{01}^4} - \frac{r\sin(\gamma - \theta_2)}{r_{02}^4} \right] \sin \gamma d\gamma \tag{2.64}$$

$$DEN(r) = -8 \int_0^\pi k(\gamma) \frac{\Gamma}{2\pi} \left[\frac{\sin\gamma - 2r\sin\theta_1 - r^2\sin(\gamma - 2\theta_1)}{r_{01}^4} \right. \tag{2.65}$$

$$\left. - \frac{\sin\gamma - 2r\sin\theta_2 - r^2\sin(\gamma - 2\theta_2)}{r_{02}^4} \right] \sin \gamma d\gamma$$

where $k(\gamma)$ is defined as:

$$k(\gamma) = 2\sin\gamma - \frac{\Gamma}{2\pi}(r^2 - 1)\left(\frac{1}{r_{01}^2} - \frac{1}{r_{02}^2}\right)$$

We observe that our control function $\delta(t)$, or displacement function of the cylinder, is a linear combination of the asymmetric unstable motion (ρ_A, α_A) of the vortices.

A close observation of the last two terms of equation (2.58) shows that the lift coefficient caused by the unsteady motion of Foppl's vortex is linearly determined by the asymmetric mode (ρ_A, α_A) and can be expressed as:

$$C_L(t) = N_1(r)\rho_A + N_2(r)\alpha_A \tag{2.66}$$

Equations (2.60) and (2.66) imply that the relation between the control function $\delta(t)$ and the lift coefficient $C_L(t)$ on the cylinder caused by the unsteady motion of

Foppl's vortices is:

$$\delta(t) = \frac{C_L(t)}{DEN(r)} \tag{2.67}$$

Equation (2.67) shows that our linear control technique relates the control function $\delta(t)$ to the unsteady lift at all times in a linear fashion. This relation will be used in an attempt to control the lift in the real viscous flow in Chapter 3.

We can also calculate the leading order steady drag and the first order unsteady drag as follows:

$$
\begin{aligned}
C_{D0} &= -\int_0^{2\pi} C_{P0}(\gamma)\cos\gamma \, d\gamma \\[2ex]
&= -\int_0^{\pi} [C_{P0}(\gamma) + C_{P0}(-\gamma)]\cos\gamma \, d\gamma \\[2ex]
&= -2\int_0^{\pi} [1 - (2\sin\gamma - \frac{\Gamma}{2\pi}(r^2-1)(\frac{1}{r_{01}^2} - \frac{1}{r_{02}^2}))^2]\cos\gamma \, d\gamma \\[2ex]
C_{D1} &= -\int_0^{2\pi} C_{P1}(\gamma)\cos\gamma \, d\gamma \\[2ex]
&= -\int_0^{\pi} [C_{P1}(\gamma) + C_{P1}(-\gamma)]\cos\gamma \, d\gamma \\[2ex]
&= -2\int_0^{\pi} [2\sin\gamma - \frac{\Gamma}{2\pi}(r^2-1)(\frac{1}{r_{01}^2} - \frac{1}{r_{02}^2})] \\[2ex]
&\quad [\frac{\Gamma}{2\pi}(2)(\frac{2r - (r^2+1)\cos(\gamma-\theta_1)}{r_{01}^4} - \frac{2r - (r^2+1)\cos(\gamma-\theta_2)}{r_{02}^4})\rho_S \\[2ex]
&\quad + \frac{\Gamma}{2\pi}(r^2-1)(2)(\frac{r\sin(\gamma-\theta_1)}{r_{01}^4} + \frac{r\sin(\gamma-\theta_2)}{r_{02}^4})\alpha_S]\cos\gamma \, d\gamma
\end{aligned}
$$

As expected, we can see that the drag on the cylinder is dependent on the symmetric mode (ρ_S, α_S) only and the displacement function $\delta(t)$ has no effect on the drag. Therefore, the drag remains the same with or without control.

Finally, we calculate the eigenvalues of our linear control system. Since our control modifies the asymmetric modes only and has no effect on the symmetric mode in the unsteady state, we consider the asymmetric modes only:

$$\frac{\partial}{\partial t}\begin{bmatrix} \rho_A \\ \alpha_A \end{bmatrix} = \begin{bmatrix} \frac{C}{r^2} & -\frac{D}{r} \\ -\frac{D}{r^3} + \frac{\Gamma}{2\pi}\frac{2}{r(r^2-1)} & -\frac{C}{r^2} \end{bmatrix}\begin{bmatrix} \rho_A \\ \alpha_A \end{bmatrix} + \begin{bmatrix} P_3 & Q_3 \\ P_4 & Q_4 \end{bmatrix}\begin{bmatrix} \frac{d\delta(t)}{dt} \\ \delta(t) \end{bmatrix}.$$

We now calculate the eigenvalues of the asymmetric modes. Recall that our linear control system shows that the cylinder displacement function $\delta(t)$ can be expressed as a linear combination of the asymmetric modes, that is:

$$\delta(t) = a\rho_A + b\alpha_A$$

By setting

$$C_{11} = \frac{C}{r^2}$$
$$C_{12} = -\frac{D}{r}$$
$$C_{21} = -\frac{D}{r^3} - \frac{1}{r^2}\frac{\Gamma}{2\pi}\left(\frac{2r}{(r^2-1)^2} - \frac{2r}{(z_1-z_2)^2}\right)$$
$$C_{22} = -\frac{C}{r^2}$$

$$\Delta = 1 - P_3 a - P_4 b$$

and

$$D_{11} = \frac{1}{\Delta}[(C_{11} + Q_3 a)(1 - P_4 b) + (C_{21} + Q_4 a)P_3 b]$$
$$D_{12} = \frac{1}{\Delta}[(C_{12} + Q_3 b)(1 - P_4 b) + (C_{22} + Q_4 b)P_3 b]$$
$$D_{21} = \frac{1}{\Delta}[(C_{21} + Q_4 a)(1 - P_3 a) + (C_{11} + Q_3 a)P_4 a]$$
$$D_{22} = \frac{1}{\Delta}[(C_{22} + Q_4 b)(1 - P_3 a) + (C_{12} + Q_3 b)P_4 a],$$

Now we can write the asymmetric mode in the compact form:

$$\frac{\partial}{\partial t}\begin{bmatrix} \rho_A \\ \alpha_A \end{bmatrix} = \begin{bmatrix} D_{11} & D_{12} \\ D_{21} & D_{22} \end{bmatrix}\begin{bmatrix} \rho_A \\ \alpha_A \end{bmatrix}.$$

The eigenvalues are given by the expression:

$$\lambda_{3,4} = \frac{1}{2}(D_{11} + D_{22} \pm \sqrt{(D_{11} - D_{22})^2 + 4D_{12}D_{21}}).$$

This result of eigenvalues is described in the next section.

2.4   Summary

In this chapter, we have used forced motions of the cylinder to actively control the potential flow of the Foppl model and have designed an active feedback method to systematically maintain the lift zero at any time $t > 0$. We have used asymptotic expansions to achieve linear control and have carried out the linear stability analysis of the control system. In particular, we have found that our control scheme has no effect on the center manifold (symmetric mode) of Foppl's vortex model, and that it modifies the stable/unstable manifold (asymmetric mode) only. Our sensor measures the lift at all times, while the actuator is the forced displacement of the cylinder counteracting any deviation of the lift from the zero value. The displacement function $\delta(t)$ is linearly determined at all times.

Figure 2.3 shows the eigenvalues of the stable/unstable manifold without and with control.

Figure 2.4 shows the coefficients $a(r), b(r)/r$ of the control function as functions of r in equations (2.61) and (2.62), where r is the distance of the point vortices to the center of the cylinder in the fixed point. In the real viscous flow, the steady position of the bubble reflects the magnitude of the Reynolds number. More precisely, the distance r increases with Reynolds number.
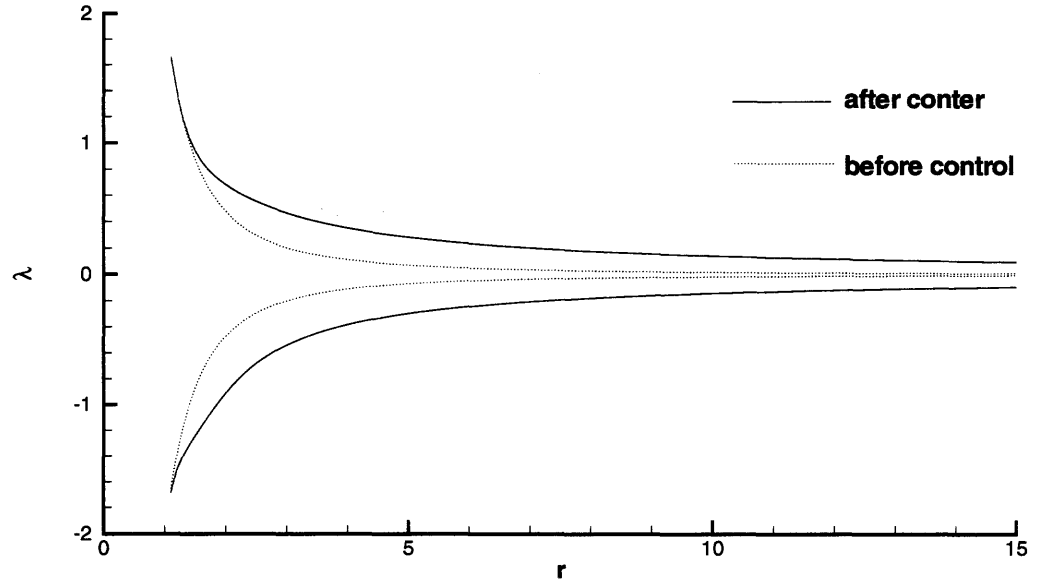
Figure 2.3 Eigenvalues of the stable/unstable manifold without and with control
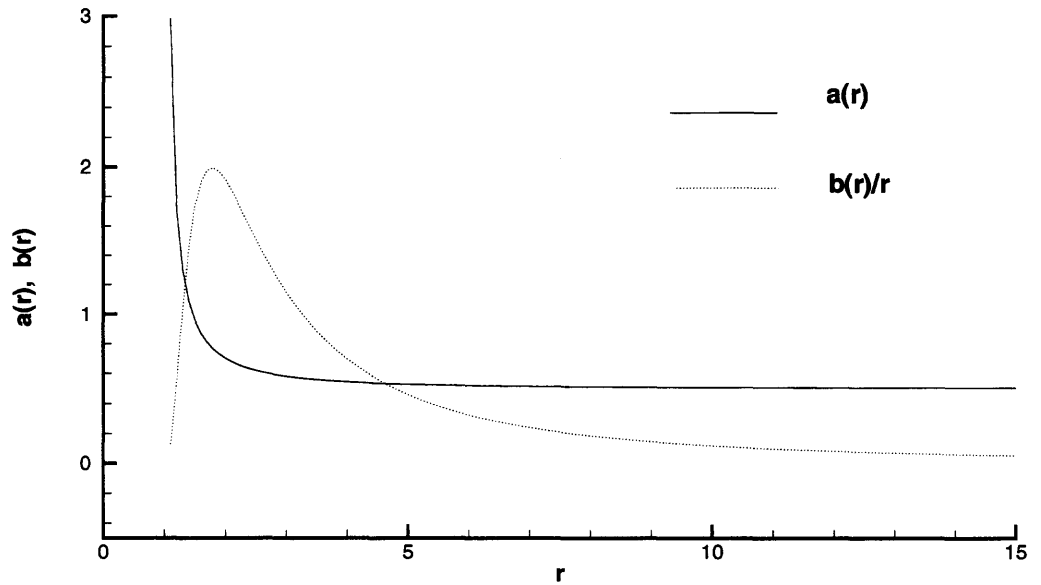
Figure 2.4 Coefficients $a(r), b(r)/r$ of the control function from equations (2.61) and (2.62)
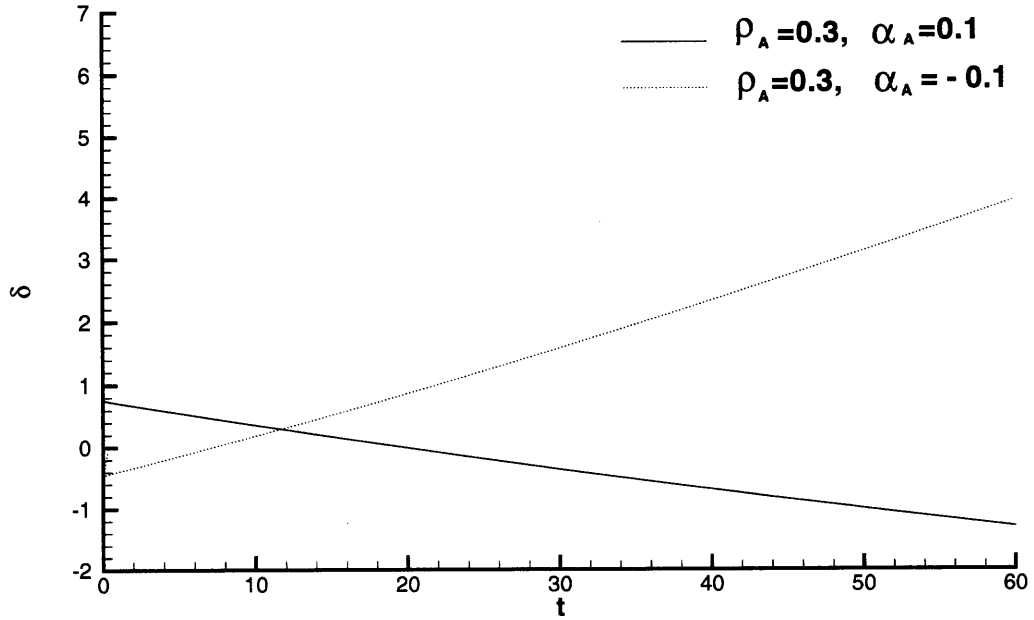
Figure 2.5 Time dependent control function $\delta(t)$ for different initial perturbations

Figure 2.5 shows the control function $\delta(t)$ in equation (2.60) for two different initial perturbations in Foppl's model $\rho_A = 0.3, \alpha_A = 0.1$; $\rho_A = 0.3, \alpha_A = -0.1$.

Figure 2.6 shows the comparison of lift $C_L(t)$ in Foppl's model without and with control for a specific asymmetric perturbation $\rho_A = 0.3$, $\alpha_A = 0.1$.
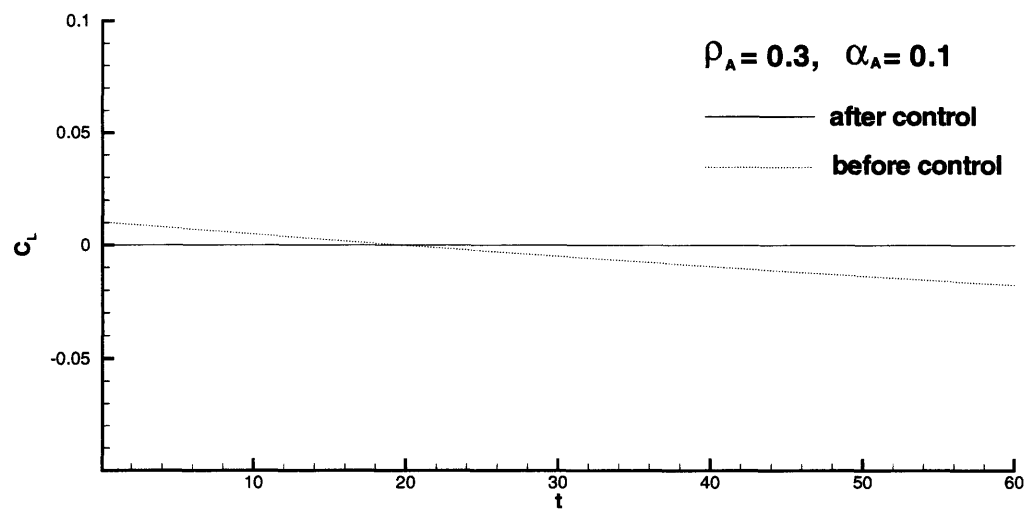
Figure 2.6 Comparison of lift on the cylinder without and with control

CHAPTER 3

FEEDBACK CONTROL OF VORTEX SHEDDING BY NUMERICAL SIMULATION

In this chapter, we apply our feedback control technique to the viscous flow by numerically integrating the Navier-Stokes equations. Our goal is to prevent the lift from becoming non-zero when vortex shedding develops. In this chapter, we confine ourselves to low Reynolds number values ($Re < 200$) where the flow is two dimensional.

Although numerical methods for simulating vortex shedding past a circular cylinder are quite mature, computations incorporating a feedback controller still remain a challenge. Until now, only a few results have been reported (Park et al. 1994, Gunzburger et al. 1996, Min & Choi 1999). Since the numerical integration of the Navier-Stokes (N-S) equations at every time step is slower than the actual response of the flow, it is unlikely that a real time, closed-loop control can be designed based on the numerical integration of the full Navier-Stokes equations alone. In this chapter, we seek to design a feedback controller capable of maintaining the lift close to zero in the viscous flow.

Our control technique is inspired by the control of Foppl's model derived in Chapter 2. For this, we consider the impulsively started flow past a cylinder at $Re = 100$. At early times, the (uncontrolled) flow consists of a bubble of counter-rotating twin vortices. As time increases, the bubble breaks and vortex shedding develops. Our control technique can be described as follows. As soon as vortex shedding starts, the flow is controlled by displacing the cylinder by a distance $\delta(t)$ measured with respect to the steady state. Our control technique consists in displacing the cylinder to counteract the motion of the twin vortices. In the numerical procedure, we first examine the lift coefficient $C_L(t)$ at each time step and test whether the latter is

within an acceptable threshold $C_{L\epsilon}$. If it is, the control is turned off. Otherwise, the control is turned on and the cylinder displaced by a certain distance $\delta(t)$ calculated at each time according to the particular state of the flow at that time. Using the terminology of control theory, our sensor is the lift, and our actuator is the motion of the cylinder itself. An appropriate displacement of the cylinder is sought in order to change the dynamics of the flow field in a desirable manner. We now present our numerical method.

3.1 Numerical Method

3.1.1 Governing Equations

We consider a flow around a fixed cylinder, the incoming free stream being U_∞. Hereafter, the fixed system of coordinates whose origin is located at the center of the cylinder is referred to as $(\widetilde{x}', \widetilde{y}')$ (figure 3.1). The superscript $'$ will therefore be used to denote the variables in the fixed system of coordinates and symbols with the notation $\sim$ will refer to dimensional variables. The two dimensional N-S equations in the fixed system of coordinates $(\widetilde{x}', \widetilde{y}')$ can then be expressed as follows:

Continuity Equation:

$$\widetilde{\nabla}' \cdot \widetilde{\mathbf{v}}' = 0 \tag{3.1}$$

Momentum Equation:

$$\frac{\partial \widetilde{\mathbf{v}}'}{\partial \widetilde{t}} + (\widetilde{\mathbf{v}}' \cdot \widetilde{\nabla}')\widetilde{\mathbf{v}}' = -\frac{1}{\rho}\widetilde{\nabla}'\widetilde{p}' + \nu \widetilde{\nabla}'^2 \widetilde{\mathbf{v}}' \tag{3.2}$$

where $\widetilde{\mathbf{v}}' = \widetilde{u}'\mathbf{i} + \widetilde{v}'\mathbf{j}$ denotes the velocity of the flow field. The variables ρ and ν denote the velocity vector of the flow field, the density of the fluid and the kinematic viscosity of the fluid, respectively. The streamfunction $\widetilde{\psi}'(\widetilde{x}', \widetilde{y}')$ and vorticity $\widetilde{\omega}' = \widetilde{\nabla}' \times \widetilde{\mathbf{v}}'$ in the fixed system of coordinates $(\widetilde{x}', \widetilde{y}')$ are defined by:

$$\widetilde{u}' = \frac{\partial \widetilde{\psi}'}{\partial \widetilde{y}'} \quad \widetilde{v}' = -\frac{\partial \widetilde{\psi}'}{\partial \widetilde{x}'} \tag{3.3}$$

$$\widetilde{\omega}' = -\frac{\partial \widetilde{u}'}{\partial \widetilde{y}'} + \frac{\partial \widetilde{v}'}{\partial \widetilde{x}'} \tag{3.4}$$

Substituting the definition of $\widetilde{\psi}'$ and $\widetilde{\omega}'$ in the continuity equation (3.1) and momentum equation (3.2), we derive the continuity and momentum equations in the fixed system of coordinates.

Streamfunction equation (continuity equation):

$$\frac{\partial^2 \widetilde{\psi}'}{\partial \widetilde{x}'^2} + \frac{\partial^2 \widetilde{\psi}'}{\partial \widetilde{y}'^2} = -\widetilde{\omega}' \tag{3.5}$$

Vorticity transport equation (momentum equation):

$$\frac{\partial \widetilde{\omega}'}{\partial \widetilde{t}} + \widetilde{u}' \frac{\partial \widetilde{\omega}'}{\partial \widetilde{x}'} + \widetilde{v}' \frac{\partial \widetilde{\omega}'}{\partial \widetilde{y}'} = \nu \widetilde{\nabla}'^2 \widetilde{\omega}' \tag{3.6}$$

In order to control the lift on the cylinder at any time $t > 0$, we displace the cylinder vertically at every time step by an appropriate distance $\delta(t)$. We then need to compute the flow past the moving cylinder. For this purpose, we use a moving system of coordinates $(\widetilde{x}, \widetilde{y})$ attached to the center of the cylinder at every time. The transformation between the fixed coordinates $(\widetilde{x}', \widetilde{y}')$ and the moving coordinates $(\widetilde{x}, \widetilde{y})$ is given by (see figure 3.1):

$$\begin{aligned} \widetilde{x}' &= \widetilde{x} \\ \widetilde{y}' &= \widetilde{y} + \widetilde{\delta}(t) \end{aligned}$$

We now proceed to derive the governing equations in the moving system of coordinates $(\widetilde{x}, \widetilde{y})$. The relation between the velocities of the flow field in the fixed system of coordinates $(\widetilde{u}', \widetilde{v}')$ and those in the system of moving coordinates $(\widetilde{u}, \widetilde{v})$ is given by:

$$\begin{aligned} \widetilde{u}' &= \widetilde{u} \\ \widetilde{v}' &= \widetilde{v} + \frac{d\widetilde{\delta}(t)}{d\widetilde{t}}. \end{aligned}$$
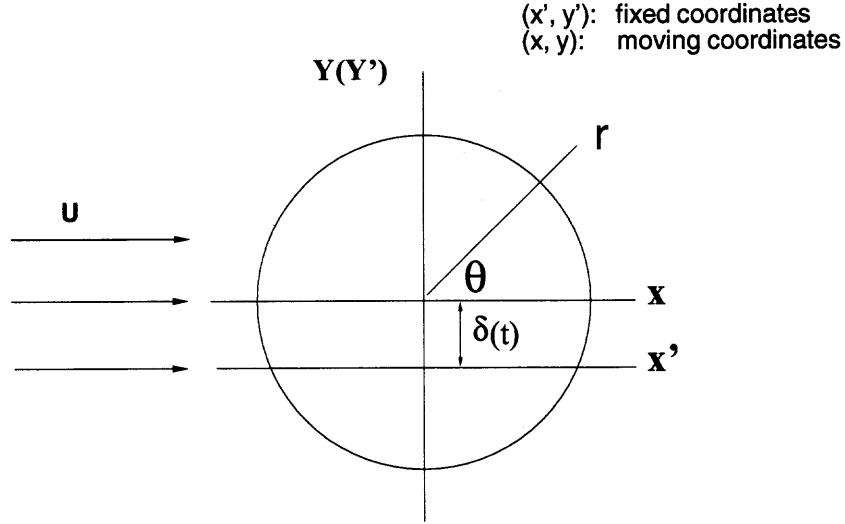
Figure 3.1 Fixed coordinates and moving coordinates

We now introduce the streamfunction $\tilde{\psi}$ and vorticity $\tilde{\omega}$ variables in the moving system of coordinates $(\tilde{x}, \tilde{y})$ through the relations:

$$\tilde{u} = \frac{\partial \tilde{\psi}}{\partial \tilde{y}} \qquad \tilde{v} + \frac{d\tilde{\delta}(t)}{d\tilde{t}} = -\frac{\partial \tilde{\psi}}{\partial \tilde{x}} \tag{3.7}$$

$$\tilde{\omega} = -\frac{\partial \tilde{u}}{\partial \tilde{y}} + \frac{\partial \tilde{v}}{\partial \tilde{x}} \tag{3.8}$$

We can see from equation (3.7) that the expression of the streamfunction $\tilde{\psi}(\tilde{x}, \tilde{y})$ includes the displacement function $\tilde{\delta}(t)$. Comparing equations (3.3), (3.4) in the fixed system of coordinates and those ((3.7), (3.8)) in the moving system of coordinates, we find that the streamfunction $\tilde{\psi}'(\tilde{x}', \tilde{y}')$ and vorticity $\tilde{\omega}'(\tilde{x}', \tilde{y}')$ in the fixed system of coordinates are identical to the streamfunction and vorticity in the moving system of coordinates $\tilde{\psi}(\tilde{x}, \tilde{y})$ and $\tilde{\omega}(\tilde{x}, \tilde{y})$. This simple relation facilitates our computational scheme. The streamfunction equation (continuity equation) and vorticity transport equation (momentum equation) in the moving system of coordinates now become:

Streamfunction equation (continuity equation):

$$\frac{\partial^2 \widetilde{\psi}}{\partial \widetilde{x}^2} + \frac{\partial^2 \widetilde{\psi}}{\partial \widetilde{y}^2} = -\widetilde{\omega} \tag{3.9}$$

Vorticity transport equation (momentum equation):

$$\frac{\partial \widetilde{\omega}}{\partial \widetilde{t}} + \widetilde{u}\frac{\partial \widetilde{\omega}}{\partial \widetilde{x}} + (\widetilde{v} + \frac{d\widetilde{\delta}(t)}{d\widetilde{t}})\frac{\partial \widetilde{\omega}}{\partial \widetilde{y}} = \nu \widetilde{\nabla}^2 \widetilde{\omega} \tag{3.10}$$

We now transform the moving Cartesian coordinates $(\widetilde{x}, \widetilde{y})$ into the (moving) polar coordinates $(\widetilde{r}, \widetilde{\theta})$ by the relation:

$$\widetilde{x} = \widetilde{r}cos\widetilde{\theta} \tag{3.11}$$

$$\widetilde{y} = \widetilde{r}sin\widetilde{\theta} \tag{3.12}$$

We then give details on the derivation of the vorticity transport equation. The derivation of the streamfunction equation can be performed in a similar manner. Equation (3.10) can be rewritten as:

$$\frac{\partial \widetilde{\omega}}{\partial \widetilde{t}} + (\widetilde{v}_r + \frac{d\widetilde{\delta}(t)}{d\widetilde{t}}sin\widetilde{\theta})\frac{\partial \widetilde{\omega}}{\partial \widetilde{r}} + (\widetilde{v}_\theta + \frac{d\widetilde{\delta}(t)}{d\widetilde{t}}cos\widetilde{\theta})\frac{\partial \widetilde{\omega}}{\widetilde{r}\partial\widetilde{\theta}} = \nu(\frac{1}{\widetilde{r}}\frac{\partial}{\partial \widetilde{r}}(\widetilde{r}\frac{\partial \widetilde{\omega}}{\partial \widetilde{r}}) + \frac{1}{\widetilde{r}^2}\frac{\partial^2 \widetilde{\omega}}{\partial \widetilde{\theta}^2})$$

where $\widetilde{v}_r = \frac{d\widetilde{r}}{d\widetilde{t}}$, $\widetilde{v}_\theta = \widetilde{r}\frac{d\widetilde{\theta}}{d\widetilde{t}}$.

We now introduce nondimensional variables, using the free stream velocity U_∞ and the radius of the cylinder a as reference and length scales:

$$\omega = \frac{\widetilde{\omega}a}{U_\infty}, \quad t = \frac{\widetilde{t}U_\infty}{a}, \quad r = \frac{\widetilde{r}}{a}, \quad \theta = \widetilde{\theta}$$

$$v_r = \frac{\widetilde{v}_r}{U_\infty}, \quad v_\theta = \frac{\widetilde{v}_\theta}{U_\infty} \quad \delta(t) = \frac{\widetilde{\delta}(t)}{a}.$$

Here we recall that the variables defined with $\sim$ are dimensional, the other variables being nondimensional. The vorticity transport equation (3.10) in the dimensionless form can be expressed as:

$$\frac{\partial \omega}{\partial t} + (v_r + \frac{d\delta(t)}{dt}sin\theta)\frac{\partial \omega}{\partial r} + (v_\theta + \frac{d\delta(t)}{dt}cos\theta)\frac{\partial \omega}{r\partial\theta} = \frac{2}{Re}(\frac{1}{r}\frac{\partial}{\partial r}(r\frac{\partial \omega}{\partial r}) + \frac{1}{r^2}\frac{\partial^2 \omega}{\partial \theta^2}) \tag{3.13}$$

where the Reynolds number is defined in terms of the diameter $2a$ of the cylinder and the free stream velocity U_∞, that is:

$$Re = \frac{U_\infty 2a}{\nu} \qquad (3.14)$$

Our computational domain is defined with exponential polar coordinates (ξ, η), such that:

$$r = e^{2\pi\xi}, \qquad \theta = 2\pi\eta \qquad (3.15)$$

Such a mapping (see figure 3.2) offers the advantage that although the computational domain is of limited size and appropriate for numerical simulations, the flow is considered in a very large physical domain and potential flow is assumed at the outer edge of the domain.

Using the differential relation between the original polar coordinates (ξ, η) and the exponential ones, $\frac{\partial}{\partial r} = \frac{1}{2\pi r}\frac{\partial}{\partial \xi}$, $\frac{\partial}{\partial \theta} = \frac{1}{2\pi}\frac{\partial}{\partial \eta}$, we derive the vorticity transport equation in the computational domain (ξ, η) from equation (3.13). The latter reads:

$$E\frac{\partial \omega}{\partial t} + \frac{\partial (V_\xi \omega)}{\partial \xi} + \frac{\partial (V_\eta \omega)}{\partial \eta} = \frac{2}{Re}\left(\frac{\partial^2 \omega}{\partial \xi^2} + \frac{\partial^2 \omega}{\partial \eta^2}\right) \qquad (3.16)$$

where the symbols E, V_ξ, V_η have the following meaning:

$$E = 4\pi^2 e^{4\pi\xi} = (2\pi r)^2$$

$$V_\xi = \frac{\partial \psi}{\partial \eta} = E^{\frac{1}{2}}\left(v_r + \frac{d\delta(t)}{dt}\sin(2\pi\eta)\right)$$

$$V_\eta = -\frac{\partial \psi}{\partial \xi} = E^{\frac{1}{2}}\left(v_\theta + \frac{d\delta(t)}{dt}\cos(2\pi\eta)\right).$$

A similar analysis applied to the streamfunction equation leads to the following equation:

$$\frac{\partial \psi^2}{\partial \xi^2} + \frac{\partial \psi^2}{\partial \eta^2} = -E\omega \qquad (3.17)$$
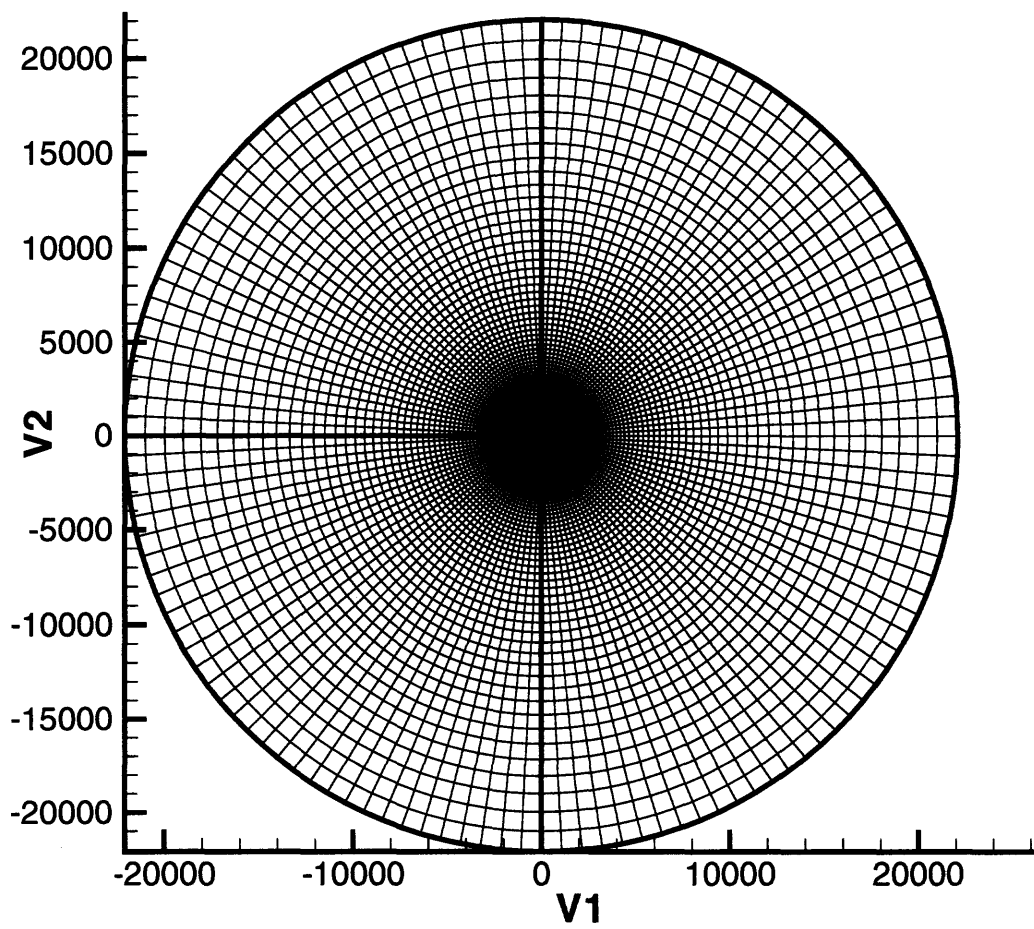
Figure 3.2 Computational domain (ξ, η)

Equations (3.16) and (3.17) are the governing equations we use to compute the flow past the moving cylinder, in the computational domain (ξ, η). We can see here that the control function $\delta(t)$ appears through the variables V_ξ and V_η in the vorticity transport equation (3.16) expressed in the computational domain (ξ, η). For zero displacement, i.e. $\delta(t) = 0$, we recover the equations of motion for a fixed cylinder. The vorticity transport equation (3.16) is solved by an Alternative-Direction Implicit (ADI) algorithm and the streamfunction equation (3.17) is integrated by means of a Fast Fourier Transform (FFT) algorithm. The accuracy of the numerical scheme is second order in space and first order in time. The details of the discretization procedure have been described in Tang & Aubry (1997) for a fixed cylinder ($\delta(t) = 0$). These authors also validated the code against numerical and/or experimental results. A good agreement with others' findings was found. Since an additional difficulty is introduced due to the motion of the cylinder in the present work, particular attention needs to be given to the numerical scheme. This will be the object of the next paragraph.

3.1.2 Numerical Details

It is well-known that vortex shedding occurs when Reynolds number exceeds a critical value $Re > Re_{cr}$. One of the most important consequences of vortex shedding consists in generating non-zero, oscillating lift on the body. Since our purpose is to control any deviation of the lift from zero value, we use the lift as sensor. In the impulsively started flow, the initial stage is characterized by a steady flow consisting of a recirculating bubble of two symmetric vortices rotating in opposite directions. At this early stage, the symmetry of the flow with respect to the centerline implies zero lift on the body. In this case, control is not applied, the cylinder is fixed ($\delta(t) = 0$) and the flow is computed in the fixed system of coordinates. As time increases, the two vortices become asymmetric and the lift starts deviating from its zero value.

At later times, vortex shedding fully develops and the lift oscillates. Our goal is to prevent the lift from deviating from zero. Our control technique is as follows. When the lift is larger than a predefined threshold in absolute value: $|C_L(t)| > C_{L\epsilon}$, control is applied and $\delta(t) \neq 0$. In this case, we calculate the flow in the system of coordinates moving with the cylinder. Since our technique consists of a closed-loop control scheme, whether the actuator is turned on or off at a particular time depends entirely on the actual flow situation at that time. We can see indeed from our results presented in the next section that actuation is not applied in a continuous fashion. Closed-loop (feedback) control is more advantageous than open-loop control for several reasons. First, it adapts to varying flow conditions; second, it requires less energy input.

There are two numerical subtleties we would like to discuss. The first point is that our computation always starts in the fixed system of coordinates since the flow consists of the symmetric bubble at early stages and the lift is nearly zero during this initial time period. We then switch our computation to the moving frame as soon as the lift $C_L(t)$ exceeds the predefined threshold $C_{L\epsilon}$ in absolute value. At any given time, we thus need to transform the expression of the streamfunction ψ and vorticity ω in the fixed mesh to a formulation in the moving mesh, and vice versa. Since each grid point (ξ_m, η_n) in the moving mesh is located within one grid element (i, j , i+1, j+1) in the fixed mesh, see figure 3.3, we calculate the streamfunction (or vorticity) value at the grid point (ξ_m, η_n) in the moving mesh by averaging the streamfunction values at the four grid vertices in the fixed mesh, that is

$$\psi(m,n) = \frac{1}{4}(\psi'(i,j) + \psi'(i+1,j) + \psi'(i,j+1) + \psi'(i+1,j+1)) \qquad (3.18)$$

The same equation holds when ψ is replaced by ω. Likewise, the transformation of the streamfunction (or vorticity) from the moving system of coordinates to the fixed
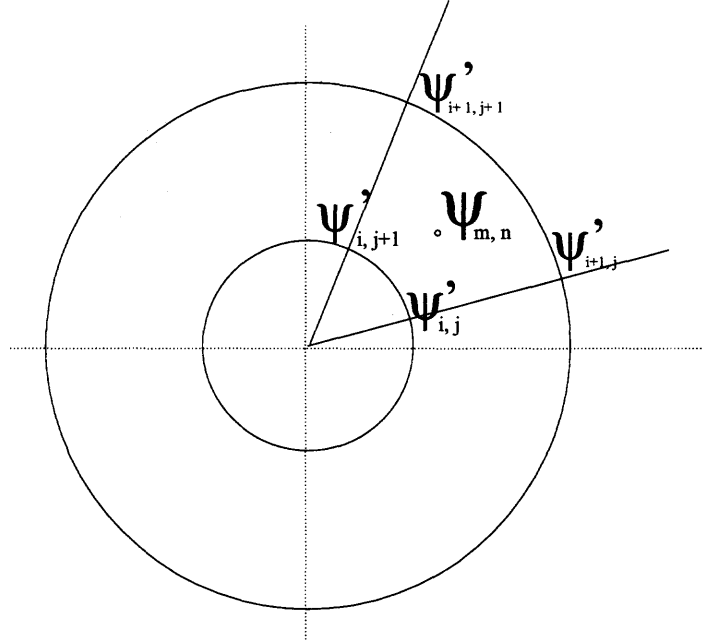
Figure 3.3 Streamfunction $\psi(m,n)$ at the point (m,n) in the moving coordinates

system of coordinates is carried out using equation (3.18) where the fixed coordinates

and moving coordinates are interchanged.

The second point is that it is important to check the vorticity flux $\frac{\partial \omega}{\partial r}$ along the

cylinder surface. Theoretically, the integral of the vorticity flux $\frac{\partial \omega}{\partial \xi}$ along the cylinder

surface is equal to zero. This can be shown from the N-S equations. We can write:

$$\frac{\partial p}{\partial \eta} = \frac{2}{Re}\frac{\partial \omega}{\partial \xi}$$

which implies:

$$C_p(0,\eta) - C_p(0,0) = \frac{2}{Re}\int_0^\eta \frac{\partial \omega(0,\eta)}{\partial \xi}d\eta$$

Since $C_p(0,1)$ and $C_p(0,0)$ actually denote the same stagnation point, the left hand

side of the previous equation is zero, and therefore, the integral in the right hand

side is also zero, that is

$$\int_0^1 \frac{\partial \omega}{\partial \xi}(0, \eta) d\eta = 0 \qquad (3.19)$$

In our numerical scheme, we use

$$\frac{\partial \omega}{\partial \xi}(0, \eta) = \frac{-3\omega(0, \eta) + 4\omega(1, \eta) - \omega(2, \eta)}{2\Delta\xi}$$

which gives us second-order accuracy to calculate the vorticity flux. This formula also meets the requirement (3.19) in a satisfactory manner.

3.2 Results and Discussions

We present our results at the Reynolds number value $Re = 100$ which is higher than the critical Reynolds number Re_{cr} (Re_{cr}=47-48). The size of the computational domain (ξ, η) is given by $\Delta\xi = 0.004$, $\Delta\eta = 1/256$ and the time step was chosen to be $\Delta T = 0.005$.

An interesting problem we need to address is to select an optimal control function $\delta(t)$ based on our analysis in Chapter 2. Since a relation between the Reynolds number of the flow and the position of the fixed point (recirculating bubble) is hard to obtain in the viscous flow, a quantitative description of the fixed point in the real flow will be helpful. Figure 3.4 shows the lift as a function of time in the uncontrolled flow at Reynolds number $Re = 100$ while figure 3.5 displays the corresponding streamlines at two different times. Figure 3.4 shows that in the initial stage, the lift is nearly zero. However, at about $t = 360$, the lift starts developing some oscillations. At that time, the streamlines still show a symmetric bubble of counter-rotating vortices whose center is located at about $r = 5$ from the center of the cylinder. At $t = 400$, lift oscillations have grown and the flow patterns exhibit vortex shedding (see figure 3.5).
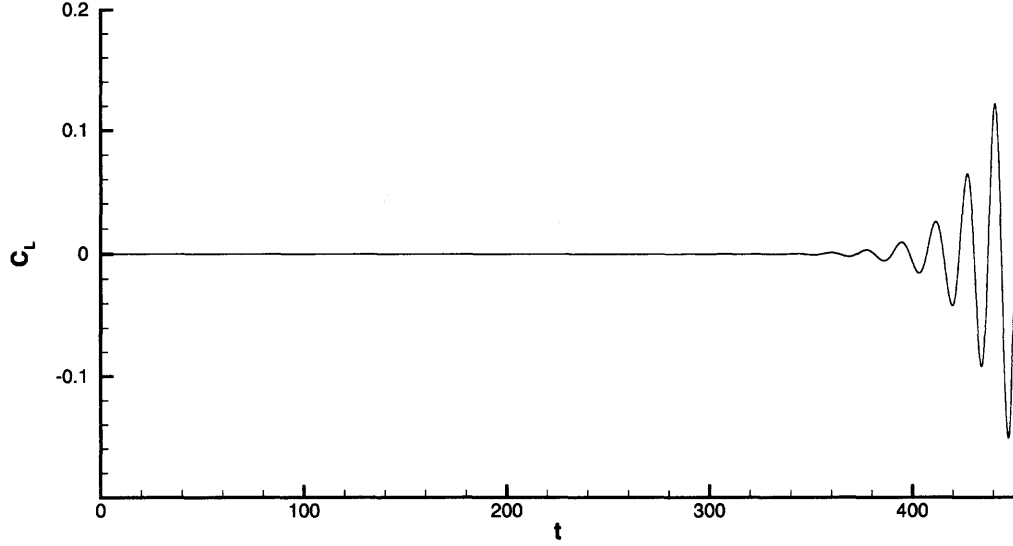
Figure 3.4 Lift in the uncontrolled flow for Re=100

One of the most important aspects of any closed-loop control technique lies in the design of the feedback control law. In the closed-loop control technique used by others and based on suction/blowing through the cylinder surface, the feedback control law is defined by:

$$u(0, \eta) = F(t)G(0, \eta) \tag{3.20}$$

where u denotes the velocity at the suction/blowing point on the cylinder, $G(0, \eta)$ is the predefined velocity profile at the suction/blowing point, and $F(t)$ refers to the feedback function defined by:

$$F(t) = K(Re)\frac{M(t, \xi = \xi_s(Re), \eta = 0)}{M_{max}(t, \xi = \xi_s(Re), \eta = 0))} \tag{3.21}$$

Here, K(Re) is the feedback coefficient (or feedback gain), $(\xi_s(Re), 0)$ is the sensor location on the centerline, downstream of the cylinder, $M(t, \xi = \xi_s(Re), \eta = 0)$ is the variable measured at the sensor location $(\xi_s(Re), 0)$ when the control is applied to the flow (forced flow), and $M_{max}(t, \xi = \xi_s(Re), \eta = 0))$ is the maximal value of the
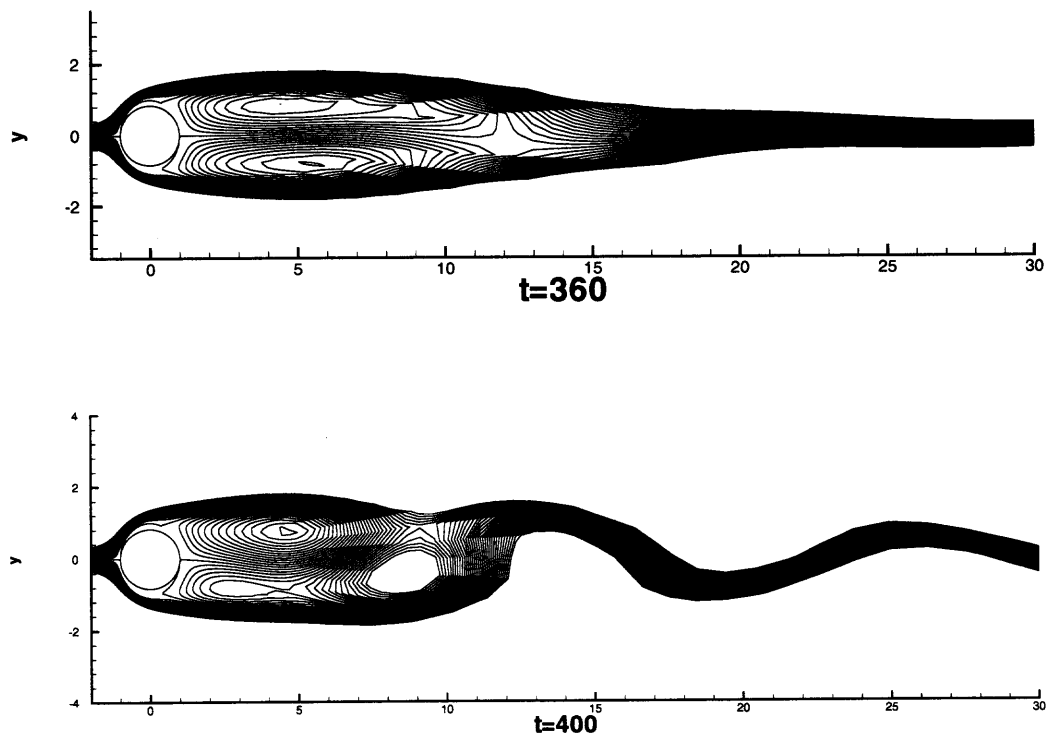
Figure 3.5 Streamline of the uncontrolled flow at $Re = 100$

variable in the uncontrolled flow. The variable measured by the sensor can be the flow velocity, vorticity, pressure or any other relevant flow parameter. Here, we use the notation $K(Re)$ and $\xi_s(Re)$ because both the feedback coefficient K and sensor location ξ_s depend on the Reynolds number.

We notice that there are three empirical parameters in the previous feedback control method which need to be selected: (i) the velocity profile $G(0, \eta)$ at the suction/blowing point(s) on the cylinder surface (for example, $G(0, \eta)$ can be taken as a parabolic (quadratic) function); (ii) the feedback coefficient(feedback gain) $K(Re)$ (usually obtained by numerical experiments), (iii) the sensor location $(\xi_s(Re), 0)$ downstream of the cylinder on the centerline. This sensitivity of the control technique to these various parameters has been documented by other researchers. Park et al. (1994), for instance, successfully suppressed vortex shedding at $Re = 60$ using suction/blowing slots on the cylinder but found that their result is only valid for a limited range of sensor positions. In addition, the sensor location must be different for various Reynolds numbers. For instance, the sensor location valid for suppressing vortex shedding at $Re = 60$ may not be successful for the control of vortex shedding at $Re = 80$. The valid region of sensor locations $(\xi = \xi_s(Re), \eta = 0)$ was determined by trial and error only.

In summary, feedback control of vortex shedding by means of suction/blowing has been achieved numerically in the past. Whether a particular control technique has been successful, however, has been strongly dependent on the selection of three parameters: the velocity profile $G(0, \eta)$, the feedback coefficient(feedback gain) K(Re) and the specific sensor location $(\xi = \xi_s(Re), \eta = 0)$.

In our control algorithm, the sensor location is not a parameter since the sensor simply measures the lift. Likewise, the position of the actuator is irrelevant due to the fact that the actuator is the motion of the cylinder itself. The amplitude of the

forced motion at each time step, however, needs to be determined. This translates into finding the displacement function, $\delta(t)$, at each time. Recall that $\delta(t)$ should be kept small compared to the radius the cylinder a, and the flow close the fixed point, in order to remain within the realm of linear control theory used in Chapter 2. Although, in some cases, linear control theory has been found to be applicable to the nonlinear regime of the flow, so far, all our attempts to control the flow after vortex shedding has settled have been unsuccessful. In practice, the lift coefficient threshold for turning the control on or off is kept small, in the order of $C_{L\epsilon} = O(10^{-3})$. Recall that if the lift is larger than the threshold in absolute value, the control is applied.

Since the threshold for the lift coefficient $C_{L\epsilon}$ is kept small, we can apply the linear control algorithm derived in Chapter 2. In this algorithm, the control function $\delta(t)$ is proportional to the lift at each time step, see equation (2.67), with the coefficient of proportionality being DEN(r). An investigation of DEN(r) in the model shows that, for the values of r relevant in the viscous flow, DEN(r) is of the order of 10^{-1}. We thus consider the linear relation:

$$\delta(t) = \frac{C_L(t)}{A} \tag{3.22}$$

where A is a constant, whose value depends on the distance of the vortices to the center of the cylinder, and therefore on Reynolds number.

As mentioned before, we computed the flow at $Re = 100$. In order to control this flow, we first chose the lift threshold $C_{L\epsilon} = 0.001$, and the control function $\delta(t) = C_L(t)/A$, where A is a constant, equal to 0.1. Figure 3.6 compares the lift without and with control. We can see that the lift on the cylinder is controlled in a satisfactory manner.

Figure 3.7 gives the corresponding displacement control function $\delta(t)$ in this case.
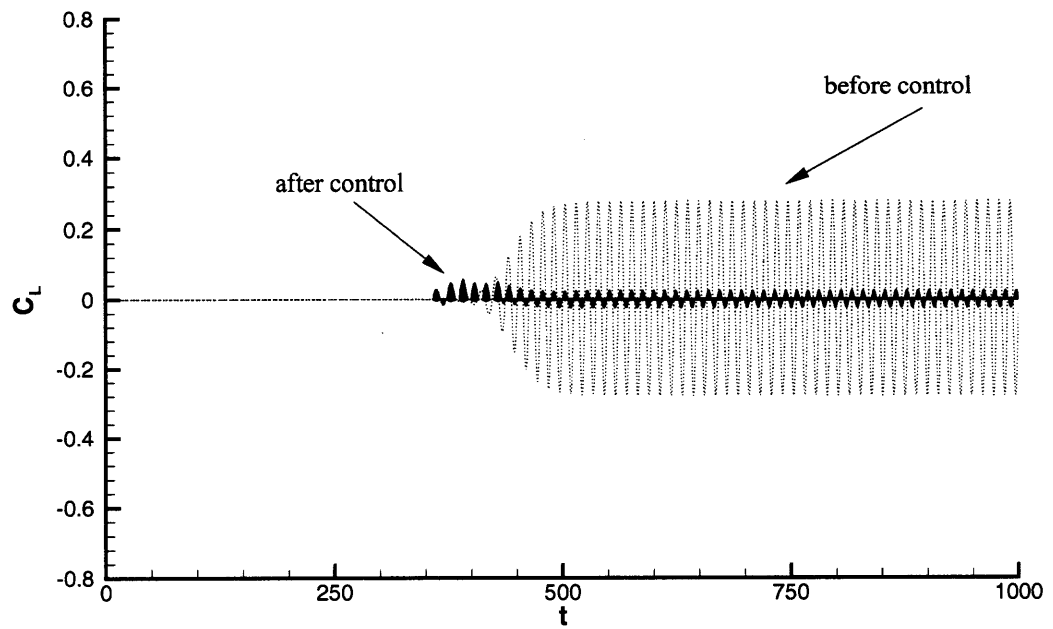
Figure 3.6 Comparison of lift coefficient without and with control at $Re = 100$, $A = 0.1$
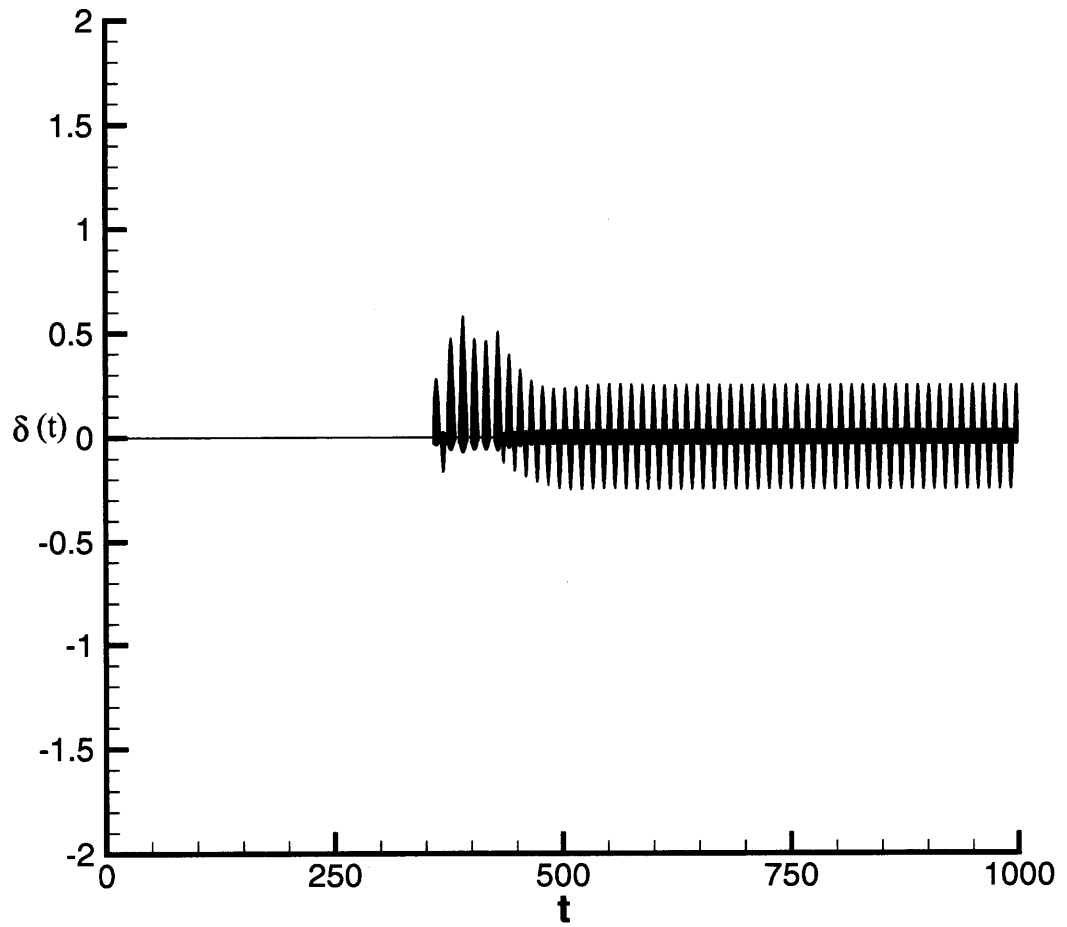
Figure 3.7 Control function $\delta(t)$ for controlled flow at $Re = 100$, $A = 0.1$

Figure 3.8 compares the streamlines of the flow without and with control. We can see that vortex shedding is fully suppressed by our control technique.

In a second attempt to control the flow at $Re = 100$, we chose the lift threshold criterion to be $C_{L_\epsilon} = 0.001$ as in the first computation, but the coefficient A in the control function $\delta(t) = C_L(t)/A$, was chosen to be $A = 0.5$.

Figure 3.9 compares the lift without and with control. Once again, we observe that the lift on the cylinder is controlled in a satisfactory manner.

Figure 3.10 gives the corresponding control function $\delta(t)$ in this case. Here, the control function $\delta(t)$ is smaller than in the previous case (Figure 3.7).

Figure 3.11 allows to compare the streamlines without and with control, showing that the control technique fully suppresses vortex shedding.

Before Control

After Control

t=410

t=410

t=420

t=420

t=430

t=430

t=440

t=440

t=450

t=450

Figure 3.8 Comparison of the streamlines without and with control for $Re = 100$, $A = 0.1$
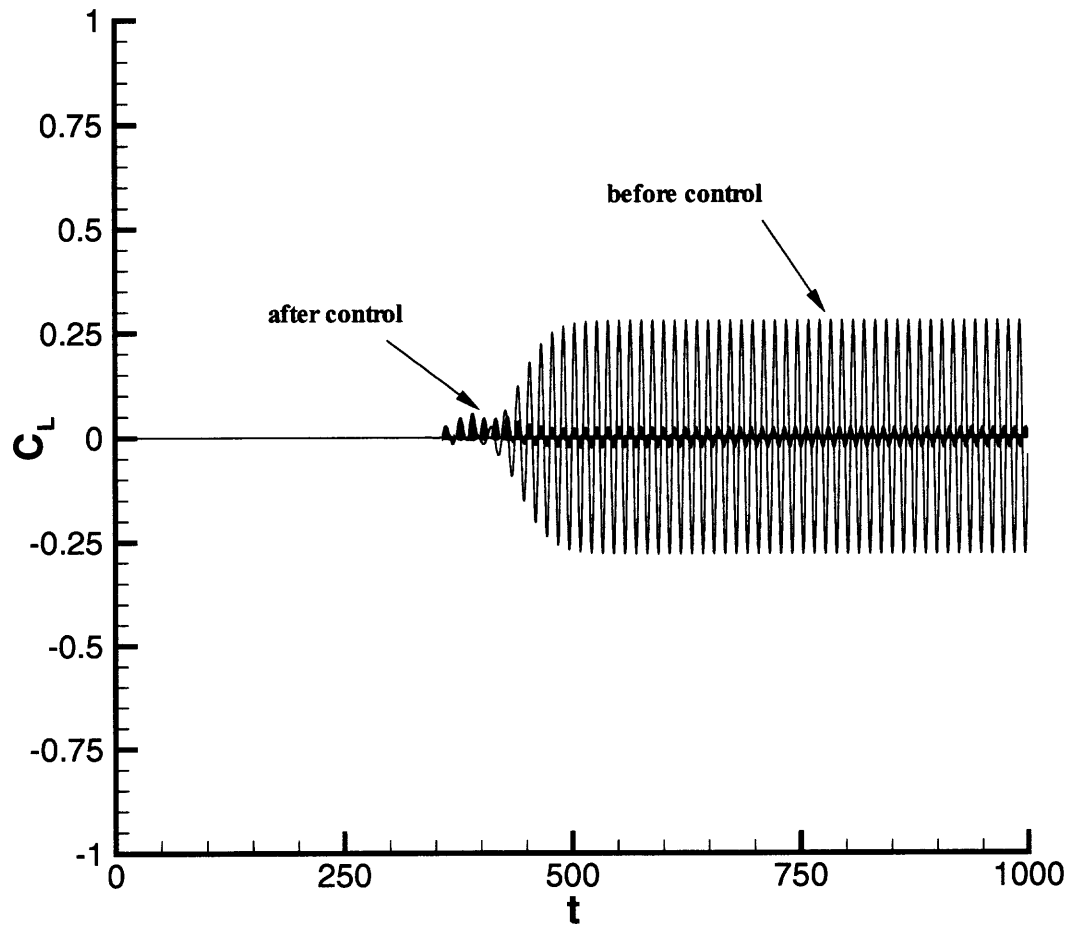
Figure 3.9 Comparison of lift coefficient without and with control for $Re = 100$, $A = 0.5$
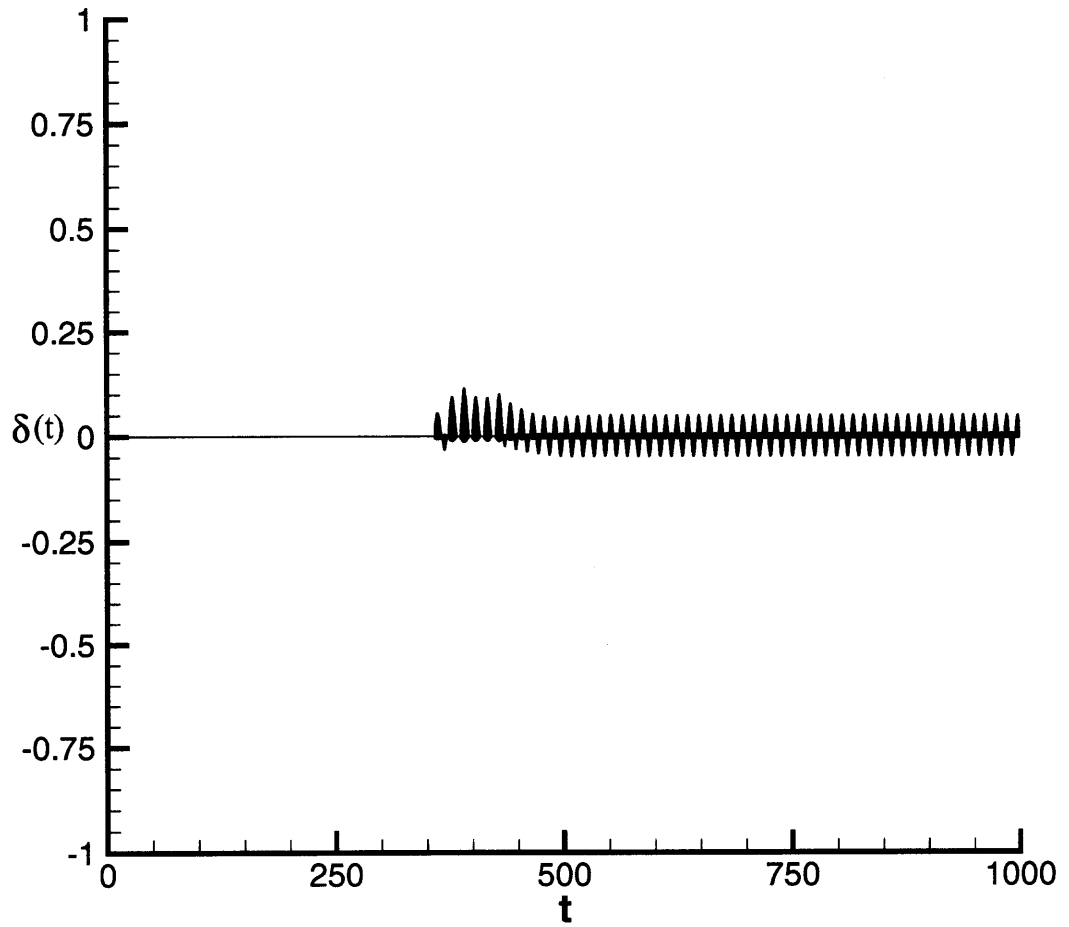
Figure 3.10 Control function $\delta(t)$ for controlled flow at $Re = 100$, $A = 0.5$
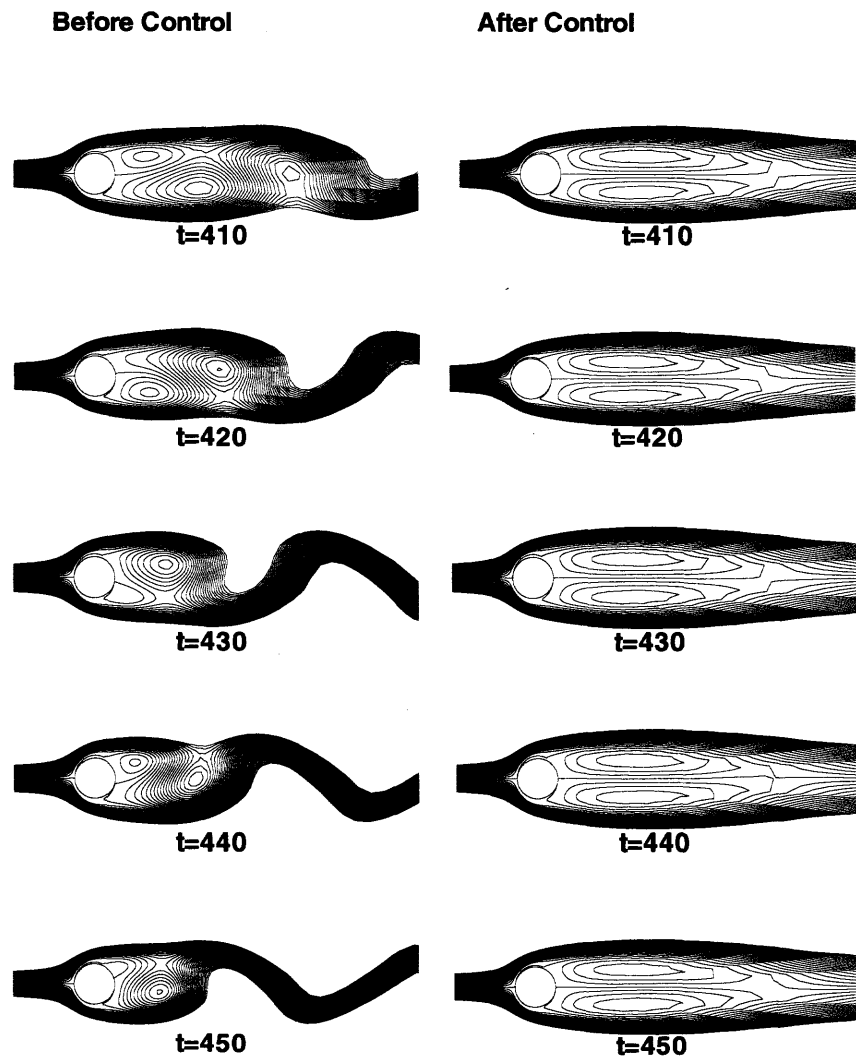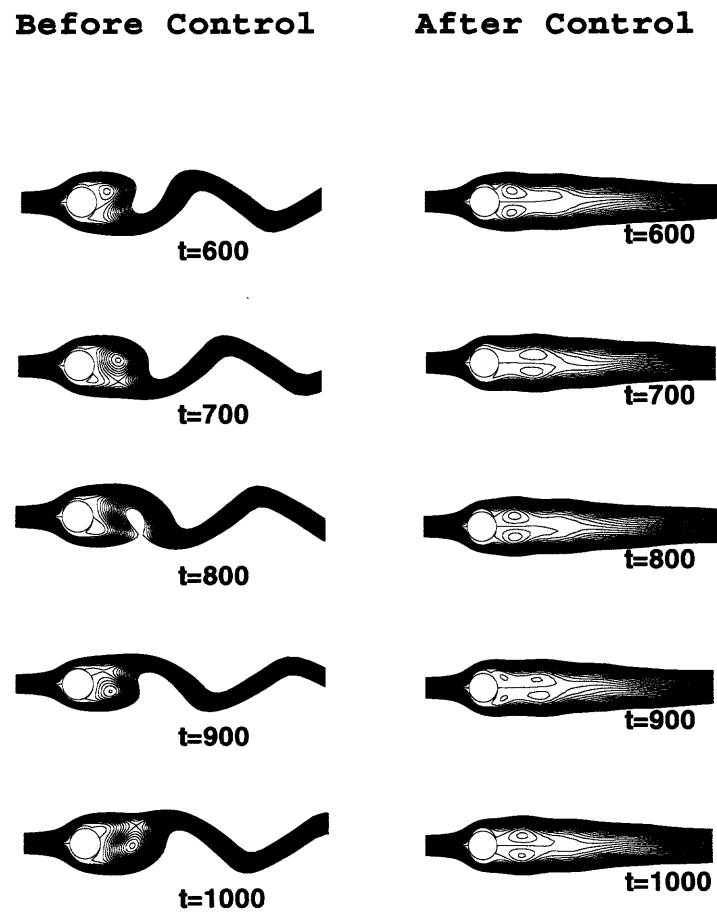
Figure 3.11 Comparison of streamlines without and with control for $Re = 100$, $A = 0.5$

CHAPTER 4

CONTROL OF FOPPL'S VORTEX MODEL BY SYMMETRIC SURFACE DEFORMATION

In this chapter, we consider the possibility to control Foppl's vortex model by an unsteady deformation of the cylinder surface. Controlling fluid flows by means of compliant walls is the subject of a certain number of investigations and has broad practical applications (Moin & Bewley 1994, Gad-el-Hak 1996, Lumley & Blossey 1998).

We consider deforming the cylinder surface in response to the actual flow situation at each time step. Here again, we concentrate on controlling the lift or the drag in the unsteady state. A deformation function $r_\epsilon(\gamma, t)$ which depends on both position γ and time t would be most appropriate. Unfortunately, the non-uniformity of the deformation along the solid surface introduces mathematical difficulties through convoluted integral equations.

In this chapter, we concentrate on the particular case of a symmetric surface deformation. Note that the motion of the cylinder treated earlier can also be considered as a particular, antisymmetric, surface deformation. The perturbation methods are very similar in these two particular cases.

We thus follow the perturbation approach described in Chapter 2 and consider a small uniform surface deformation $r_\epsilon(t)$ at each time t, see figure 4.1. The deformation is mathematically introduced by a uniform source distribution function $Q_\epsilon(t)$ placed along the cylinder surface, which, at every time, takes care of the new boundary condition. We first present our mathematical model and then proceed with our analysis in the following sections.

71

Solid line: Steady state circular cylinder at $t_0=0$

Dashed line: Cylinder surface after displacement at time $t>0$
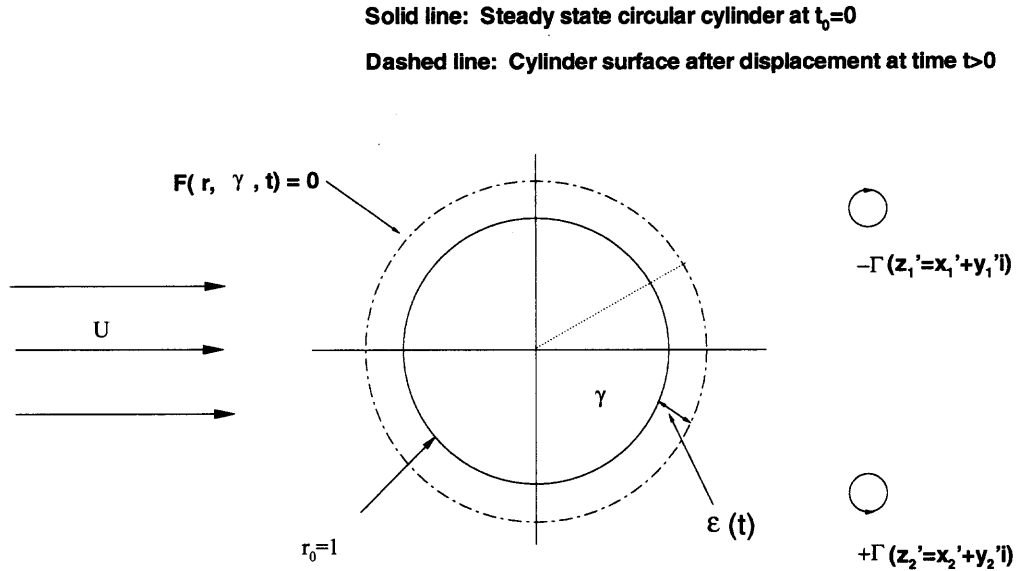
Figure 4.1 Control of vortex shedding by symmetric surface deformation

4.1   Mathematical Model

As in our previous analysis, we represent the cylinder surface by the function $F(r, \gamma, t) = 0$ where the variables (r, γ) denote the position of the point in polar coordinates; the flow-tangency boundary condition is given by the equation:

$$\frac{DF}{Dt} = \frac{\partial F}{\partial t} + \vec{u} \cdot \nabla F = 0 \qquad (4.1)$$

at all points on the body surface $F(r, \gamma, t) = 0$. Here, $\vec{u}$ is the velocity at any point on the surface. In this symmetric surface deformation case, a small source distribution $Q_\epsilon(t)$ is imposed on the boundary surface to satisfy the boundary condition. Here, we assume $Q_\epsilon(t) \ll 1$.

Let $r_\epsilon(t)$ be a small deformation of the body surface with respect to the initial circular cylinder $r_0 = 1$ where $r_\epsilon(t) \ll 1$, $\frac{dr_\epsilon(t)}{dt} \ll 1$. The goal of our study is to find a control function $r_\epsilon(t)$ which either controls the lift or the drag at any time.

As in the previous sections, we decompose the velocity into three terms:

$$\vec{u} = \vec{u}^U + \vec{u}^v + \vec{u}^c$$

where $\vec{u}^U$ refers to the velocity induced by the free-stream velocity U, $\vec{u}^v$ denotes the velocity induced by Foppl's vortices, and $\vec{u}^c$ is the velocity induced by the source distribution $Q_\epsilon(t)$ on the cylinder surface. Equation (4.1) now becomes:

$$\frac{\partial F}{\partial t} + (u_r^U + u_r^v + u_r^c)\frac{\partial F}{\partial r} + (u_\gamma^U + u_\gamma^v + u_\gamma^c)\frac{1}{r}\frac{\partial F}{\partial \gamma} = 0 \qquad (4.2)$$

where the subscripts r and γ denote the radial and azimuthal components, respectively.

The function $F(r, \gamma, t)$ defining the deformable solid surface is expressed by

$$F(r, \gamma, t) = r - r_0 - r_\epsilon(t). \qquad (4.3)$$

This gives us:

$$\frac{\partial F}{\partial t} = -\frac{dr_\epsilon(t)}{dt}$$
$$\frac{\partial F}{\partial r} = 1$$
$$\frac{\partial F}{\partial \gamma} = 0$$

Substituting these derivatives in equation (4.2) and expressing the velocity in terms of the zeroth order (basic state) and first order (perturbation) components, we have

$$-\frac{dr_\epsilon(t)}{dt} + [(u_{r0}^U + u_{r1}^U) + (u_{r0}^v + u_{r1}^v) + (u_{r0}^c + u_{r1}^c)] = 0$$

where the indices 0 and 1 refer to zeroth and first order terms, respectively.

We notice that the velocities u_{r0}^c is identically zero since the source distribution $Q_\epsilon(t)$ is not applied in the basic state, i.e. $u_{r0}^c = 0$ and assume that $r_\epsilon(t) \ll 1$, $\frac{dr_\epsilon(t)}{dt} \ll 1$. The first order term of the boundary condition then becomes:

$$u_{r1}^U + u_{r1}^v + u_{r1}^c = \frac{dr_\epsilon(t)}{dt}. \qquad (4.4)$$

In the next section, we will seek expressions for u_{r1}^{U}, and u_{r1}^{v}, u_{r1}^{c} in terms of the control function $r_{\epsilon}(t)$.

4.2 Induced Velocity at a Point on the Deformable Surface

4.2.1 Velocity Induced by the Free Stream

We use a perturbation method similar to that used in Chapter 2. At any time $t > 0$, we consider an arbitrary point $z_0'(r_0', \gamma)$ on the deformable surface $F(r, \gamma, t) = 0$. The unsteady flow can be treated in terms of the steady flow and a small perturbation. The velocity induced by the free stream at any point $z_0'(r_0', \gamma)$ can be obtained from the complex potential:

$$w(z_0') = U(z_0' + \frac{r_0'^2}{z_0'})$$

The corresponding induced velocity is given by:

$$\frac{d\overline{z_0'}}{dt} = \frac{dw}{dz_0'} = U(1 - \frac{r_0'^2}{z_0'^2})$$

We now deduce the expression of the radial and azimuthal components of the induced velocity. Expressing the fact that there is no azimuthal perturbation on the solid surface, we have:

$$r_0'(t) = r_0 + r_\epsilon(t)$$

$$z_0'(t) = r_0' e^{i\gamma}$$

Using equations (2.12), (2.13), (2.14) from Chapter 2, we can write:

$$u_r' - iu_\gamma' = \frac{U}{r_0'}(z_0' - \frac{r_0'^2}{z_0'}) = i2\sin\gamma$$

Expressing the unsteady velocity in terms of the leading order term (steady state) and first order terms, we obtain the velocity at any point on the deformable surface induced by the free stream, that is:

$$u_{r0}^U(\gamma) = 0 \tag{4.5}$$

$$u_{\gamma 0}^U(\gamma) = -2\sin\gamma \tag{4.6}$$

$$u_{r1}^{U}(\gamma, t) = 0 \tag{4.7}$$

$$u_{\gamma 1}^{U}(\gamma, t) = 0 \tag{4.8}$$

The zeroth order term of the radial velocity $u_{r0}^{U} = 0$ reflects the normal boundary condition on the solid surface in the basic state.

4.2.2 Velocity Induced by the Point Vortices

Similarly, we can calculate the velocity at the point z_0' on the deformable surface induced by Foppl's two point vortices located at points z_1', z_2' and their images located at points $\frac{1}{\overline{z'}_1}, \frac{1}{\overline{z'}_2}$ in the controlled flow.

Using the same procedure as that in Chapter 2, we suppose that the positions of the two vortices in the basic state are $z_1(r_1, \theta_1)$, $z_2(r_2, \theta_2)$ respectively, and that small perturbations (ρ_1, α_1), (ρ_2, α_2) are applied to these positions such that ρ_1, $\rho_2 \ll 1$, θ_1, $\theta_2 \ll 1$. The new position of the point vortices are defined by $z_1'(r_1', \theta_1')$, $z_2'(r_2', \theta_2')$ respectively, such that:

$$r_1' = r_1 + \rho_1$$

$$\theta_1' = \theta_1 + \alpha_1$$

$$r_2' = r_2 + \rho_2$$

$$\theta_2' = \theta_2 + \alpha_2.$$

The flow dynamics induced by the point vortices at the point z_0' on the deformable surface is given by:

$$\frac{d\overline{z'}_0}{dt} = -\frac{\Gamma}{2\pi i}\frac{1}{z_0' - z_1'} + \frac{\Gamma}{2\pi i}\frac{1}{z_0' - \frac{r_0'^2}{\overline{z'}_1}} + \frac{\Gamma}{2\pi i}\frac{1}{z_0' - z_2'} - \frac{\Gamma}{2\pi i}\frac{1}{z_0' - \frac{r_0'^2}{\overline{z'}_2}}$$

Using expression (2.12) in Chapter 2, we deduce:

$$u_r'^v(z_0') - iu_\gamma'^v(z_0') = \frac{z_0'}{r_0'}[-\frac{\Gamma}{2\pi i}\frac{(z_1'\overline{z'}_1 - r_0'^2)}{(z_0' - z_1')(z_0'\overline{z'}_1 - r_0'^2)} + \frac{\Gamma}{2\pi i}\frac{(z_2'\overline{z'}_2 - r_0'^2)}{(z_0' - z_2')(z_0'\overline{z'}_2 - r_0'^2)}] \tag{4.9}$$

Noticing that $z'_0 \overline{z'_0} = r'^2_0$, we can write:

$$u'^v_r(z'_0) - iu'^v_\gamma(z'_0) = \frac{1}{r'_0}\left[\frac{\Gamma}{2\pi i}\frac{(z'_1 \overline{z'}_1 - r'^2_0)}{r^2_{0'1'}} - \frac{\Gamma}{2\pi i}\frac{(z'_2 \overline{z'}_2 - r'^2_0)}{r^2_{0'2'}}\right] \qquad (4.10)$$

where: $r_{0'1'} = |z'_0 - z'_1|$ is the distance between Foppl's Vortex 1 and the cylinder surface in the unsteady state, $r_{0'2'} = |z'_0 - z'_2|$ the distance between Foppl's Vortex 2 and the cylinder surface in the unsteady state.

Expanding the velocity in the controlled state in terms of the leading order (basic state) and first order terms and using the linearization of the position coordinates after perturbation in the unsteady state (2.15) derived in Chapter 2, we can expand equation (4.10) as follows:

$$u'^v_r(z'_0) - iu'^v_\gamma(z'_0)$$

$$= \quad = \frac{1}{r'_0}\left[\frac{\Gamma}{2\pi i}\frac{(z'_1 \overline{z'}_1 - r'^2_0)}{r^2_{0'1'}} - \frac{\Gamma}{2\pi i}\frac{(z'_2 \overline{z'}_2 - r'^2_0)}{r^2_{0'2'}}\right]$$

$$= \quad \frac{1}{r_0}\left[\frac{\Gamma}{2\pi i}\frac{(z_1 \overline{z}_1 - 1)}{r^2_{01}} - \frac{\Gamma}{2\pi i}\frac{(z_2 \overline{z}_2 - 1)}{r^2_{02}}\right]$$

$$\quad -\frac{r_\epsilon}{r^2_0}\left[\frac{\Gamma}{2\pi i}\frac{(z_1 \overline{z}_1 - 1)}{r^2_{01}} - \frac{\Gamma}{2\pi i}\frac{(z_2 \overline{z}_2 - 1)}{r^2_{02}}\right]$$

$$\quad +\frac{1}{r_0}\left[\frac{\Gamma}{2\pi i}\frac{2r_1\rho_1 - 2r_\epsilon}{r^2_{01}} - \frac{\Gamma}{2\pi i}\frac{2r_2\rho_2 - 2r_\epsilon}{r^2_{02}}\right]$$

$$\quad +\frac{1}{r_0}\left[-\frac{\Gamma}{2\pi i}\frac{r^2 - 1}{r^4_{01}}(2r_1\rho_1 + 2r_\epsilon - 2(\rho_1 + r_1 r_\epsilon)\cos(\gamma - \theta_1) - 2r_1\alpha_1\sin(\gamma - \theta_1))\right]$$

$$\quad +\frac{1}{r_0}\left[+\frac{\Gamma}{2\pi i}\frac{r^2 - 1}{r^4_{02}}(2r_2\rho_2 + 2r_\epsilon - 2(\rho_2 + r_2 r_\epsilon)\cos(\gamma - \theta_2) - 2r_2\alpha_2\sin(\gamma - \theta_2))\right]$$

$$= \quad \frac{1}{r_0}\left[\frac{\Gamma}{2\pi i}\frac{r^2 - 1}{r^2_{01}} - \frac{\Gamma}{2\pi i}\frac{r^2 - 1}{r^2_{02}}\right]$$

$$-\frac{r_\epsilon}{r_0^2}\left[\frac{\Gamma}{2\pi i}\frac{r^2-1}{r_{01}^2}-\frac{\Gamma}{2\pi i}\frac{r^2-1}{r_{02}^2}\right]+\frac{(-2*r_\epsilon)}{r_0}\left[\frac{\Gamma}{2\pi i}\frac{1}{r_{01}^2}-\frac{\Gamma}{2\pi i}\frac{1}{r_{02}^2}\right]$$

$$+\frac{(-2r_\epsilon)}{r_0}\left[\frac{\Gamma}{2\pi i}\frac{(r^2-1)(1-r_1\cos(\gamma-\theta_1))}{r_{01}^4}-\frac{\Gamma}{2\pi i}\frac{(r^2-1)(1-r_2\cos(\gamma-\theta_2))}{r_{02}^4}\right]$$

$$+\frac{1}{r_0}\left[\frac{\Gamma}{2\pi i}\frac{2r_1\rho_1}{r_{01}^2}-\frac{\Gamma}{2\pi i}\frac{r^2-1}{r_{01}^4}(2r_1\rho_1-2\rho_1\cos(\gamma-\theta_1)-2r_1\sin(\gamma-\theta_1)\alpha_1)\right]$$

$$+\frac{1}{r_0}\left[-\frac{\Gamma}{2\pi i}\frac{2r_2\rho_2}{r_{02}^2}+\frac{\Gamma}{2\pi i}\frac{r^2-1}{r_{02}^4}(2r_2\rho_2-2\rho_2\cos(\gamma-\theta_2)+2r_2\sin(\gamma-\theta_2)\alpha_2)\right]$$

$$=-\frac{\Gamma}{2\pi i}(2r^2)\left(\frac{1}{r_{01}^2}-\frac{1}{r_{02}^2}\right)r_\epsilon+\frac{\Gamma}{2\pi i}(r^2-1)^2\left(\frac{1}{r_{01}^4}-\frac{1}{r_{02}^4}\right)r_\epsilon$$

$$+\frac{\Gamma}{2\pi}(2)\left(\frac{2r-(r^2+1)\cos(\gamma-\theta_1)}{r_{01}^4}\rho_1-\frac{2r-(r^2+1)\cos(\gamma-\theta_2)}{r_{02}^4}\rho_2\right)$$

$$+\frac{\Gamma}{2\pi}(r^2-1)(2)\left(\frac{r\sin(\gamma-\theta_1)}{r_{01}^4}\alpha_1-\frac{r\sin(\gamma-\theta_2)}{r_{02}^4}\alpha_2\right)$$

where r_{01}, r_{02} r, r_1, r_2 have the same definition as those in Chapter 2.

The zeroth and first order terms of the various velocity components can thus be deduced, these terms correspond to the velocity at the point z_0' on the solid surface induced by the two point vortices and their images at time t:

$$u_{r0}^v = 0 \tag{4.11}$$

$$u_{\gamma 0}^v = (r^2-1)\frac{\Gamma}{2\pi}\left(\frac{1}{r_{01}^2}-\frac{1}{r_{02}^2}\right) \tag{4.12}$$

$$u_{r1}^v = 0 \tag{4.13}$$

$$u_{\gamma 1}^v = -\frac{\Gamma}{2\pi}(2r^2)(\frac{1}{r_{01}^2} - \frac{1}{r_{02}^2})r_\epsilon(t) + \frac{\Gamma}{2\pi}(r^2 - 1)^2(\frac{1}{r_{01}^4} - \frac{1}{r_{02}^4})r_\epsilon(t)$$

$$+\frac{\Gamma}{2\pi}(2)\left(\frac{2r-(r^2+1)\cos(\gamma-\theta_1)}{r_{01}^4}\rho_1 - \frac{2r-(r^2+1)\cos(\gamma-\theta_2)}{r_{02}^4}\rho_2\right) \qquad (4.14)$$

$$+\frac{\Gamma}{2\pi}(r^2 - 1)(2)\left(\frac{r\sin(\gamma-\theta_1)}{r_{01}^4}\alpha_1 - \frac{r\sin(\gamma-\theta_2)}{r_{02}^4}\alpha_2\right)$$

Here, the leading order radial velocity $u_{r0}^v = 0$ reflects the normal boundary condition on the solid surface satisfied by the basic state.

We can compare the result of the first order velocity u_{r1}^v (4.13) and $u_{\gamma 1}^v$ (4.14) with those (2.33), (2.34) obtained in Chapter 2. We can see that the first order term of the velocity component u_{r1}^v, $u_{\gamma 1}^v$ consists of two parts: the first part is caused by the deformation of the cylinder surface $r_\epsilon(t)$ ($\delta(t)$ in Chapter 2); the second part is caused by the perturbation of the point vortices (ρ_1, α_1), (ρ_2, α_2). In both the symmetric surface deformation (expressed by $r_\epsilon(t)$ in this chapter) and the antisymmetric surface deformation (expressed by $\delta(t)$ in Chapter 2), the perturbation of the point vortices (ρ_1, α_1), (ρ_2, α_2) does not affect the normal velocity u_{r1}^v and its effect on the azimuthal velocity $u_{\gamma 1}^v$ remains the same.

4.2.3 Velocity Induced by the Source Distribution on the Cylinder Surface

In order to satisfy the no-slip normal boundary condition on the solid surface (2.1) at any time t, we place a small source distribution $Q_\epsilon(t)$ along the surface. The velocity at any surface point $(\cos\gamma, \sin\gamma)$ induced by the source distribution is given by:

$$v_x(\gamma) = \int_0^{2\pi} \frac{Q_\epsilon(t)}{2\pi} \frac{x - x_{Q_\epsilon}}{(x - x_{Q_\epsilon})^2 + (y - y_{Q_\epsilon})^2} d\tau$$

$$= \int_0^{2\pi} \frac{Q_\epsilon(t)}{2\pi} \frac{\cos\gamma - \cos\tau}{(\cos\gamma - \cos\tau)^2 + (\sin\gamma - \sin\tau)^2} d\tau$$

$$v_y(\gamma) = \int_0^{2\pi} \frac{Q_\epsilon(t)}{2\pi} \frac{y - y_{Q_\epsilon}}{(x - x_{Q_\epsilon})^2 + (y - y_{Q_\epsilon})^2} d\tau$$

$$= \int_0^{2\pi} \frac{Q_\epsilon(t)}{2\pi} \frac{\cos\gamma - \cos\tau}{(\cos\gamma - \cos\tau)^2 + (\sin\gamma - \sin\tau)^2} d\tau.$$

In polar coordinates, the velocity becomes:

$$v_r^c(\gamma, t) = \int_0^{2\pi} \frac{Q_\epsilon(t)}{2\pi} \frac{(\cos\gamma - \cos\tau)\cos\gamma + (\sin\gamma - \sin\tau)\sin\gamma}{(\cos\gamma - \cos\tau)^2 + (\sin\gamma - \sin\tau)^2} d\tau$$

$$= \frac{1}{2} Q_\epsilon(t)$$

$$v_\gamma^c(\gamma, t) = \int_0^{2\pi} \frac{Q_\epsilon(t)}{2\pi} \frac{-(\cos\gamma - \cos\tau)\sin\gamma + (\sin\gamma - \sin\tau)\cos\gamma}{(\cos\gamma - \cos\tau)^2 + (\sin\gamma - \sin\tau)^2} d\tau$$

$$= 0$$

This implies that the velocity induced by the source distribution at a point on the solid surface is:

$$v_r^c(\gamma, t) = \frac{1}{2} Q(t) \tag{4.15}$$

$$v_\theta^c(\gamma, t) = 0 \tag{4.16}$$

This result can be explained as follows. Since we apply the uniform surface source distribution $Q_\epsilon(t)$ which depends on time t only, the normal velocity $v_r^c(\gamma, t)$ is also only time dependent and there is no azimuthal velocity at any point $(r_0' \cos\gamma, r_0' \sin\gamma)$.

4.2.4 Source Distribution Function on the Cylinder Surface

Summarizing the previous results (4.11), (4.12), (4.13), (4.14), (4.15), (4.16), the various induced velocities at any point on the solid surface take the expressions:

$$u_{r0}^U(\gamma) = 0 \tag{4.17}$$

$$u_{\gamma 0}^U(\gamma) = -2\sin\gamma \tag{4.18}$$

$$u_{r0}^v(\gamma) = 0 \tag{4.19}$$

$$u_{\gamma 0}^v(\gamma) = (r^2 - 1)\frac{\Gamma}{2\pi}(\frac{1}{r_{01}^2} - \frac{1}{r_{02}^2}) \tag{4.20}$$

$$u_{r1}^U(\gamma, t) = 0 \tag{4.21}$$

$$u_{\gamma 1}^U(\gamma, t) = 0 \tag{4.22}$$

$$u_{r1}^v(\gamma, t) = 0 \tag{4.23}$$

$$u_{\gamma 1}^v(\gamma, t) = -\frac{\Gamma}{2\pi}(2r^2)(\frac{1}{r_{01}^2} - \frac{1}{r_{02}^2})r_\epsilon + \frac{\Gamma}{2\pi}(r^2 - 1)^2(\frac{1}{r_{01}^4} - \frac{1}{r_{02}^4})r_\epsilon$$

$$+\frac{\Gamma}{2\pi}(2)(\frac{2r - (r^2 + 1)\cos(\gamma - \theta_1)}{r_{01}^4}\rho_1 - \frac{2r - (r^2 + 1)\cos(\gamma - \theta_2)}{r_{02}^4}\rho_2) \tag{4.24}$$

$$+\frac{\Gamma}{2\pi}(r^2 - 1)(2)(\frac{r\sin(\gamma - \theta_1)}{r_{01}^4}\alpha_1 - \frac{r\sin(\gamma - \theta_2)}{r_{02}^4}\alpha_2)$$

$$u_{r1}^c(\gamma, t) = \frac{1}{2}Q(t) \tag{4.25}$$

$$u_{\gamma 1}^c(\gamma, t) = 0 \tag{4.26}$$

The zeroth order term of the radial velocities $u_{r0}^U = 0$ and $u_{r0}^v = 0$ guarantees the no-slip normal boundary condition on the solid surface for the basic state. We can see that this term is the same as that calculated in Chapter 2 in the case of the displacement $\delta(t)$ of the cylinder. The first order term, however, is different reflecting different perturbations applied to the cylinder.

Substituting results (4.21),(4.23),(4.25) into the boundary condition (4.4), we obtain the source distribution along the surface:

$$Q(t) = 2\frac{dr_\epsilon(t)}{dt} \tag{4.27}$$

We observe here the source distribution function $Q_\epsilon(t)$ is proportional to the deformation velocity of the surface of the cylinder, representing the mass input or output along the cylinder surface per unit time corresponding to the cylinder surface.

4.3 Control by Symmetric Deformation of the Cylinder Surface

4.3.1 Linearization of the Control System

Following the procedure presented in Chapter 2, we assume that the point vortices are perturbed from the location z_1, z_2 to z_1', z_2', and that a point on the solid surface is perturbed from z_0 to z_0'. The dynamics of the perturbed point vortex model in Cartesian coordinates is given by:

$$\frac{d\overline{z'}_1}{dt} = 1 - \frac{r_0'^2}{z_1'^2} + \frac{\Gamma}{2\pi i}\frac{1}{z_1' - z_2'} + \frac{\Gamma}{2\pi i}\frac{1}{z_1' - \frac{r_0'^2}{\overline{z'}_1}} - \frac{\Gamma}{2\pi i}\frac{1}{z_1' - \frac{r_0'^2}{\overline{z'}_2}} + \frac{1}{2\pi}\int_0^{2\pi}\frac{Q_\epsilon(t)}{z_1' - z_0'}d\gamma$$

$$\frac{d\overline{z'}_2}{dt} = 1 - \frac{r_0'^2}{z_2'^2} - \frac{\Gamma}{2\pi i}\frac{1}{z_2' - z_1'} + \frac{\Gamma}{2\pi i}\frac{1}{z_2' - \frac{r_0'^2}{\overline{z'}_1}} - \frac{\Gamma}{2\pi i}\frac{1}{z_2' - \frac{r_0'^2}{\overline{z'}_2}} + \frac{1}{2\pi}\int_0^{2\pi}\frac{Q_\epsilon(t)}{z_2' - z_0'}d\gamma.$$

Using the expression (2.12) in Chapter 2, we convert the control system from Cartesian coordinates to polar coordinates:

$$\frac{dr_1'}{dt} - ir_1'\frac{d\theta_1'}{dt} = \frac{1}{r_1'}(z_1' - \frac{r_0'^2}{z_1'} + \frac{\Gamma}{2\pi i}\frac{z_1'}{z_1' - z_2'} + \frac{\Gamma}{2\pi i}\frac{r_0'^2}{z_1'\overline{z'}_1 - r_0'^2} - \frac{\Gamma}{2\pi i}\frac{r_0'^2}{z_1'\overline{z'}_2 - r_0'^2}$$

$$+ \frac{1}{2\pi}\int_0^{2\pi}\frac{Q_\epsilon(t)z_1'}{z_1' - z_0'}d\gamma)$$

$$\frac{dr_2'}{dt} - ir_2'\frac{d\theta_2'}{dt} = \frac{1}{r_2'}(z_2' - \frac{r_0'^2}{z_2'} - \frac{\Gamma}{2\pi i}\frac{z_2'}{z_2' - z_1'} + \frac{\Gamma}{2\pi i}\frac{r_0'^2}{z_2'\overline{z'}_1 - r_0'^2} - \frac{\Gamma}{2\pi i}\frac{r_0'^2}{z_2'\overline{z'}_2 - r_0'^2}$$

$$+ \frac{1}{2\pi}\int_0^{2\pi}\frac{Q_\epsilon(t)z_2'}{z_2' - z_0'}d\gamma)$$

Here, we use the same notation (as in the chapter 2) to linearize the system with respect to the fixed point positions $z_1(r_1, \theta_1)$, $z_2(r_2, \theta_2)$ and the circular cylinder surface $z_0(r_0, \gamma)$. The positions of the vortices are perturbed by means of small disturbances (ρ_1, α_1), (ρ_2, α_2), where ρ_1, $\rho_2 \ll 1$, θ_1, $\theta_2 \ll 1$.

Using Cauchy formula, we can show that:

$$\int_0^{2\pi} \frac{1}{z_1 - z_0} d\gamma = \frac{i}{z_1} \int_{|r|=1} \left(\frac{1}{z_0} + \frac{1}{z_1 - z_0}\right) dz_0 = -\frac{2\pi}{z_1}$$

$$\int_0^{2\pi} \frac{1}{z_2 - z_0} d\gamma = \frac{i}{z_2} \int_{|r|=1} \left(\frac{1}{z_0} + \frac{1}{z_2 - z_0}\right) dz_0 = -\frac{2\pi}{z_2}.$$

Lineariztion of the control system with respect to the fixed point leads to:

$$\frac{d\rho_1}{dt} = -\frac{\rho_1}{r_1^2} Re[z_1 - \frac{1}{z_1} + \frac{\Gamma}{2\pi i} \frac{z_1}{z_1 - z_2} + \frac{\Gamma}{2\pi i} \frac{1}{z_1 \bar{z}_1 - 1} - \frac{\Gamma}{2\pi i} \frac{1}{z_1 \bar{z}_2 - 1}]$$

$$+ \frac{1}{r_1} Re[z_1(\frac{\rho_1}{r_1} + i\alpha_1) + \frac{1}{z_1^2} z_1(\frac{\rho_1}{r_1} + i\alpha_1)$$

$$+ \frac{\Gamma}{2\pi i}(\frac{1}{z_1 - z_2} z_1(\frac{\rho_1}{r_1} + i\alpha_1) - \frac{z_1}{(z_1 - z_2)^2}(z_1(\frac{\rho_1}{r_1} + i\alpha_1) - z_2(\frac{\rho_2}{r_2} + i\alpha_2))$$

$$- \frac{\Gamma}{2\pi i} \frac{2r_1 \rho_1}{(r_1^2 - 1)^2} + \frac{\Gamma}{2\pi i} \frac{1}{(z_1 \bar{z}_2 - 1)^2}(z_1 \bar{z}_2(\frac{\rho_1}{r_1} + i\alpha_1) + z_1 \bar{z}_2(\frac{\rho_2}{r_2} - i\alpha_2))]$$

$$- \frac{Q_\epsilon(t)}{r_1}$$

$$\frac{d\alpha_1}{dt} = \frac{2\rho_1}{r_1^3} Im[z_1 - \frac{1}{z_1} + \frac{\Gamma}{2\pi i} \frac{z_1}{z_1 - z_2} + \frac{\Gamma}{2\pi i} \frac{1}{z_1 \bar{z}_1 - 1} - \frac{\Gamma}{2\pi i} \frac{1}{z_1 \bar{z}_2 - 1}]$$

$$- \frac{1}{r_1^2} Im[z_1(\frac{\rho_1}{r_1} + i\alpha_1) + \frac{1}{z_1^2} z_1(\frac{\rho_1}{r_1} + i\alpha_1)$$

$$+ \frac{\Gamma}{2\pi i}(\frac{1}{z_1 - z_2} z_1(\frac{\rho_1}{r_1} + i\alpha_1) - \frac{z_1}{(z_1 - z_2)^2}(z_1(\frac{\rho_1}{r_1} + i\alpha_1) - z_2(\frac{\rho_2}{r_2} + i\alpha_2))$$

$$- \frac{\Gamma}{2\pi i} \frac{2r_1 \rho_1}{(r_1^2 - 1)^2} + \frac{\Gamma}{2\pi i} \frac{1}{(z_1 \bar{z}_2 - 1)^2}(z_1 \bar{z}_2(\frac{\rho_1}{r_1} + i\alpha_1) + z_1 \bar{z}_2(\frac{\rho_2}{r_2} - i\alpha_2))]$$

$$\frac{d\rho_2}{dt} = -\frac{\rho_2}{r_2^2}Re[z_2 - \frac{1}{z_2} - \frac{\Gamma}{2\pi i}\frac{z_2}{z_2 - z_1} + \frac{\Gamma}{2\pi i}\frac{1}{z_2\bar{z}_1 - 1} - \frac{\Gamma}{2\pi i}\frac{1}{z_2\bar{z}_2 - 1}]$$

$$+ \frac{1}{r_2}Re[z_2(\frac{\rho_2}{r_2} + i\alpha_2) + \frac{1}{z_2^2}z_2(\frac{\rho_2}{r_2} + i\alpha_2)$$

$$- \frac{\Gamma}{2\pi i}(\frac{1}{z_2 - z_1}z_2(\frac{\rho_2}{r_2} + i\alpha_2) - \frac{z_2}{(z_2 - z_1)^2}(z_2(\frac{\rho_2}{r_2} + i\alpha_2) - z_1(\frac{\rho_1}{r_1} + i\alpha_1))$$

$$- \frac{\Gamma}{2\pi i}\frac{1}{(z_2\bar{z}_1 - 1)^2}(z_2\bar{z}_1(\frac{\rho_2}{r_2} + i\alpha_2) + z_2\bar{z}_1(\frac{\rho_1}{r_1} - i\alpha_1)) + \frac{\Gamma}{2\pi i}\frac{2r_2\rho_2}{(r_2^2 - 1)^2}]$$

$$- \frac{Q_\epsilon(t)}{r_2}$$

$$\frac{d\alpha_2}{dt} = \frac{2\rho_2}{r_2^3}Im[z_2 - \frac{1}{z_2} - \frac{\Gamma}{2\pi i}\frac{z_2}{z_2 - z_1} + \frac{\Gamma}{2\pi i}\frac{1}{z_2\bar{z}_1 - 1} - \frac{\Gamma}{2\pi i}\frac{1}{z_2\bar{z}_2 - 1}]$$

$$- \frac{1}{r_2^2}Im[z_2(\frac{\rho_2}{r_2} + i\alpha_2) + \frac{1}{z_2^2}z_2(\frac{\rho_2}{r_2} + i\alpha_2)$$

$$- \frac{\Gamma}{2\pi i}(\frac{1}{z_2 - z_1}z_2(\frac{\rho_2}{r_2} + i\alpha_2) - \frac{z_2}{(z_2 - z_1)^2}(z_2(\frac{\rho_2}{r_2} + i\alpha_2) - z_1(\frac{\rho_1}{r_1} + i\alpha_1))$$

$$- \frac{\Gamma}{2\pi i}\frac{1}{(z_2\bar{z}_1 - 1)^2}(z_2\bar{z}_1(\frac{\rho_2}{r_2} + i\alpha_2) + z_2\bar{z}_1(\frac{\rho_1}{r_1} - i\alpha_1)) + \frac{\Gamma}{2\pi i}\frac{2r_2\rho_2}{(r_2^2 - 1)^2}].$$

Adding and subtracting the equations of motion for the two vortices and using the symmetric and asymmetric modes as those defined in Chapter 2, we have:

$$\frac{d\rho_S}{dt} = \frac{1}{r}(\frac{A(r)}{r}\rho_S - B(r)\alpha_S) - \frac{1}{r}\frac{\Gamma}{2\pi}\frac{2r^2}{(z_1 - z_2)^2}\alpha_S - \frac{2Q_\epsilon(t)}{r}$$

$$\frac{d\alpha_S}{dt} = -\frac{1}{r^2}(\frac{B(r)}{r}\rho_S + A(r)\alpha_S) - \frac{1}{r^2}\frac{\Gamma}{2\pi}\frac{2r}{(r^2 - 1)^2}\rho_S$$

$$\frac{d\rho_A}{dt} = \frac{1}{r}(\frac{C(r)}{r}\rho_A - D(r)\alpha_A)$$

$$\frac{d\alpha_A}{dt} = -\frac{1}{r^2}(\frac{D(r)}{r}\rho_A + C(r)\alpha_A) - \frac{1}{r^2}\frac{\Gamma}{2\pi}(\frac{2r}{(r^2-1)^2} - \frac{2r}{(z_1-z_2)^2})\rho_A$$

where $A(r)$, $B(r)$ $C(r)$, $D(r)$ are the same as those defined in (2.50), (2.51), (2.52), (2.53) in Chapter 2.

We can rewrite the above control system in the following matrix form.

Symmetric mode:

$$\frac{\partial}{\partial t}\begin{bmatrix} \rho_S \\ \alpha_S \end{bmatrix} = \begin{bmatrix} \frac{A}{r^2} & -\frac{B}{r} - \frac{\Gamma}{2\pi}\frac{2r}{(z_1-z_2)^2} \\ -\frac{B}{r^3} - \frac{\Gamma}{2\pi}\frac{2}{r(r^2-1)^2} & -\frac{A}{r^2} \end{bmatrix}\begin{bmatrix} \rho_S \\ \alpha_S \end{bmatrix} + \begin{bmatrix} \frac{4}{r} & 0 \\ 0 & 0 \end{bmatrix}\begin{bmatrix} \frac{dr_\epsilon(t)}{dt} \\ r_\epsilon(t) \end{bmatrix}$$

Asymmetric mode:

$$\frac{\partial}{\partial t}\begin{bmatrix} \rho_A \\ \alpha_A \end{bmatrix} = \begin{bmatrix} \frac{C}{r^2} & -\frac{D}{r} \\ -\frac{D}{r^3} + \frac{\Gamma}{2\pi}\frac{2}{r(r^2-1)} & -\frac{C}{r^2} \end{bmatrix}\begin{bmatrix} \rho_A \\ \alpha_A \end{bmatrix}.$$

As expected, this shows that a uniform surface deformation $r_\epsilon(t)$ of the cylinder has an effect on the symmetric mode only, without influencing the asymmetric mode. This implies that our symmetric control scheme will alter the center manifold of the fixed point, without affecting the stable/unstable manifold. We now discuss whether a control scheme based on such a deformation can control the force (lift and drag) exerted on the solid body.

4.3.2 Pressure Distribution on the Solid Surface

We now proceed with our analysis and calculate the pressure distribution on the cylinder surface. We recall the expressions of the zeroth order (steady state) and first order terms of the pressure coefficient (??), (??) in Chapter 2 substitute in the azimuthal induced velocity expressions (4.18), (4.20), (4.22), (4.24), (4.26), we can

calculate the zeroth and first order terms of the pressure coefficient for a point (r_0', γ) on the surface of the cylinder.

$$C_{p0}(\gamma) = 1 - [2\sin\gamma - \frac{\Gamma}{2\pi}(r^2 - 1)(\frac{1}{r_{01}^2} - \frac{1}{r_{02}^2})]^2 \qquad (4.28)$$

$$C_{p1}(\gamma) = 2[2\sin\gamma - \frac{\Gamma}{2\pi}(r^2 - 1)(\frac{1}{r_{01}^2} - \frac{1}{r_{02}^2})]$$

$$[-\frac{\Gamma}{2\pi}(2r^2)(\frac{1}{r_{01}^2} - \frac{1}{r_{02}^2})r_\epsilon + \frac{\Gamma}{2\pi}(r^2 - 1)^2(\frac{1}{r_{01}^4} - \frac{1}{r_{02}^4})r_\epsilon$$

$$\qquad (4.29)$$

$$+\frac{\Gamma}{2\pi}(2)(\frac{2r - (r^2+1)\cos(\gamma-\theta_1)}{r_{01}^4}\rho_1 - \frac{2r - (r^2+1)\cos(\gamma-\theta_2)}{r_{02}^4}\rho_2)$$

$$+\frac{\Gamma}{2\pi}(r^2 - 1)(2)(\frac{r\sin(\gamma-\theta_1)}{r_{01}^4}\alpha_1 - \frac{r\sin(\gamma-\theta_2)}{r_{02}^4}\alpha_2)]$$

We then deduce the differential pressure coefficient between two points located symmetrically with respect to the centerline:

$$\Delta C_p = C_{p1}(\gamma) - C_{p1}(-\gamma)$$

$$= 2[2\sin\gamma - \frac{\Gamma}{2\pi}(r^2 - 1)(\frac{1}{r_{01}^2} - \frac{1}{r_{02}^2})]$$

$$\qquad (4.30)$$

$$[\frac{\Gamma}{2\pi}(2)(\frac{2r - (r^2+1)\cos(\gamma-\theta_1)}{r_{01}^4} + \frac{2r - (r^2+1)\cos(\gamma-\theta_1)}{r_{02}^4})\rho_A$$

$$+\frac{\Gamma}{2\pi}(r^2 - 1)(2)(\frac{r\sin(\gamma-\theta_1)}{r_{01}^4} - \frac{r\sin(\gamma-\theta_2)}{r_{02}^4})\alpha_A]$$

which is only a function of the asymmetric variables (ρ_A, α_A).

We now calculate the lift on the cylinder. Since the leading order term of the induced azimuthal velocities $u_{\gamma 0}^U$, $u_{\gamma 0}^v$ is the same as those in Chapter 2, the leading order term of the lift coefficient is still zero, that is:

$$C_{L0} = 0$$

The first order term of the lift coefficient is:

$$C_{L1} = -\int_0^{2\pi} C_{P1}(\gamma) \sin\gamma d\gamma$$

$$= -\int_0^{\pi} \Delta C_{P1}(\gamma) \sin\gamma d\gamma$$

Since the differential pressure $\Delta C_{P1}(\gamma)$ (4.30) only depends on the asymmetric mode (ρ_A, α_A) and does not depend on the surface deformation function $r_\epsilon(t)$, we can conclude that any symmetric deformation of the cylinder has no effect on the vertical component of the force, i.e. the lift. In contrast, we now show that a symmetric surface deformation can control the horizontal component of the force, i.e. the drag. For this purpose, we impose the first order term of the drag coefficient to be zero at all times $t > 0$. The leading order term of the drag coefficient is the same as that given in Chapter 2, that is:

$$C_{D0} = -\int_0^{2\pi} C_{P0}(\gamma) \cos\gamma d\gamma$$

$$= -\int_0^{\pi} [C_{P0}(\gamma) + C_{P0}(-\gamma)] \cos\gamma d\gamma$$

$$= -2\int_0^{\pi} [1 - (2\sin\gamma - \frac{\Gamma}{2\pi}(r^2-1)(\frac{1}{r_{01}^2} - \frac{1}{r_{02}^2}))^2] \cos\gamma d\gamma.$$

The first order term of the drag coefficient is given by:

$$C_{D1} = -\int_0^{2\pi} C_{P1}(\gamma) \cos\gamma d\gamma$$

$$= -\int_0^{\pi} [C_{P1}(\gamma) + C_{P1}(-\gamma)] \cos\gamma d\gamma$$

$$= -2\int_0^{\pi} [2\sin\gamma - \frac{\Gamma}{2\pi}(r^2-1)(\frac{1}{r_{01}^2} - \frac{1}{r_{02}^2})]$$

$$[-\frac{\Gamma}{2\pi}(4r^2)(\frac{1}{r_{01}^2} - \frac{1}{r_{02}^2})r_\epsilon + \frac{\Gamma}{2\pi}(2)(r^2 - 1)^2(\frac{1}{r_{01}^4} - \frac{1}{r_{02}^4})r_\epsilon$$

$$+\frac{\Gamma}{2\pi}(2)(\frac{2r - (r^2 + 1)\cos(\gamma - \theta_1)}{r_{01}^4} - \frac{2r - (r^2 + 1)\cos(\gamma - \theta_2)}{r_{02}^4})\rho_S$$

$$+\frac{\Gamma}{2\pi}(r^2 - 1)(2)(\frac{r\sin(\gamma - \theta_1)}{r_{01}^4} + \frac{r\sin(\gamma - \theta_2)}{r_{02}^4})\alpha_S]\cos\gamma d\gamma.$$

We conclude here that the first order term of the drag coefficient depends on both the symmetric mode (ρ_S, α_S) and the deformation function $r_\epsilon(t)$. It is therefore possible to obtain a symmetric deformation control function $r_\epsilon(t)$ by imposing $C_{D1} = 0$. We now present the function obtained in this manner:

$$r_\epsilon(t) = e(r)\rho_S + f(r)\alpha_S \tag{4.31}$$

where e(r), f(r) are defined by:

$$e(r) = \frac{M_1(r)}{DEM(r)} \tag{4.32}$$

$$f(r) = \frac{M_2(r)}{DEM(r)} \tag{4.33}$$

$$M_1(r) = 4\int_0^\pi k(\gamma)\frac{\Gamma}{2\pi}[\frac{2r - (r^2 + 1)\cos(\gamma - \theta_1)}{r_{01}^4} - \frac{2r - (r^2 + 1)\cos(\gamma - \theta_2)}{r_{02}^4}]\cos\gamma d\gamma \tag{4.34}$$

$$M_2(r) = 4\int_0^\pi k(\gamma)\frac{\Gamma}{2\pi}(r^2 - 1)[\frac{r\sin(\gamma - \theta_1)}{r_{01}^4} + \frac{r\sin(\gamma - \theta_2)}{r_{02}^4}]\cos\gamma d\gamma \tag{4.35}$$

$$DEM(r) = -4\int_0^\pi k(\gamma)[-\frac{\Gamma}{2\pi}(2r^2)(\frac{1}{r_{01}^2} - \frac{1}{r_{02}^2}) + \frac{\Gamma}{2\pi}(r^2 - 1)^2(\frac{1}{r_{01}^4} - \frac{1}{r_{02}^4})]\cos\gamma d\gamma \tag{4.36}$$

where $k(\gamma)$ is defined as:

$$k(\gamma) = 2\sin\gamma - \frac{\Gamma}{2\pi}(r^2 - 1)(\frac{1}{r_{01}^2} - \frac{1}{r_{02}^2})$$

By deforming the cylinder surface with the control function (4.31), we can force the drag of the perturbed flow to keep the value as it has in the basic state.

4.4   Results and Discussions

In this chapter, we have considered the possibility of controlling the perturbed flow of Foppl's potential flow model by deforming the surface of the cylinder. We have considered a particular deformation only, a time dependent and uniform deformation. This was achieved by means of a deformation control function $r_\epsilon(t)$ chosen by forcing the drag to keep the value the same as it has in the basic state. Such a deformation was realized by introducing a symmetric source distribution $Q_\epsilon(t)$ along the surface of the cylinder to ensure that the boundary condition on the solid boundary is satisfied at each time.

We can linearize the control system around the fixed point. The linearized motion of the symmetric and asymmetric modes are given by the following expression.

Symmetric mode:

$$\frac{\partial}{\partial t}\begin{bmatrix} \rho_S \\ \alpha_S \end{bmatrix} = \begin{bmatrix} \frac{A}{r^2} & -\frac{B}{r} - \frac{\Gamma}{2\pi}\frac{2r}{r(z_1-z_2)^2} \\ -\frac{B}{r^3} - \frac{\Gamma}{2\pi}\frac{2}{r(r^2-1)^2} & -\frac{A}{r^2} \end{bmatrix} \begin{bmatrix} \rho_S \\ \alpha_S \end{bmatrix} + \begin{bmatrix} \frac{4}{r} & 0 \\ 0 & 0 \end{bmatrix} \begin{bmatrix} \frac{dr_\epsilon(t)}{dt} \\ r_\epsilon(t) \end{bmatrix}$$

Asymmetric mode:

$$\frac{\partial}{\partial t}\begin{bmatrix} \rho_A \\ \alpha_A \end{bmatrix} = \begin{bmatrix} \frac{C}{r^2} & -\frac{D}{r} \\ -\frac{D}{r^3} + \frac{\Gamma}{2\pi}\frac{2}{r(r^2-1)} & -\frac{C}{r^2} \end{bmatrix} \begin{bmatrix} \rho_A \\ \alpha_A \end{bmatrix}$$

As expected, the symmetric deformation affects the center manifold only and has no effect on the lift coefficient C_L. However, it can control the drag coefficient C_D. This is achieved by choosing a suitable deformation function $r_\epsilon(t)$ in equation (4.31).

CHAPTER 5

CONCLUSION

In this thesis, we have designed two active, closed loop control algorithms aiming at manipulating the flow undergoing the previous instability. In the first algorithm, the lift is kept at zero value, while in the second scheme, the drag is maintained at the drag value of the steady recirculation bubble.

The two algorithms were derived analytically via a reduced model which we choose to be Foppl's potential flow model. In this model, the fixed point represents the recirculation bubble which is always unstable. The linear stability analysis of the fixed point showed that there is a two-dimensional center eigenspace spanned by symmetric modes, a one-dimensional stable eigenspace spanned by an asymmetric mode and a one-dimensional eigenspace spanned by another asymmetric mode. Our goal was to control the solution perturbed away from the fixed point in order to either keep the lift to zero or keep the drag to the drag value of the fixed point. In both control algorithms, the actuator consists of a change in the boundary condition at the surface of the cylinder. This change was treated analytically through the domain perturbation method and asymptotic expansions.

In the first algorithm, the cylinder is displaced by a distance $\delta(t)$, which plays the role of our control function. The motion of the cylinder is represented by a vortex distribution at the surface of the cylinder. We have used asymptotic expansions to derive the control system and to express the distance $\delta(t)$ required at all times in order to cancel the non-zero lift in the solution perturbed away from the fixed point. The control function $\delta(t)$ was found to be a linear function of the asymmetric eigenspace, thus implying that the displacement of the cylinder has no effect on the symmetric (center) eigenspace of the fixed point. We could thus successfully impose zero lift on

the cylinder at all times $t > 0$ by displacing the cylinder vertically. The application of the control algorithm to a numerical simulation of the viscous, impulsively started flow past a cylinder (based on the full Navier-Stokes equations), showed that we could keep the lift close to zero in the viscous flow as well, when the controller was applied before vortex shedding sets in. Compared to the more commonly used feedback control technique based on suction/blowing, our control approach is less dependent on the control parameters such as sensor location, velocity profile, etc..

In the second algorithm, the surface of the cylinder was deformed in a uniform manner along the surface, so that at every time, the solid body is a cylinder whose radius varies in time. Here, our control function is the change in radius, $r_\epsilon(t)$, compared to the radius of the cylinder in the original Foppl's model. Mathematically, this uniform surface deformation was represented by a source distribution along the surface of the cylinder. We have used asymptotic expansions to derive the control system and have found that the control function $r_\epsilon(t)$ is determined solely by the symmetric eigenspace of the fixed point, thus implying that it has no effect on the asymmetric mode. In this manner, we could control the drag in order to prevent the latter from deviating away from the drag value of the steady state.

REFERENCES

1. Abergei, F.& Termam, R. 1990   On some control problems in fluid mechanics. Theor. Comput. Fluid Dyn. **1**, 303.

2. Albarede, P. & Provansal, M. 1995   Quasi-periodic cylinder wakes and the Ginzburg-Landau model.   J. Fluid Mech. **291**, 191-222.

3. Barkley, D. & Henderson, R. D. 1996   Three dimensional Floquet stability analysis of the wake of a circular cylinder.   J. Fluid Mech. **332**, 215-241.

4. Berger, E. 1967   Suppression of vortex shedding and turbulence behind oscillating cylinders.   Phys. Fluids **10**, S191-S193.

5. Blackburn, H. M. & Henderson, R. D. 1999   A study of two-dimensional flow past an oscillating cylinder.   J. Fluid Mech. **385**, 255-286.

6. Brika, D. & Laneville, A 1993   Vortex-induced vibrations of a long flexible circular cylinder.   J. Fluid Mech. **250**, 481-508.

7. Chen, Z. 2000   Electro-magnetic control of cylinder wake.   Doctoral Dissertation Proposal, Dept. of Mech. Engr., NJIT.

8. Cortelezzi, L. 1996   Nonlinear feedback control of the wake past a plate with a suction point on the downstream wall.   J. Fluid Mech. **327**, 303-324.

9. Crow, S. C., 1970   Stability Theory for a Pair of Trailing Vortices.   AIAA J. **8** (12), 2172-2179.

10. Dusek, J., Gal, P. L. & Fraunie P. 1994   A numerical and theoretical study of the first Hopf bifurcation in a cylinder wake.   J. Fluid Mech. **264**, 59-80.

11. Ffowcs Williams, J. E. & Zhao, B. C. 1989   The active control of vortex shedding.   J. Fluids Struct. **3**, 115-122.

12. Gad-el-Hak, M. 1996   Modern developments in flow control.   Appl. Mech. Rev. **49** (7), 365-379.

13. Gunzburger, M. D., & Lee, H. C., 1996   Feekback control of Kanman vortex shedding.   J. Appl. Mech. **63** (9), 828-835.

14. Hannemann, K. & Oertel, H. 1989   Numerical simulation of the absolutely and convectively unstable wake.   J. Fluid Mech. **199**, 55-88.

15. Henderson, R. D. & Barkley, D. 1996   Secondary instability in the wake of a circular cylinder.   Phys. Fluid, **8**, 1683.

16. Jackson, C. P. 1987   A finite-element study of the onset of vortex shedding in flow past variously shaped bodies.   J. Fluid Mech. **182**, 23-45.

17. Karniadakis, G. E. & Triantafyllou, G. S., 1989   Frequency selection and asymptotic states in laminar wakes.   J. Fluid Mech. **199**, 441-469.

18. Kang, S. & Choi, H. 1996   Laminar flow past a rotating circular cylinder. Phys. Fluids **8**, 479.

19. Keefe, L. R. 1993   Two nonlinear control schemes contrasted on a hydrodynamiclike model.   Phys. Fluids A 5(4), 931-947.

20. Koumoutsakos, P. & Leonard, A. 1995   High-resolution simulations of the flow around an impulsively started cylinder using vortex methods.   J. Fluid Mech. **296**, 1-38.

21. Kwon, K. & Choi, H. 1996   Control of laminar vortex shedding behind a circular cylinder using splitter plates.   Phys. Fluids **8**, 479.

22. Lumley, j. & Blossey, P. 1998   Control of Turbulence.   Annu. Rev. Fluid Mech. **30**, 311-327.

23. Min, C. & Choi, H. 1999   Suboptimal feedback control of vortex shedding at low Reynolds numbers.   J. Fluid Mech. **401**, 123-156.

24. Moin, P. & Bewley, T. 1994   Feedback control of turbulence.   Appl. Mech. Rev. **47** (6), s3-s13.

25. Monkewitz, P. A. 1992   Wake Control.   *Bluff-Body Wakes, Dynamics and Instabilities* (ed. H. Eckelmann, J. M. R, Graham, P. Huerre & P. A. Monkewitz), pp. 227-240. Springer-Verlag.

26. Monkewitz, P. A., Schumm, M. & Berger E. 1994   Self-excited oscillations in the wake of two-dimensional bluff bodies and their control.   J. Fluid Mech. **271**, 17-53.

27. Newman, D. J. & Karniadakis, G. E. 1996   Simulations of flow over a flexible cable: A comparison of forced and flow induced vibration.   J. Fluids Struct. **10**, 439-453.

28. Newman, D. J. & Karniadakis, G. E. 1997   A direct numerical simulation study of flow past a freely vibrating cable.   J. Fluid Mech. **344**, 95-136.

29. Oertel, H. Jr. 1990   Wakes behind blunt bodies.   Annu. Rev. Fluid Mech. **22**, 539-64.

30. Ongoren, A. & Rockwell, D. 1988   Flow structure from an oscillating cylinder. Part 1: Mechanism of phase shift and recovery in the near wake.   J. Fluid Mech. **191**, 197-223.

31. Park, D. S., Ladd, D. M. & Hendricks, E. W. 1994   Feedback control of von Karman vortex shedding behind a circular cylinder at low Reynolds numbers.   Phys. Fluids **6** (7), 2390-2405.

32. Provansal, M., Mathis, C. & Boyer, L. 1987   Benard-von Karman instability: transient and forced regimes.   J. Fluid Mech. **182**, 1-22.

33. Roussopoulos, K. 1992   Aspects of bluff body wake control.   *Bluff-Body Wakes, Dynamics and Instabilities* (ed. H. Eckelmann, J. M. R, Graham, P. Huerre & P. A. Monkewitz), pp. 249-252. Springer-Verlag.

34. Roussopoulos, K. 1993   Feedback control of vortex shedding at low Reynolds numbers.   J. Fluid Mech. **248**, 267.

35. Rusak, Z., & Seginer, A., 1991   The three-dimensional stability of Foppl Vortices.   Rensselaer Polytechnic Inst., Aeronautical Engineering Rept. 99, Troy, NY.

36. Schumm, M., Berger, E. & Monkewitz, P. A. 1994   Self-excited oscillations in the wake of two-dimensional bluff bodies and their control.   J. Fluid Mech. **271**, 17-53.

37. Shermer, R. 1991   Control of vortex shedding in a two-dimensional flow past a plate.   Phys. Rev. A **46** (12).

38. Smith, A. C. 1973   On the stability of Foppl's Vortices.   J. Appl. Mech. (6), 610-612.

39. Smith, P. A., & Stansby, P. K. 1988   Impulsively started flow around a circular cylinder by the vortex method.   J. Fluid Mech. **194**, 45-77.

40. Sreenivasan, K. R., Strykowski, P.J. & Olinger, D.J. 1987   Hopf bifurcation, Landau equation and vortex shedding behind circular cylinders.   *Proc. Forum on Unsteady Flow Separation*. ASME Applied Mechanics, Bio Engineering and Fluid Engineering Conference. Cincinnati, Ohio. June 11-17.

41. Strykowski, P. J. & Sreenivasan K. R. 1990   On the formation and suppression of vortex shedding at low Reynolds numbers.   J. Fluid Mech. **218**, 77-107.

42. Tang, S. & Aubry, N. 1997   On the symmetry breaking instability leading to vortex shedding.   Phys. Fluids **9** (9), 2550-61.

43. Tokumaru, P. T. & Dimotakis, P. E. 1991   Rotary oscillation control of a cylinder wake.   J. Fluid Mech. **224**, 77-90.

44. Unal, M. F. & Rockwell, D. 1988   On vortex formation from a cylinder. Part 2: Control by splitter-plate interference   J. Fluid Mech. **190**, 513.

45. Williamson, C. H. K. 1996   Vortex dynamics in the cylinder wake.   Annu. Rev. Fluid Mech. **28**, 477-539.

46. Williamson, C. H. K. & Roshko, A. 1988   Vortex formation in the wake of an oscillating cylinder.   J. Fluids Struct. **2**, 2355-2381.

47. Widnall, S. E. 1975   The structure and dynamics of vortex filaments.   Annu. Rev. Fluid Mech. **7** 141-165.

48. Widnall, S., 1985   Review of three-dimensional vortex dynamics: implications for the computation of seperated and turbulent flow.   *Studies of Vortex Dominated Flows* (ed. M. Y. Hussaini & M. D. Salas). 16-32.

49. Zielinska, B. J. A. & Wesfreid, J. E. 1995   On the spatial structure of global modes in wake flow.   Phys. Fluids **7** (6), 1418-1424.

50. Zhang, H. Q. et al. 1995   On the transition of the cylinder wake.   Phys. Fluids **7** (4), 779-794.